Investigating the functions and interactions of *Salmonella* effector SspH2 with intracellular innate immune receptors

By: Cole J. Delyea

A thesis submitted in partial fulfillment of the requirements for the degree of

Master of Science

in

Immunology

Department of Medical Microbiology and Immunology

University of Alberta

Abstract:

As part of its pathogenesis, *Salmonella enterica* serovar *typhimurium* delivers effector proteins into host cells. One such effector is SspH2, a member of the novel E3 ubiquitin ligase (NEL) family, which has been reported to interact with, and enhance, NOD1 pro-inflammatory signaling. It is still unknown as to how SspH2 is specifically mediating increased NLR activity. I transfected host NLRs and bacterial SspH2 in mammalian epithelial cell culture and monitored various aspects of SspH2 interactions in host cells. I demonstrate that SspH2 interacts with two out of three different regions on NOD1, namely its central Nucleotide binding domain, and its C-terminal Leucine rich repeat domain by using co-immunoprecipitations (co-IP). Using the same methods, I also determined that SspH2 also interacts with NOD2, a closely related NLR to NOD1. This interaction induces super-activation of NOD2, resulting in increased IL-8 secretion that was measured by ELISA. Furthermore, I show that catalytically active SspH2 significantly increases NLR-mediated cytokine secretion via the NF-κB pathway. With the help of Shu Luo from the Julien lab, I immunoprecipitated NOD1 in the presence of SspH2 and utilized liquid chromatography with tandem mass spectrometry (LC-MS/MS) to uncover specific sites of ubiquitination on NOD1. I then semi-quantitatively analyzed the peptide fragment intensities of LC-MS/MS and identified lysines of statistical importance. Based off of these identified lysines, I mutated them to arginine residues, such that they could no longer be ubiquitinated. These NOD1 variants retained their interaction with SspH2 and showed similar basal activity compared to wildtype NOD1 through analysis by co-IP. Interestingly by utilizing IL-8 ELISAs, I identified 4 key lysine residues in NOD1 that are specifically required for enhanced cytokine secretion in the presence of SspH2. Here, I provide evidence for post-translational modification of NOD1 by ubiquitin, and uncover a unique mechanism of targeted ubiquitination to enhance the activation

of an archetypal NLR. To my knowledge this is the first demonstration that NLRs are specifically ubiquitinated by bacterial effectors.

Preface

This thesis is composed of original work by Cole Delyea. Throughout, it contains content co-authored by collaborators.

Dedication

I'd like to dedicate this thesis to my grandmother, Jary Wagner. Her unwavering support,

guidance, emphasis on education, and love is a treasure beyond value.

Acknowledgements

I would first like to thank my supervisor, Dr. Amit Bhavsar for giving me the opportunity to pursue graduate studies on his lab. Thank you for your mentorship and support during all of the long days, endless weeks, and pandemic that has occurred through the course of my thesis. I value all of the times that I have been able to pop my head into your office to get your immediate input on experiments as they are happening to allow me to effectively guide decisions in the moment. I appreciate all the opportunities to learn and implement new techniques and travel to present science while being a part of your lab. You have been a role model for what it means to exhibit perseverance in the face of hardship and continue to work steadfastly towards goals. Your balanced perspective has helped me to hone my skills as an independent and critically thinking scientist. I hope that your first graduating student is an omen of many more successful students to come.

I would also like to thank the past and present members of the Bhavsar lab for their support and friendship, without whom coming in to the lab would have been a bleak experience. Asna Latif, Ivan Domingo, Ghazal Babolmorad, Bradley Dubrule, and Ashley Wagner. An additional thank you to all the Bhavsar Lab undergraduate students, it was a treat to teach and learn beside you

I would like to thank the MMI office staff, especially Tabitha Nguyen and Debbie Doudiet. Alongside all of the MMI students, and staff. Throughout my graduate studies I have had the pleasure to be surrounded by inspiring intellects and big-hearted individuals. Thank you to the MMI students for being a group of amazing, resilient, and supportive group of friends that all work towards the collective success of everyone involved. If I can be of any help in the future, please reach out.

Table of Contents

List of Tables

List of Figures

Appendix

List of abbreviations and notations

CARD	Caspase activation and recruitment domain
Co-IP	co-immunoprecipitation
DAMP	Damage associated molecular pattern
ELISA	enzyme-linked immunosorbent assay
ER	Endoplasmic reticulum
HECT	homologous to E6-associated protein C-terminus
iE-DAP	gamma-D-glutamyl-*meso*-diaminopimelic acid
IKK	I-kappa-B kinase
IL-1β	Interleukin 1 beta
IL-8	Interleukin 8
IP	immunoprecipitation
LC-MS/MS	liquid chromatography mass spectrometry
LPS	Lipopolysaccharide
LRR	Leucine rich repeat
MAMP	Microbial-associated molecular pattern
NEL	Novel E3 ubiquitin ligase
NF-κB	Nuclear factor kappa B
NLR	NOD-like receptor
NLRP3	NLR family pyrin domain containing 3
NOD1	Nucleotide-binding oligomerization domain containing protein 1
NOD2	Nucleotide-binding oligomerization domain containing protein 2
PKN1	Serine/Threonine-protein kinase N1
PRR	Pattern recognition receptors
RING	Really interesting new gene
RIP2	Receptor-interacting serine/threonine-protein kinase 2
S. Typhimurium	*Salmonella enterica* serovar Typhimurium
SPI-1	*Salmonella* pathogenicity island-1
SPI-2	*Salmonella* pathogenicity island-2

SspH1	*Salmonella* secreted protein H1
SspH2	*Salmonella* secreted protein H2
T3SS	Type 3 secretion system
Tri-DAP	tripeptide diaminopimelate
YopM	*Yersinia* outer protein M

CHAPTER 1 – INTRODUCTION

1.1 *Salmonella* Typhimurium

1.1.1 *Salmonella* Typhimurium Overview

Salmonella enterica is a Gram-negative, rod-shaped, primarily flagellated, facultative anaerobic

bacterial species that contains over 2600 different serovars (1, 2). This bacterium is deposited in

the environment due to contaminated fecal matter from humans and animals (1, 3). *S. enterica* is

primarily differentiated between typhoidal (e.g., *S. enterica* serovar Typhi), and non-typhoidal

Salmonella (e.g., *S. enterica* serovar Typhimurium) (1). Typhoidal *Salmonella* serovars cause

enteric fever, which is an invasive, life-threatening systemic disease that is endemic in the

developing world as a result of lack of sanitation (2, 4). Non-typhoidal *Salmonella* causes

diarrhoeal disease, and enterocolitis worldwide, and annually result in an estimated 1.3 billion

infections, 3 million deaths, and 33 million healthy life years being lost (5, 6). Non-typhoidal

Salmonella is spread by fecal contamination of produce, animal product, and can be a result of

person to person contact and from contact with pets (2). To experience enterocolitis that results

in diarrhoea, >50,000 bacteria need to be consumed, and symptoms typically occur 6-72 hours

after consumption. This infection will typically resolve in 5-7 days without the need for

treatment in otherwise healthy individuals. Furthermore, Non-typhoidal *Salmonella* serotypes

can persist in the gut for 6 weeks – 3 months, allowing for shedding during this time (4, 6).

After being ingested, *S. enterica* serovar Typhimurium (*S.* Typhimurium) enters the

gastrointestinal tract and accesses the epithelial layer of the terminal ileum by utilizing its

flagella (7). *Salmonella* must compete with resident commensal intestinal microbiota. To

compete with commensal bacteria, *S.* typhimurium uses virulence factors which induce intestinal

inflammation to facilitate a competitive advantage over the gut commensals (8). Furthermore, *S.*

Typhimurium elicit significantly higher levels of neutrophil chemoattractant IL-8 from the cells that they infect to aid in their pathogenesis (9). Neutrophil recruitment leads to increased inflammation in epithelial cells, allowing *S.* typhimurium to sequester key nutrients away from the host, and promote transmission through diarrhoea (7, 10).

Many adhesins and fimbriae are necessary to mediate attachment of *S.* typhimurium to epithelial cells in the gut (11). Subsequent invasion of intestinal epithelial cells can be mediated in many different fashions. For example, this can be accomplished through M cells in the Follicle-associated epithelium covering Peyer's Patches, which are a critical entry site for antigens and pathogens from the lumen to the lamina propria (12). Invasion can also occur by disrupting tight junctions to invade through paracellular pathways, or by utilizing cells that intercalate between epithelial cells, like CX3CR1[+] macrophages/Dendritic cells (13-16). *Salmonella* can also be internalized by non-phagocytic enterocytes by using its Type III Secretion System (T3SS) encoded on *Salmonella* Pathogenicity Island-1 (SPI-1) that translocates effector proteins into the cytosol of the epithelial cell. This induces actin rearrangement, membrane ruffling, and non-phagocytic uptake of the bacteria into host cells (17-19). Once *Salmonella* have been phagocytosed (either as a result of crossing the Peyer's Patches, and being uptaken by macrophages, or through induced phagocytosis of epithelial cells), it begins to express a 2nd T3SS via its *Salmonella* pathogenicity island-2 (SPI-2), which allows *Salmonella* to begin replicating (8).

1.1.2 Type III Secretion System structural overview

To facilitate bacterial survival in host organisms, many gram-negative bacteria such as *Salmonella enterica* serovar *typhimurium, Shigella flexneri, Enteropathogenic/ enterohemorrhagic E. coli* (EPEC/EHEC)*, Yersinia* spp., and *Pseudomonas aeruginosa* use the

remarkably conserved type III secretion system (T3SS). This structure is used to targets animals and plants, and is found to be essential for bacterial pathogenicity. The T3SS has a syringe-like appearance with a wide base embedded into the membrane of bacteria and a thin extracellular membrane-spanning needle, capped by a tip complex that senses host cells that protrudes into the extracellular space. The export apparatus is where the bacterial proteins gather for injection, and the ATPase complex recruits ATP to power the structure (20, 21) (Fig. 2). This complex nanomolecular machine is over 3.5 MDa, and consists of more than 20 uniquely named protein subunits (22). Phylogenetic analysis of the conserved proteins show that the T3SS was first used to transport extracellular components of the flagellum, before being co-opted by different bacteria to exploit niches which engage with eukaryotic cells (23).The Non-Flagellar-T3SS is also used by pathogenic bacteria to translocate effector proteins across three membrane layers: the bacterial inner membrane, the bacterial outer membrane, and the host membrane, to allow bacterial proteins to easily gain access to, and interact with, host cells (23).

The proteins that make up this structure, and the way it behaves and assembles are detailed in great length elsewhere (22, 24-26).
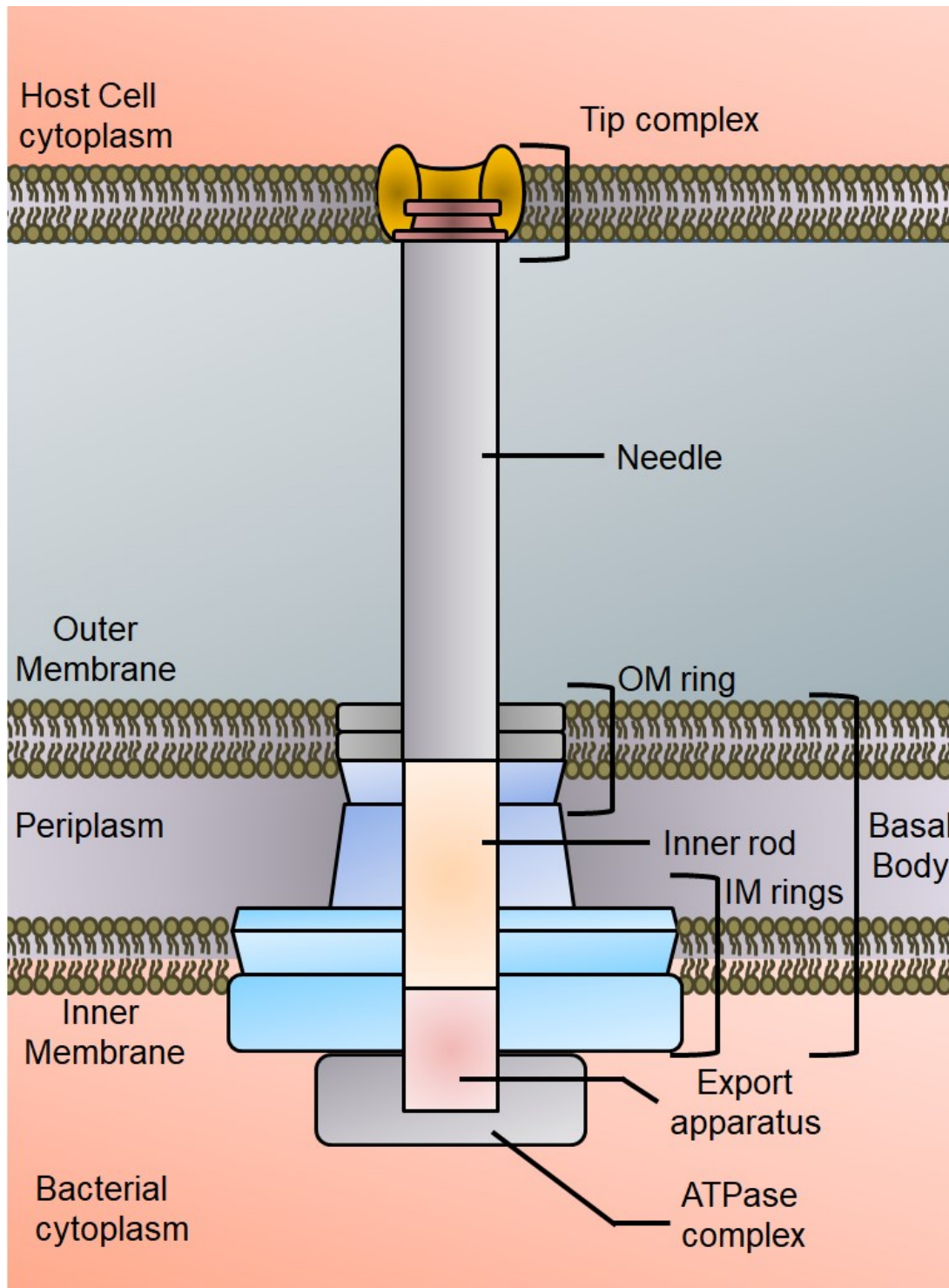
Figure 1.1. Summary of the non-flagellar type III secretion system structure.

OM, outer membrane; IM, inner membrane. Adapted from (22, 24-26).

1.1.3 *Salmonella* pathogenicity island 1

S. Typhimurium has multiple different *Salmonella* pathogenicity islands (SPIs), which are clusters of virulence associated genes that are responsible for encoding many virulence genes that can contribute to host specificity (27). These are thought to have been transferred to *Salmonella* spp. through horizontal gene transfer due to the different GC content from the rest of the bacterial genome (28).

To mediate the transfer of effector proteins into the host cell, *S.* typhimurium utilizes SPI-1; a 40kb locus that encodes a T3SS important for initial phagocytosis (27, 29, 30). SPI-1 proteins transferred into host cells are required for the invasion of epithelial cells and macrophages, alongside inducing macrophage apoptosis (31). *Salmonella* bacteria containing mutations in some of these regions show reduced ability to infect mice through oral administration. However, mutations in SPI-I do not have on effect on mice infected intraperitonally (32).

SptP, SopE, and SopE2 comprise a subset of proteins that are used to modify the signaling transduction pathway inside host cells. This allows for cytoskeletal rearrangement leading to non-phagocytic host cell (epithelial cell) invasion. This is carried out by interfering with small GTPases, Cdc42, Rac-1 and Rho, to mediate the formation of the cytoskeleton and F-actin filaments. SopE and SopE2 act as GTP exchange factors, activating Cdc42 to cause the formation of actin filaments at the site of protein translocation (33). To ensure host cell survival after bacterial invasion, which allows for *S.* typhimurium replication, SptP functions as a GTPase activating factor, in opposition to SopE/E2, inactivating Cdc42 and Rac-1, leading to stoppage of actin polymerization and membrane ruffling (34). Macrophage apoptosis is mediated by SipB induction of caspase-1 and caspase-2. This also causes the release of pro-inflammatory IL-8, causing other immune cells to congregate (35, 36). SopA, SopB, and SopD are related to the

induction of diarrheal symptoms of *Salmonella* infections. SopB is an inositol phosphate phosphatase, resulting in the activation of chloride channels in the membrane of targeted epithelial cell in the intestinal lumen (37). SopA and SopD are not as well understood, but both contribute to diarrhea in a bovine model of *Salmonella* infection (38). Furthermore, SspH1, a bacterial E3 ligase which contributes to virulence in calves, has been shown to be translocated by SPI-1 (39).

1.1.4 Salmonella pathogenicity island 2

SPI-2 is a 40kb locus that encodes a second T3SS that is involved in intracellular survival (27, 40). SPI-2 presence is considered an evolutionary step towards species specific colonization of warm-blooded animals (41). Mutation of genes inside this region caused attenuation of virulence in oral and intraperitoneal infections of mice, indicating that it is used after initial epithelial infection (40). Mutation of SPI-2 genes also attenuates infection in porcine models (42).

To mediate systemic infections, this locus is required for replication inside of *Salmonella* containing vesicles (SCVs) in macrophages (31, 38). To allow proliferation of *Salmonella* inside of SCVs, SPI-2 proteins prevent colocalization of phagocyte oxidase (43) and nitric oxide synthetase (44). As a result of this activity, intracellular *Salmonella* are protected against antimicrobial activity of peroxynitrate, formed by the combination of reactive oxygen and nitrogen intermediates (38). SifA, an effector protein not found in SPI-2 itself, but translocated by SPI-2 encoded T3SS, is essential in maintaining the integrity of SCV phagosome membranes (38). SpiC is translocated by the SPI-2 T3SS to interfere with cellular trafficking (45). Furthermore, SspH1 and SspH2, bacterial E3 ubiquitin ligases that contribute to virulence in calves, have been shown to be translocated inside host cells only once bacteria have successfully invaded the host cell (39).

SPI-2 also encodes genes responsible for tetrathione reductase expression (ttrBCA and ttrRS) (46). During anaerobic respiration, tetrathionate utilization as an electron acceptor is a specific trait used for the identification and enrichment of *Salmonella* spp. in clinical specimens (38).

This information is covered in more detail by in-depth reviews by Marcus *et. al.* and Schmidt *et. al.* (30, 38).

1.1.5 SspH2

Salmonella secreted protein H2 (SspH2) is a commonly found protein during *S. typhimurium* infection (39, 47-49). SspH2 was first discovered by looking at protein homology to sspH1 in 1999 by Miao *et. al* (39). SspH2 are present in human cells infected with *Salmonella* species, and are also found in calves, where it contributes to virulence alongside SspH1 (39). The SsrAB virulon controls expression of SPI-2, which encodes the SPI-2 T3SS, enabling injection of SspH2 (50, 51).

SspH2 is an 87 kDa protein that has 69% homology to SspH1, 40% sequence homology to IpaH4.5 (found in *Shigella* spp), and 33% homology to YopM (found in *Yersinia pestis*) (39). These proteins (except YopM) all share a similar structure. They have 2 major domains: an amino terminal leucine rich repeat (LRR) domain, and a carboxy terminal active domain (52) (Fig. 1.2). The LRR domain of SspH2, which is similar to YopM, (residues 171-481) consists of 12 repeats of the LRR motif (LxxLPxxLxxLx$_5$VxLxxNPL) that are capped at both termini by α-helices (52). To allow SspH2 to be translocated into the host cell, it requires 143 amino acids at the N terminus. These amino acids are also correlated to a conserved sequence set found across 7 proteins on SPI-2 (53). The C terminus of the LRR domain serves as a connecting loop to the NEL domain, which starts at 492 and is helical with unique folding (52). Cys580 in the NEL

7

region is the residue responsible for the catalytic activity of SspH2 (52). In an inactive state, the amino terminus LRR shields the active site in a closed conformation. Upon activation, SspH2 dimerizes in a way similar to IpaH9.8 to un-inhibit the active site, allowing substrate mediated activity (54).

Upon injection into host cells, SspH2 is localized to the plasma membrane (52). This function is mediated by the Cys9 residue which is stably palmitoylated (55). This brings SspH2 in close proximity to many host proteins like the immune receptor NOD1. SspH2 interacts with both NOD1 and SGT1 to increase SGT1-dependent NOD1 activity (56).

It is known that SspH2 mediates ubiquitination in host cells (52, 56). It has also been shown that SspH2 selectively binds the E2 enzyme, UbcH5. This protein complex is found to bind to ubiquitin better than UbcH5 alone (57). Upon closer investigation of this phenomenon, it was discovered that SspH2 binds regions of UbcH5 previously not thought to be important for E3 ligase binding to mediate poly-ubiquitination directly to UbcH5 *in vitro* (57).

There is also evidence that SspH2 interacts with mammalian actin cross-linking protein, filamin through the conserved N terminal amino acids 1-61 and interacts with profilin through the carboxy terminal end (58). Through this interaction, it is thought that SspH2 may play a role in cross-linking actin causing cell morphology changes. This is supported by observing inhibited actin formation in the presence of SspH2 *in vitro* (58).

Full length SspH2 can also be used to inhibit effective host response to bacterial infection. Along with many other injected *Salmonella* proteins, SspH2 can inhibit T cell activation via disturbing normal dendritic cell priming (59). Additionally, SspH2 has been shown to inhibit dendritic cell chemotaxis (60).

SspH2 has also been proposed to be used for therapeutic or vaccine related purposes. The amino terminal proteins can be used as a scaffold for fusion proteins. These fusion proteins can be translocated into cells and reduce bacterial infection. An example of this is shown with SspH2-EscI fusion protein (61). When SspH2 is fused to EscI and used for immunization, SspH2-EscI immunized mice were able to clear wild-type *Salmonella* infections after 6 days compared to other fusion protein vaccinations. This shows a possible role for attenuated bacteria being used as a vaccine candidate through caspase dependent immunity (62). Furthermore, the amino terminal end can also be used for translocating fusion constructs that can be used for priming CD4 and CD8 dependent immune responses for a more classical vaccine response (63).
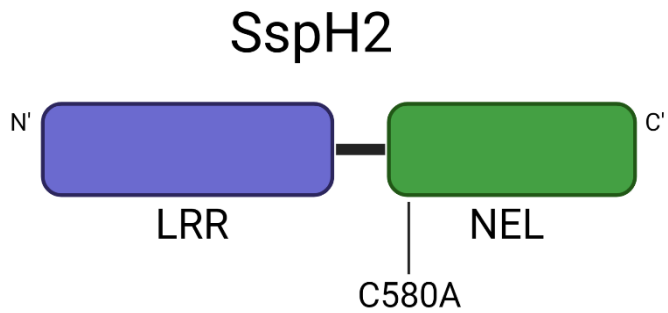
Figure 1.2. Domain structure of SspH2.

SspH2 is a 87 kDa protein that is composed of an amino-terminal LRR domain connected to a

carboxy-terminal NEL domain, which holds the catalytically active cysteine responsible for its

ubiquitin E3 ligase function. Created with Biorender.com

1.2 Ubiquitination

1.2.1 Ubiquitination Overview

Ubiquitin is a 76 amino acid, ~8.5 kDa protein, that is ubiquitously expressed in eukaryotic organisms (64, 65). Ubiquitin belongs to the ubiquitin-like (UBL) protein family, and shares structural and sequential homology with proteins like the Small Ubiquitin-like Modifier (SUMO)-1 (~11 kDa) (66, 67), Interferon stimulated gene 15 (ISG15) (~15kDa) (68), and Neural precursor cell expressed, developmentally down-regulated 9 (NEDD9) (~8kDa) (69). Ubiquitin-like proteins that share some similarities in structure and conjugation systems have also recently been identified in bacteria (70, 71).

Ubiquitination is a reversible way that eukaryotic organisms utilize to post-translationally modify host proteomes with the conserved protein, ubiquitin. Ubiquitination results in many different functions in the cell. It was first identified to serve as a trigger for 26S proteosome degradation, but has since been identified for other functions such as inducing signal transduction, and selective autophagy (64, 65, 72). Ubiquitination of substrate proteins is mediated by ubiquitin covalently binding, via the C-terminal glycine residue, to the ε-amino group of a substrate lysine (73, 74). This process starts with an ATP-dependent, ubiquitin-activating enzyme (E1) that first recruits ubiquitin. Ubiquitin is then transferred to a ubiquitin-conjugating enzyme (E2) via a thioester linkage. A ubiquitin ligase (E3) subsequently binds substrate and transfers the ubiquitin from E2 to the final substrate which varies in mechanism of action depending on the type of E3 (Fig. 1.3) (65, 75-78).

Encoded in the human genome, there are two E1 enzymes, 37 E2 enzymes and >600 E3 ligases that account for the multitude of protein modifications (79, 80). There are two main groups of E3 enzymes that function endogenously in slightly different fashions, namely Really Interesting

New Gene (RING) and homologous to E6-associated protein C-terminus (HECT) (79). RING E3s function by acting as scaffolds, bringing E2s and the targeted substrates into proximity and mediating the direct exchange of ubiquitin between the two (81). HECT E3s function by binding both the E2 and substrate, but by using their conserved cysteine to act as an intermediary for ubiquitin prior to substrate ubiquitination (81).

The type of ubiquitin chain signal present on substrate changes the type of biological effect that it has. K48 and heterotypic K11/K48 chains serve as a trigger for substrates to be degraded by the 26S proteosome. Alternatively, mono-ubiquitination or linear ubiquitination with K6, K27, K33, or K63 are typically involved in selective autophagy, DNA damage repair, and innate immunity autophagy (Fig 1.4A) (72). Targeted substrate proteins can be modified by mono-ubiquitination, or by the addition of polymeric ubiquitin chains. Polymeric chains can be made through multiple combinations of homo- or heterotypic branching or linear internal lysine linkages (K6, K11, K29, K33, K48, K63) or N-terminal methionine linkages (Fig. 1.4B) (72, 82-85).

The type of ubiquitin chain present on substrates can be effectively interpreted by proteins containing ubiquitin-binding domains, which identify terminal chain-specific residues at linker regions connecting ubiquitin molecules (86-89). De-ubiquitinating enzymes act to remove ubiquitinating enzymes on substrate proteins (90, 91).
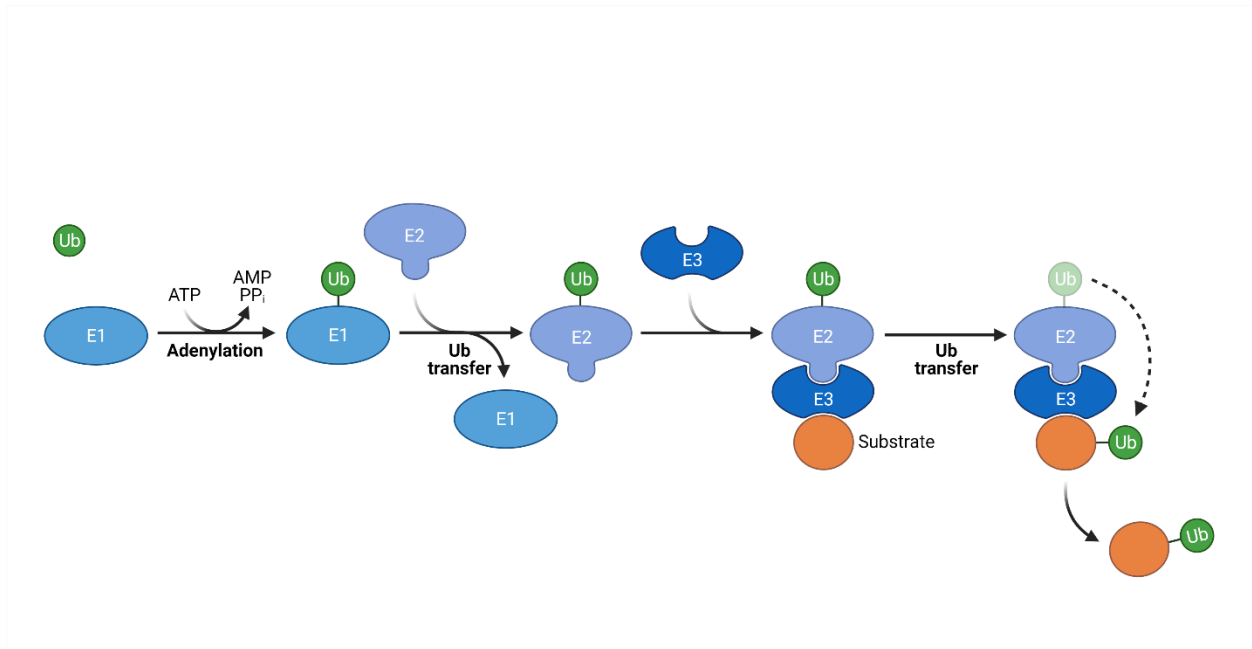
Figure 1.3. General Protein Ubiquitination Pathway.

Ubiquitin chain formation proceeds through multiple steps, during which ubiquitin attaches to an E1 enzyme through adenylation. This ubiquitin gets transferred from the E1 enzyme to an E2 enzyme. The E3 enzyme then binds to both the E2 enzyme and substrate and facilitates transfer of ubiquitin to the substrate. Created with Biorender.com.
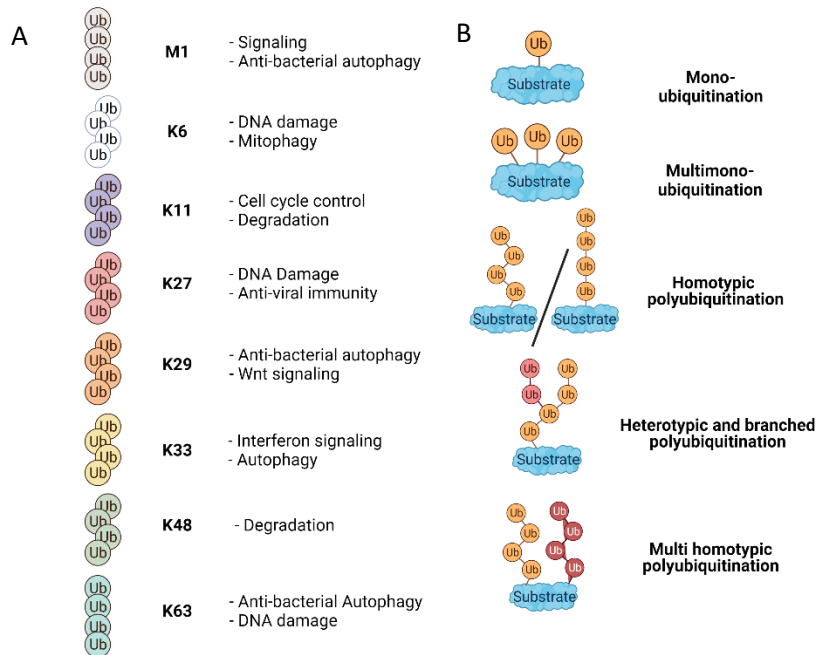
Figure 1.4. Functions of different types of ubiquitination.

A) The repertoire of ubiquitin chains, linked through methionine (M) 1 (linear/head-to-tail) or through the internal lysine (K) residues 6, 11, 27, 29, 33, 48 and 63 with a short description of their cellular function. **B)** Overview of several modes of substrate ubiquitination including different forms of mono- and polyubiquitination. Adapted from (80). Created with Biorender.com.

1.2.2 Pathogenic ubiquitination

Ubiquitin ligase mimicry is a mechanism used by pathogens to enable effective utilization of host resources. In plants, *Pseudomonas syringae*, which is a bacterial pathogen of *Arabidopsis thaliana* cells and tomatoes, utilizes AvrPtoB effector that has a RING domain on its carboxy-terminal end, to mediate its virulence (92). Viruses can also alter host post-translational pathways by encoding their own de-ubiquitination enzymes, or E3 ligases (93, 94).

Pathogenic bacteria like *Legionella*, *Shigella,* and *Salmonella* can also subvert ubiquitination in mammalian cells. They can do this through utilizing HECT-like, RING/U-box-like and Novel E3 ligase (NEL) effectors (92). There are at least 15 NELs, which function similarly to HECT E3 ligases. Like HECT E3 ligases, NELs utilize a catalytic cysteine residue for ubiquitin transfer (52, 95-98). NEL proteins primarily share a conserved structure pattern composed of an amino-terminal LRR domain and an entirely helical carboxy-terminal NEL catalytic domain, which is distinct from other E3s (99).

NELs can perform many different functions inside of the host cell. In *Shigella* spp. one of the most common effector proteins upon contact with human cells are the IpaH proteins. As a proof-of-concept experiment in yeast, IpaH9.8 has been shown to possess E3 ubiquitin ligase activity used to initiate proteasomal degradation of MAPKK Ste7 (100). IpaH9.8 functions to remove granule binding proteins from *Shigella flexneri* to help the bacteria evade the host immune response (101), and to inhibit NF-κB signaling by degrading NEMO (92). Other IpaH proteins which include IpaH1.4, 2.5, and 4.5 are also known to inhibit NF-κB activity (92, 101).

Other NEL proteins have also been identified that do not share the exact same domain structure. *Legionella* NELs, such as SidC and SdcA, have an amino-terminal ubiquitin ligase (SNL) domain, and contain a phosphatidylinositol-4 phosphate binding domain, and function to alter

protein trafficking in the host cell (101). This is accomplished by SidA through mono-ubiquitination of Rab which induces the maturation of the host *Legionella*-containing vacuole (101). *Yersinia* bacteria also inject a protein that contains NEL-like function. YopM is peculiar, in that it does not have a designated catalytic cysteine. It has been shown to function by inhibiting the inflammasome formation by ubiquitinating NLRP3, marking it for proteasomal degradation (102).

Salmonella contains 3 different NELs, SspH1, SspH2, and SlrP. SspH1 is an E3 ligase, which utilizes the mammalian protein PKN1 as a substrate, and translocates to the nucleus, preventing NF-κB activity (100). SlrP functions to induce host cell death by ubiquitinating thioredoxin (102).

1.3 NLR signaling

1.3.1 NLR Overview

The recognition of microbial- or damage-associated molecular patterns (MAMPs and DAMPs, respectively) on the surface, or in the cytosolic compartment of host cells is critical for host immunity. Pattern recognition receptors (PRRs) play an important part in recognizing these molecular patterns, acting as first line defenders against infectious agents. These include Toll-like receptors (TLRs), NOD-like receptors (NLRs), RIG-like receptors (RLRs), and AIM2-like receptors (ALRs). Nod-like receptors (NLRs) are associated with sensing MAMPs alongside DAMPs, and ER stress in mammalian cells (103). There are 22 identified members of the NLR family in humans (104, 105). NLRs are characterized by their tripartite structure consisting of: i) a variable amino terminal domain, which is critical for interactions with downstream effector proteins, ii) a central nucleotide binding domain (NBD) that facilitates NLR oligomerization, and iii) a carboxy terminal leucine-rich repeat (LRR) domain that senses bacterial structures. NOD1

and NOD2 are the founding members of the NLRs, first described by Inohara *et al.* in 1999

(106), and have since been grouped as NLRCs as they contain a characteristic amino terminal

caspase activation and recruitment domain (CARD). NOD1 and NOD2 are commonly found in

the cytosol of host cells (106). To mediate their activation, these receptors localize to actin-rich

regions in the plasma membrane (107, 108). NLRP proteins contain a Pyrin domain in the

amino-terminal region of the protein. NLRP3 activation, used as a mechanism for antimicrobial

activity, induces interaction with caspase-1, which facilitates induction of the inflammasome,

leading to inflammatory cell death (109).

1.3.2 NOD1

NOD1 is a canonical NLR, characterized by its nucleotide-binding and oligomerization domain

(NOD) (106). This 108 kDa protein is a tri-partite protein encoded by the gene *card4* in humans,

and is similar in function to nematode CED-4/Apaf-1 cell death family proteins (110). Each of

the domains play important roles in how NOD1 is able to activate and signal through NF-κB. An

overview of general NOD1 structure, and activation pathways is shown below for convenience

(Fig. 1.5).

The CARD region is the distinct region that places NOD1 in the NLRC family. NOD1 CARD

consists of an arrangement of 6 alpha-helices closely packed around a hydrophobic core (111).

NOD1 CARD is a dimer at pH 6.0 and a monomer at pH 7.0 (112). This suggests that upon

activation, NOD1 dimerizes to induce pro-inflammatory cytokine function. When crystallized,

the CARD region forms a dimer by swapping of the 6th helices between helices 1 and 5 at the

carboxy termini (113). Upon closer inspection, this homodimerization is stabilized by the

formation of an interchain disulfide bond between Cys39 residues. Furthermore, R35 & D95

have been found to be necessary for homodimerization (112). It has also been found that amino

acids 107-138 are important for NOD1 CARD protein stability (111). NOD1 CARD is also responsible for the homophilic domain interaction with RIP2 (106, 114). In the mere presence of both NOD1 and RIP2, it is known that both proteins spontaneously interact (114). NOD1 E53, D54, and E56 (on its exposed major acidic patch) are part of the interaction surface while R69 mediates protein stabilization between the RIP2 residues R444, R483, and R488 (111). In further findings, NOD1 L40A, V41A, D42K, triple mutant, and L40A-D42K & D42K-L44A double mutants have impaired ability to bind RIP2. These residues form a cluster adjacent to the acidic residues and likely forms a peripheral part of the interaction surface (111).

NOD1 NBD is an internal ATP/GTPase domain which includes a Walker A box, P-loop and Walker B box, and Mg^{2+} binding site that helps to facilitate oligomerization and activation (106, 114). To maintain function, NOD1 must maintain ATPase activity by keeping D248 and K208 conserved; mutations at these points renders NOD1 non-functional (115). Furthermore, the Walker A and B box, Sensor 1 and GxP motif are critical for activation of both NOD1 and NOD2 (108).

The NOD1 LRR domain is made up of a series of 10 repeating Leucine rich repeats, folded into a right-handed, curved solenoid structure which contain a putative alpha helix and beta sheet, characteristic of LRRs as a whole (106, 116). The LRR domain is thought to be present in a closed conformation when inactive and in its absence, NOD1 induces increased pro-inflammatory cytokines (106, 114). In particular, it has also been shown that NOD1 648-668 deletions resulted in increased basal activity (115). NOD1 requires its LRR domain to interact with its ligand, tri-DAP and iE-DAP (117). It has also been shown that NOD1 interacts with HSP70/90, keeping it in its closed conformation, and it is thought that this interaction occurs at the LRR domain, similar to other related LRR structures (118). Therefore, distal LRRs of NOD1

are essential for suppression of the constitutive activation of these proteins as well as for recognition of bacterial components (115).

One of the first things noted about NOD1 is that overexpression causes the activation of NF-κB (106). It was initially thought that NOD1 can recognize lipopolysaccharide (LPS) through its LRR domain. However, this LPS activation was determined to be because of contamination of the samples (114). As it was later revealed, NOD1 is critical in epithelial sensing of intracellular bacteria through peptidoglycan sensing of GlcNAc-MurNAc (GM)-tripeptide diaminopimelate-containing N-acteylglucosamine-N-acetylmuramic acid tripeptide motif (Tri-DAP) (119). NOD1 also recognizes γ-D-glutamyl-*meso*-diaminopimelic acid (iE-DAP) in bacterial peptidoglycan (120). NOD1 is particularly robust in its ability to sense these peptides. For example, NOD1 can detect iE-DAP even after it was subjected to harsh acidic treatment, harsh basic treatment, and boiling (121). Additionally, to induce activation in the cell, peptidoglycan recognizing protein-L might play a role in degrading bacterial cell wall components and potentiates the detection of peptides by NOD1 (122). Changing meso-DAP to L-ornithine makes it so that NOD1 is unable to detect PGN (122). The recognition of TriDAP is done through interactions with NOD1 LRR domain in the centre of the concave surface (LRR 5,6,8) (116). This interaction stimulates protein oligomerization (123). Furthermore, this oligomerization elevates NOD1 binding to RIP2 and increases RIP2 phosphorylation (117).

NOD1 activation also results in the binding of ATP, which allows direct binding to pro-apoptotic protein BID, which results in increased NOD1 activity (123). It has also been shown that ER stress induces NOD1 signaling independent of peptidoglycan through stimulation with thapsigargin (124). However, upon closer investigation it was posited that the ER stress causes cellular perturbations that affect intracellular Ca^{2+}. This reaction can trigger internalization of

peptidoglycan trace contaminants found in culture serum, thereby stimulating pro-inflammatory signaling. This is what is likely being seen when thapsigargin induces NOD1 signaling (125).

NOD1 is present in multiple tissues which include: epithelial cells, heart, placenta, lung, skeletal muscle, liver, spleen, kidney, thymus, and ovary (106). It has also been identified that NOD1 proteins are found in eosinophils and neutrophils (126). Through closer examination of activated NOD1, it has been determined that NOD1 localizes to actin rich regions of the plasma membrane (107, 108). Furthermore, NOD1 recruits the autophagy protein ATG16L1 to the plasma membrane at sites of bacterial entry (107). This interaction allows NOD1 to induce autophagy of intracellular bacteria (107).

Interestingly, it has been documented that NOD1 stimulatory molecules can also be detected from bacteria growing outside of host cells. Thus, it is not strictly necessary for bacteria to infect cells to be able to activate NOD1 signaling (121). However, inside the cell NOD1 interacts with many different host proteins. Alongside interacting with RIP2 to mediate NF-κB activation, it also interacts with Caspase 1, 2, 4, 8, and 9 and CLARP (106). When interacting with Caspase 9, NOD1 enhances activity, and mediates this interaction between CARD regions (106). Furthermore, NOD1 can induce pro-apoptotic activity independent of NF-κB (114).

When activated, NOD1 canonically induces NF-κB signaling through its association with RIP2. This activation of NOD1 and RIP2 is mediated by RelA (p65) (114). Activation of tri-DAP induces BID (a BCL2 family protein) phosphorylation. BID interacts with NOD1 on its NBD alongside interacting with IκB kinase (IKK) complex, mediating the interaction with NOD1 (127). Transforming growth factor (TGF)-beta-activated kinase 1 (TAK1) is the kinase essential for NOD1-induced signaling, and causes the phosphorylation of IκBα of the IKK complex (128). Centaurin beta (CENTB1) is an ADP-ribosylation factor that also interacts with NOD1.

CENTB1 expression is induced by TNF-a, IL-1β, iE-DAP, and MDP and found in the cytoplasm. CENT1B inhibits NOD1 dependent NF-κB activation (129). ATG16L1 is also known to inhibit NOD1 activation by interfering with poly-ubiquitination of RIP2.

There is also some evidence that ubiquitin is able to interact with NOD1. Using nuclear magnetitic resonance and *in vitro* experiments, it has been found that lysine 63, and linear Met-1-linked ubiquitin chains binds to NOD1 CARD on Tyr88 and Glu84 residues (130, 131). This interaction interrupts the ability of NOD1 to interact with RIP2, inhibiting activation (131). Another study looked at the crystal structure of NOD1 CARD, and found that ubiquitin interacts with NOD1 on many interfaces. Linear ubiquitin chains interact with NOD1 at Tyr88:Ile44 and Cys59:Phe4 (CARD:Ub) (132). However, it remains to be seen whether NOD1 is actually ubiquitinated on its lysine residues.

Furthermore, NOD1 function is not limited to innate immune activity. It has been found that NOD1 triggers, and synergizes with TLRs, and primes Th1, Th2, and Th17 cells in vivo (133). While alone, NOD1 agonist primes antigen specific T and B cell immunity with a Th2 polarization profile, functioning in adaptive immunity (133).
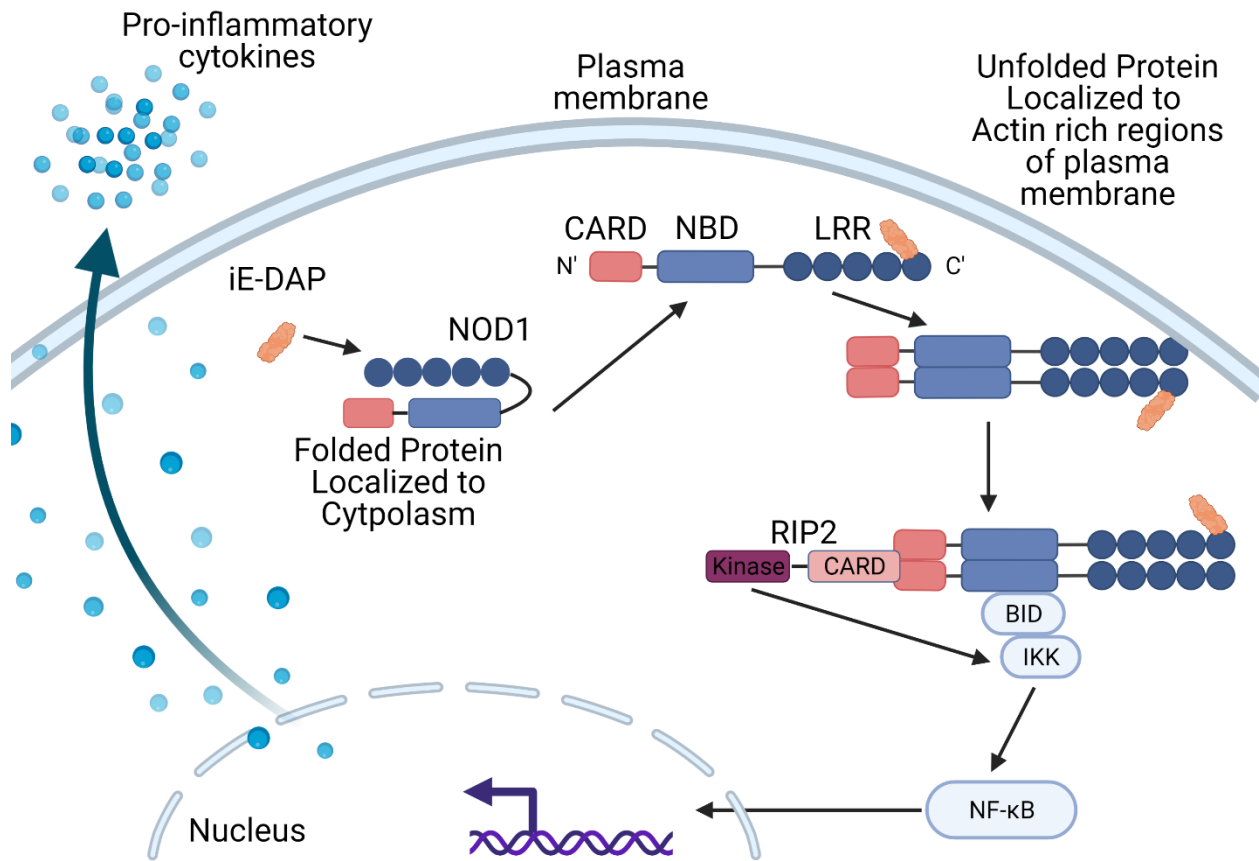
Figure 1.5. General activation pathway of NOD1.

NOD1 is found in an auto-inhibited form, and upon activation with iE-DAP it dimerizes and

localizes to actin-rich regions of the plasma membrane. This allows for association with RIP2,

which facilitates the NF-κB signaling cascade resulting in the secretion of pro-inflammatory

cytokines like IL-8. Image created with Biorender.com.

1.3.3 NOD2

NOD2 is another canonical NLR protein in the NRLC family. NOD2 has 34% amino acid identity to NOD1, is encoded by the human *card15* gene, and is 110 kDa. NOD2 contains two amino terminal CARD domains, a central NBD and a carboxy terminal LRR that has 10 repeats in it to form a predicted alpha helix and beta sheet sequence (134). An overview of general NOD2 structure, and activation pathways is shown below for convenience (Fig. 1.6).

NOD2 can interact with many proteins inside the cell, like NLRP1, NLRP3, and NLRP12 through its CARD region (135). NOD2 also interacts with RIP2 by utilizing both of the CARD regions in a similar fashion to NOD1 (134-136). Specifically, E69, D70, and E71, amino acids found in the CARD1 domain of NOD2, mediate interaction with RIP2 (135). Upon investigation into which amino acids were essential for NOD2 function, mutations of residues Q31, E69, T91, A106, L145, P177 and R180 exhibited complete loss/ greatly reduced activity in response to MDP. Furthermore, F161 P177 and R180 are crucial for protein stability and expression. Whereas, A31, A106, and L145 are important in the ability to associate with RIP2. Finally, L145P mutation inhibited the ability of RIP2 to activate NF-κB in the presence or absence of MDP (115).

The NBD region of NOD2 is similar in nature to that of NOD1, containing an ATP/GTPase domain which includes a Walker A box, P-loop and Walker B box, and Mg^{2+} binding site which functions to facilitate oligomerization and activation. NOD2 also utilizes oligomerization at the NBD region to induce association with RIP2 (134). Furthermore, the Walker A and B box, Sensor 1, and GxP motif are critical for activation of NOD2 (108). NOD2 has 21 residues that are critical for active signaling. Of particular note, D379 in the Walker B box is required for Mg^{2+}-substrate and nucleotide hydrolysis, and R334W and R334Q act as hyper-active

mutants (115). Additionally, mutation of the extended Walker B box leads to auto-activation of NOD2, while mutating K305 prevents activation (108, 134).

The NOD2 LRR domain functions in multiple ways. Most notably, the NOD2 LRR is used in auto-inhibition of inactivated NOD2; when the LRR domain is absent NF-κB activity is enhanced (134). The specific amino acids responsible for this action are 664-854. This was determined by observing that deletions of this region resulted in increased basal activity indicating a regulatory region (115). NOD2 LRR domain also recognizes bacterial peptidoglycan muramyl dipeptide (MDP) (116). NOD2 LRR 855-1040 are required for MDP sensing (115). This MDP recognition occurs in the middle of the LRR horseshoe fold, where R877, W932, and S933 are important, and R877 interacts with the 2'-N-acetyl group of MDP (137).

PGRP-L might play a role in degrading bacterial cell wall components, leading to activation of NOD2 (122). NOD2 senses MDP, that is present in both Gram-negative and Gram-positive bacteria (122, 138). Like NOD1, NOD2 was falsely thought to recognize LPS through their LRR regions (116, 141). The interaction with MDP is direct and is pH dependent; pH 5.0-6.5 gives optimal binding (139). Activation with MDP results in NOD2 hydrolyzing ATP (136). As a result, NOD2 homo-oligomerization, NOD2 and RIP2 hetero-oligomerization, and MDP binding are enhanced by ATP binding (136). It was also determined that ATP is not required for binding of MDP, but is a result of it (139). It has also been shown that ER stress induces NOD2 signaling independent of peptidoglycan (124). However, like NOD1, it was concluded that ER stress that causes cellular perturbations affects intracellular Ca^{2+}, which can trigger internalization of trace contaminants of peptidoglycan found in culture serum (125).

For NOD2 to become effectively activated, membrane targeting in intestinal epithelial cells is required for activation by MDP (140). This causes the ubiquitination of NEMO (component of

24

NF-κB signaling complex) (141). GRIM-19 (a novel cell death-related gene) binds to NOD2 when NOD2 is in vesicles. Furthermore, GRIM-19 is required for NF-κB activation following stimulation with MDP (142). Additionally, HSP70 interacts with NOD2 and increases NOD2 response to cell wall fragments by increasing NOD2 half-life (143).

NOD2 is most abundant in monocytes, and also found in eosinophils, neutrophils and in epithelial crypts in the intestine (126, 134, 144). In murine neutrophils activation of NOD2 by MDP induces increased cytokine response mediated by RIP2 (145). In APC's and monocyte-derived DC's NOD2 activation with MDP induces autophagy. To appropriately activate autophagy, this requires the proteins: RIP2, PI3K, ATG5, ATG7, and ATG16L (146).

Within cells, NOD2 is found primarily in the cytosol (138). However, upon activation NOD2 localizes to actin-rich regions in the plasma membrane, and when identifying intracellular bacteria, activates ATG16L1 to induce autophagy (107). This interaction with the plasma membrane in epithelial cells is mediated through NOD2 LRR domain (140). Interestingly, NOD2 mutated protein found in Crohn's disease (L1007C) does not allow for localization to the plasma membrane, suggesting a reason for how NOD2 causes disease (107).

To modulate NF-κB activation, activation of MDP induces BID (a BCL2 family protein) phosphorylation. BID interacts with NOD2 on its NBD alongside interacting with IκB kinase (IKK) complex, mediating the interaction with NOD2 (127). CENT1B also inhibits NOD2 dependent NF-kB activation (129). Furthermore, TAK1 interacts with NOD2. The LRR domain of NOD2 regulates TAK1 activation to have an antagonistic effect on NF-κB activation (147). To subsequently regulate NF-κB, GRIM-19 acts downstream of NOD2 and is required for NF-κB activation. This is important to note because patients with IBD commonly have decreased levels of GRIM-19 in their inflamed mucosa (142).

Compared to NOD1, much more is known about ubiquitination of NOD2. When NOD2 senses

bacterial infections through MDP recognition, it stimulates K63-linked ubiquitination of RIP2

(148). Pellino3 is a key mediator of NOD2 signaling by acting as an E3 ligase for RIP2,

promoting its K63 linked ubiquitination and triggering downstream activation of NF-kB and

expression of pro-inflammatory proteins (148). NOD2 CARD Ile104 and Leu200 are important

in binding ubiquitin in a similar fashion to NOD1, blocking interaction with RIP2 (130, 131).

Ubiquitination sites have also been predicted at K436 and K445 (130). Furthermore, ATG16L1

functions in a similar fashion with NOD2 as NOD1, suppressing activation (130).

There are multiple proteins that induce degradation of NOD2 through ubiquitination. For

example, PARKIN mediates NOD2 K48-linked chain degradation (130). Tripartite motif-

containing 27 protein (TRIM27) regulates NOD2 through a direct interaction and ubiquitination

leading to degradation. The PRY-SPRY domain of TRIM27 interacts with NOD2 NBD, which

gets K48-linked ubiquitinated and sent for 26S proteasomal degradation (130). Meanwhile,

suppressor of cytokine signaling 3 (SOCS3) was found to be recruited upon conformational

change of NOD2 to enable ATP hydrolysis. This resulted in reduced affinity for Hsp90, whereby

SOCS3 ubiquitinated NOD2 to facilitate proteasomal degradation (130). Interestingly, TRIM22

has been identified as a positive regulator of NOD2 through polyubiquitination (130).

NOD2 helps to strengthen adaptive immune responses by functioning as an adjuvant to TLR

ligands in mouse neutrophils and APCs when activated by MDP (145, 149). NOD2 helps T cells

to create Th1 immunity by interacting with NIK (NF-κB inducing kinase) and c-Rel. However,

the interaction between NOD2 and c-Rel upregulates transcription of IL-2 (150). This interaction

of NOD2 and TLRs is also used to help increase type 1 cytokine production and recruitment of

CD4 and CD8 T cells in response to *Mycobacterium bovis* bacillus Calmette-Guerin. (151).

Furthermore, NOD2 negatively regulates TLR2 driven activation of NF-κB subunit c-Rel (152).

NOD2 stimulation also leads to MHC class II localization with microtubule-associated protein

1A/1B/light chain-3 (LC3) autophagy dependent upregulation of surface MHC class II and

generation of antigen-specific CD4 T cell responses. (146).
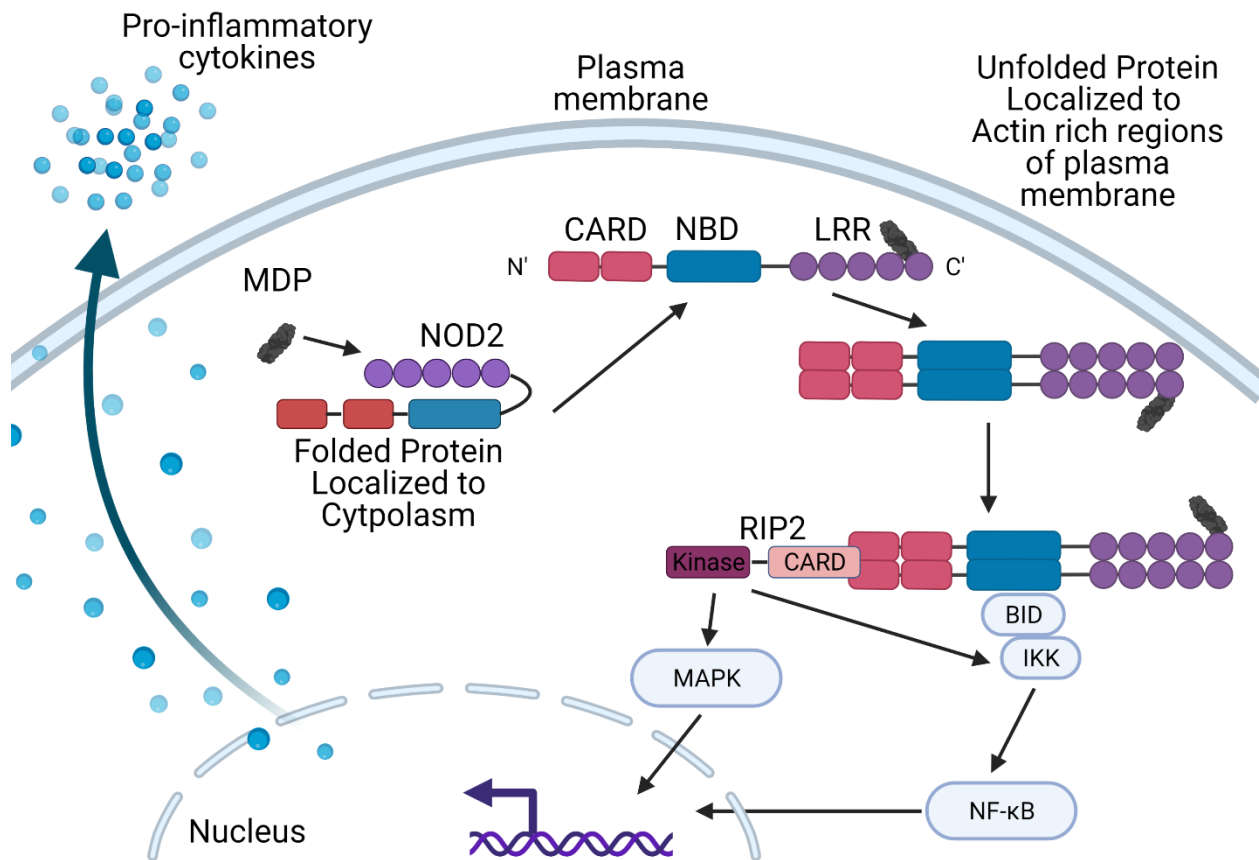
Figure 1.6. General activation pathway of NOD2.

NOD2 is found in an auto-inhibited form in the cellular cytosol, and upon activation with MDP it dimerizes and localizes to actin-rich regions of the plasma membrane. This allows for association with RIP2, which facilitates the NF-κB and MAPK signaling cascade resulting in the secretion of pro-inflammatory cytokines like IL-8. Image created with Biorender.com.

1.3.4 RIP2

RIP2 is a serine/threonine protein kinase. It is made up of a carboxy-terminal caspase activation and recruitment domain (CARD) which recognizes upstream signals through homomeric domain interactions, and an amino terminal kinase domain that can dimerize and phosphorylate downstream factors (153).

RIP2 interacts specifically with NOD1/NOD2 to mediate NF-κB signaling in mouse and human models and is required for MDP-mediated enhancement of immune responses (154, 155). Ubiquitinated RIP2 acts as a platform for TAK1 and IKK, which facilitate NF-κB and MAPK activation (148). Polyubiquitination of RIP2 at K63 and K209 in the RIP2 kinase domain, is required for activation and oligomerization upon NOD1 or NOD2 stimulation (128, 154). This oligomerization induces NF-κB activation by forming RIP2 CARD homodimers/-oligomers (114, 135). RIP2 ubiquitination mediates recruitment of TAK1. RIP2 is also phosphorylated at Ser 176 upon engagement with NOD2, through presumed autophosphorylation, and is essential for downstream TAK1 activation (156).

Activation of NEMO through K63 poly-ubiquitination on NEMO K285 was also found to occur through agonist dependent activation of NOD2. CYLD (de-ubiquitinating enzyme) can reverse this NEMO-dependent ubiquitination (141). Additionally, TRAF2/5 are required to interact with RIP2 for NOD1 mediated NF-κB activation (128). Cellular inhibitors of apoptosis proteins (cIAPs) cIAPs 1 and 2 are E3 ligases that are required for RIP2 K63 ubiquitination, which physically interact with RIP2 in its N terminal kinase region, facilitate NOD signaling (157).

XIAP also mediates signaling from NOD activation. XIAP interacts with RIP2 via XIAP's baculoviral IAP-repeat 2 (BIR2) domain mediating linkage to RIP2 C-terminal CARD domain to facilitate downstream NF-κB activation (158). Pellino3-induced ubiquitination of RIP2 may also

facilitate subsequent linear ubiquitination of RIP2 signaling complex by XIAP (148). Furthermore, LRRK2 is a positive regulator of RIP2, promoting inflammatory cytokine production. LRRK2 enhances RIP2 activity by promoting phosphorylation of RIP2 at Ser176 (159).

1.3.5 NLRP3

The NLRP3 (NALP3/cryopyrin) inflammasome and all of its components is an extensively studied topic, and is discussed in great detail by numerous reviews (160-165). Below is a summary of the major points relevant to my thesis. An overview of general NLRP3 structure, and activation pathways is shown below for convenience (Fig. 1.7).

The *Nlrp3* (CIAS1) gene encodes for NLRP3. This tri-partite protein includes an amino terminal pyrin domain, a central nucleotide-binding domain, and a carboxy-terminal LRR domain (166). The LRR domain contains 12 repeats (167). In the absence of activators, NLRP3 exists in an auto-inhibited state via the interaction of its NOD and LRR domains (168). Thereby, it is assumed that NLRP3 exists in a monomeric state prior to activation. When activated, by its ligands, NLRP3 domains dissociate with each other to allow interaction between NLRP3 and ASC (168). It has been observed that NLRP3 is constitutively active in the absence of its LRR domain, thus indicating its importance in NLRP3 activity (169).

NLRP3 is activated by many different sources, but has not been found to directly interact with any particular exogenous motifs (164). When NLRP3 senses danger signals, it oligomerizes to interact with the pyrin domain (PYD) of apoptosis-associated speck-like protein containing a caspase recruitment domain (ASC), an adaptor protein, through homophilic interactions (170). ASC then utilizes its CARD region to recruit the cysteine protease, pro-caspase-1 (170). This

causes the auto-catalysis and activation of caspase-1, which also triggers to the production of cytokine precursors, pro-IL-1β and pro-IL-18. These cytokine precursors get cleaved into their active forms by caspase-1 into IL-1β and IL-18, which in turn get secreted from the cell. This sequence of events under certain conditions leads to pyroptosis, a form of programmed inflammatory cell death (171-173).

NLRP3 is primed, and up-regulated by the activation of the TLR/NF-κB pathway through multiple mechanisms (174, 175). NLRP3 is activated by various actions from bacterial and viral PAMPs. It can also be activated by DAMPs and other cellular perturbation signals such as potassium influx, ATP recognition, lysosomal destabilization and rupture, pore-forming toxins, and detection of mitochondrial ROS. This initiates the assembly of multi-protein complexes containing NLRP3, ASC, and pro-capase-1 (176-178).

The mitotic serine/threonine kinase NEK7 is important for NLRP3 activation via direct interaction during interphase (167). In the LRR domain, the amino acids E800, D748, E743 are important and, Y916, E862, V705 are partially important for activity with NEK7. The NLRP3 NBD amino acids Q636, E637, and E683 are all also required together for activity with NEK7 (167). NLRP3 can also interact with NOD2 to process IL-1β in a CARD independent fashion (135). In macrophages, both NOD2 and NLRP3 play roles in MDP-induced IL-1β secretion (179).

NLRP3 is found at baseline levels in primarily in immune and inflammatory cells, whereby activation of the cells by inflammatory stimuli causes an increased production of NLRP3 (174, 180). Inside the cell it is found in the cytosol, where it fully assembles into the inflammasome complex in the cytoplasm (162). It is also found in the ER, and upon activation it has been observed to relocate to the Membrane-Associated ER Membranes (MAMs), and the Golgi (162).

IL-1β is a key pro-inflammatory cytokine that mediates inflammation in various tissues and cell types. It plays a role in sensing disturbances in cellular homeostasis (165). Activation of the inflammasome serves to reduce bacterial levels in *Vibrio cholerae* and *Streptococcus pneumoniae* infections in mouse models (181, 182). Effector proteins, translocated through the T3SS can also activate the NLRP3 inflammasome. For example, the effector protein, YopJ, from *Yersinia pestis* subspecies KIM is an acetyltransferase that induces apoptosis through the inactivation of MAPK and IκB kinases, activating the inflammasome (183, 184). NLRP3 activation can play a role in protecting the host against viral, parasitic and fungal pathogens. Through the roles of IL-1β and IL-18, Influenza A infections can be controlled by the NLRP3 inflammasome *in vivo* (185, 186). *Candida albicans* and *Leishmania* infections can also be controlled through the release of IL-1β stemming from NLRP3 inflammasome activation (187, 188).

NLRP3 activity also plays a role in maintaining homeostasis. It plays a regulatory role in the intestinal epithelium homeostasis, and mediating antimicrobial activity by maintaining expression of colonic defensins. This has been tested in mice in an experimental colitis model (189, 190). The NLRP3 inflammasome can also be a double-edged sword though, as it is also involved in multiple systemic inflammatory diseases that are characterized by recurrent fevers, leukocytosis, and elevated acute phase proteins (191, 192). Furthermore, it is also highly associated with multiple autoinflammatory and autoimmune diseases (192, 193).
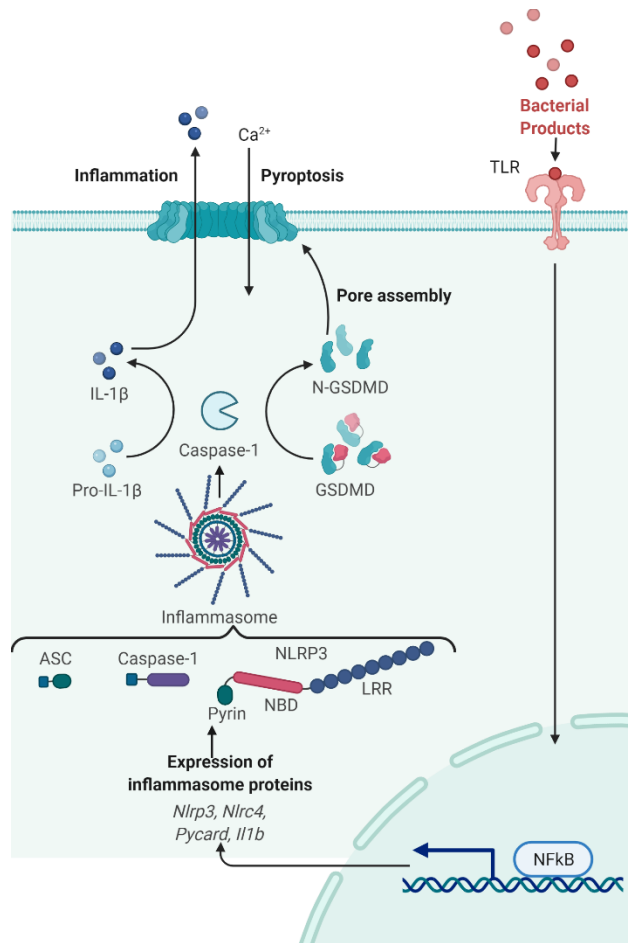
Figure 1.7. General activation pathway of NLRP3.

NNLRP3 is up-regulated when bacterial products/cellular damage is identified by the cell. NLRP3 is found in an auto-inhibited form in the cellular cytosol, and upon activation oligomerizes with ASC and caspase-1 to create the inflammasome complex in the cytosol. This allows for caspase-1 to cleave pro-IL-1β into IL-1β inside the cell, whereby the pro-inflammatory IL-1β is secreted from the cell through a pore created by modified gasdermin-D (GSDMD). Image created with Biorender.com.

1.4 Rationale

The data in this thesis investigates the functional results of SspH2 interaction with NLRs. Even though SspH2 has been implicated in the super-activation of NOD1 (56), it remains to be determined exactly how SspH2 is modulating this action on NOD1. In addition, the pathway of NOD1 super-activation by SspH2 still remains to be elucidated. It is thus tempting to hypothesize that SspH2 mediates super-activation through NOD1 activation because a catalytic mutant cannot do this (52). If this is truly the case, this prompts the question: where on NOD1 is SspH2 acting upon?

Furthermore, it remains to be seen whether SspH2 is capable of interacting with other host receptors once inside of the cell. If SspH2 interacts with other host receptors, this then begs the question: what sort of functional effect does this interaction induce?

1.5 Hypotheses

I hypothesize that: SspH2 is ubiquitinating NOD1 at specific lysines to mediate super-activation of NOD1, and that mutating these sites will reduce NOD1 super-activation.

I am going to test this hypothesis by observing ubiquitination sites present on NOD1 in the presence of SspH2, SspH2C580A, and EV by utilizing LC-MS/MS. I will identify the resultant NOD1 ubiquitination sites unique to the presence of SspH2. I will then follow this up by identifying sites of ubiquitination that have higher intensity in SspH2 compared to SspH2C580A. These lysines will be mutated so that they cannot be ubiquitinated (K→R mutation). These NOD1 lysine mutants will then be transiently transfected into HeLa cells and assessed for their ability to react to NOD1 stimulation, and super-activation in the presence of SspH2 via IL-8 ELISA.

I hypothesize that: SspH2 is interacting with other NLR proteins, and causes super-activation of the NLRs that SspH2 interacts with.

I am going to test this hypothesis by transiently transfecting other NLRs (NOD2 and NLRP3) into cells alongside SspH2 and assessing their ability to interact via reciprocal immunoprecipitations. I will also assess whether the ability to interact with SspH2 is reliant upon catalytic activity by observing interaction with SspH2C580A and NLRs. I will further determine whether the ability to interact with NLRs is a characteristic of *S*. Typhimurium NELs, by transiently expressing SspH1, and comparing whether this effect is specific to SspH2. The activity of these possible interactions will be assessed via secretion of IL-8 or IL-1β.

CHAPTER 2 – METHODS

2.1 Tissue culture

HEK293T (ATCC CRL-3216) and HeLa (ATCC CCL-2) cells were cultured in Dulbecco's

modified eagle medium (DMEM) containing 4500mg/Litre glucose 4500mg/Litre L-glutamine,

and 4500mg/Litre sodium bicarbonate (Sigma) supplemented with 10% fetal bovine serum

(FBS) (123483-020; Gibco), and 1% Penicillin-Streptomycin (1 unit penicillin/ml and 0.1 mg

streptomycin/ml, P4333; Sigma) and routinely grown at 37°C and 5% CO_2.

THP-1 cells (ATCC, Manassas, VA, USA), were modified by CRISPR Cas9 and generously

provided by the Muruve lab (UCalgary) (194) were grown in RPMI-1640 (Thermo Fisher

Scientific, Waltham, MA, USA) supplemented with 10% heat inactivated FBS (Thermo Fisher

Scientific, Waltham, MA, USA), 1% Penicillin-Streptomycin (Sigma-Aldrich, Saint Luis, MO,

USA) and with 1mM sodium pyruvate (11360-070; Gibco), and routinely grown at 37 °C and

5% CO_2.

2.2 Cloning

Domain truncation variants of NOD1 were generated by PCR amplification of NOD1 domains

using pcDNA3-Nod1-FLAG (APB 117) as a template. Primer sequences can be found in

supplementary Table 1. Truncation fragments were cloned into pcDNA3.1 using the *KpnI* and

XhoI restriction enzymes to replace wt NOD1. To create the NOD1 domain mutants the

following primer combinations were used. CARD: NOD1_CARD_For1 and

NOD1_CARD_Rev2; NBD: NOD1_NBD_For1 and NOD1_NBD_Rev1; LRR:

NOD1_LRR_For2 and NOD1_LRR_Rev1; ΔCARD: NOD1_NBD_For1 and

NOD1_LRR_Rev1; ΔLRR: NOD1_CARD_For1 and NOD1_NBD_Rev1. ΔNBD was created by

separately amplifying the CARD and LRR domains using primer pairs:

NOD1_CARD_For1/NOD1_CARD_Rev1 and NOD1_LRR_For1/NOD1_LRR_Rev1. These 2

PCR fragments were then combined together using NOD1_CARD_For1 and NOD1_LRR_Rev1 by crossover PCR. The lysine variants of NOD1 were generated in the pcDNA3.1NOD1 background, using the Quikchange II site directed mutagenesis kit (Agilent) according to the outlined protocol from Agilent. In brief, primers to mutate the adenine to guanine in the lysine codon were generated using the QuickChange Primer Design tool (Agilent). All PCR-amplified products were sequence verified. All constructs were propagated in *E. coli* DH5α using standard methods.

Table 2.1. Primers used for cloning

Primer name	Nucleotide sequence
NOD1_a71g	5'-ccccacattcaattactgagaagcaatcgggaacttctg-3'
NOD1_a71g_antisense	5'-cagaagttcccgattgcttctcagtaattgaatgtgggg-3'
NOD1_a209g	5'-cctgacaaggtccgcagaattctggacctggta-3'
NOD1_a209g_antisense	5'-taccaggtccagaattctgcggaccttgtcagg-3'
NOD1_a425g	5'-ggccgtgactccaggttcgtgctgtgc-3'
NOD1_a425g_antisense	5'-gcacagcacgaacctggagtcacggcc-3'
NOD1_a728g	5'-gcatgttcagctgcttcagggaaagtgacaggc-3'
NOD1_a728g_antisense	5'-gcctgtcactttccctgaagcagctgaacatgc-3'
NOD1_a971g	5'-cagtgggaagctgctcaggggggctag-3'
NOD1_a971g_antisense	5'-ctagcccccctgagcagcttcccactg-3'
NOD1_a983g	5'-ctcaaggggggctagcaggctgctcacagc -3'
NOD1_a983g_antisense	5'-gctgtgagcagcctgctagcccccttgag -3'
NOD1_a1418g	5'-ccggggcatggagaggagcctctttgtct-3'
NOD1_a1418g_antisense	5'-agacaaagaggctcctctccatgccccgg-3'
NOD1_a1745g	5'-cgggaagacctcttcaagaacagggatcacttcca-3'
NOD1_a1745g_antisense	5'-tggaagtgatccctgttcttgaagaggtcttcccg-3'
NOD1_a1799g	5'-ggctgttgtccaaagccagacagaaactcctgcg-3'
NOD1_a1799g_antisense	5'-cgcaggagtttctgtctggctttggacaacagcc-3'
NOD1_a1853g	5'-cctgaggagaaagcgcagggccctgtg-3'
NOD1_a1853g_antisense	5'-cacagggccctgcgctttctcctcagg-3'

NOD1_a2111g	5'-cctgcatcacttccccaggcggctggc-3'
NOD1_a2111g_antisense	5'-gccagccgcctggggaagtgatgcagg-3'
NOD1_a2237g	5'-cactgacggtgggggtaagggtgctaagcg-3'
NOD1_a2237g_antisense	5'-cgcttagcacccttaccccaccgtcagtg-3'
NOD1_a2261g	5'-gctaagcgaagagctgaccagatacaaaattgtgacctatt-3'
NOD1_a2261g_antisense	5'-aataggtcacaattttgtatctggtcagctcttcgcttagc-3'
NOD1_a2333g	5'-gccaggtacgtcaccagaatcctggatgaatgc-3'
NOD1_a2333g_antisense	5'-gcattcatccaggattctggtgacgtacctggc-3'
NOD1_a2351g	5'-ccaaaatcctggatgaatgcagaggcctcacgc-3'
NOD1_a2351g_antisense	5'-gcgtgaggcctctgcattcatccaggattttgg-3'
NOD1_a2405g	5'-caagtgaaggagggaggtatctcgccctggc-3'
NOD1_a2405g_antisense	5'-gccagggcgagatacctccctccttcacttg-3'
NOD1_a2426g	5'-ctcgccctggctgtgaggaacagcaaatcaatct-3'
NOD1_a2426g_antisense	5'-agattgatttgctgttcctcacagccagggcgag-3'
NOD1_a2696g	5'-gaaatgttgaaagtcaaccagacgttaaggcatttatggcttatc-3'
NOD1_a2696g_antisense	5'-gataagccataaatgccttaacgtctggttgactttcaacatttc-3'
NOD1_a2810g	5'-ttgcctaaatggaaacctgataagaccagaggaggc-3'
NOD1_a2810g_antisense	5'-gcctcctctggtcttatcaggtttccatttaggcaa-3'
NOD1_CARD_For1	5'-gaggggtaccgatatcaccatgg-3'
NOD1_CARD_Rev1	5'-ctggaagtgatccttgttcatgtagatctcctccag-3'
NOD1_CARD_Rev2	5'-gaggctcgagcatgtagatctcctccag-3'
NOD1_NBD_For1	5'-gaggggtaccgatatcaccatggacaccatcatggagctggttggc-3'
NOD1_NBD_Rev1	5'-gaggctcgagcttgaagaggtcttcccg-3'

NOD1_LRR_For1	5'-ctggaggacgatctacatgaacaacaaggatcacttccag-3'
NOD1_LRR_For2	5'-gaggggtaccgatatcaccatgaacaaggatcacttccag-3'
NOD1_LRR_Rev1	5'-gaggctcgaggaaacagataatccg-3'

Table 2.2. Mutated NOD1 descriptions

Mutation	Stock name	Strain number	Strain description
a71g	pcDNA3-NOD1FLAG-a71g	APB 218	NOD1-FLAG was cloned with a Kozak sequence into pcDNA3 between *KpnI* and *XhoI* restriction sites. This clone gives a 2.8kb dropout when cut with these enzymes. site directed mutagenesis causes a71g which is K24R
a209g	pcDNA3-NOD1FLAG-a209g	APB 219	NOD1-FLAG was cloned with a Kozak sequence into pcDNA3 between *KpnI* and *XhoI* restriction sites. This clone gives a 2.8kb dropout when cut with these enzymes. site directed mutagenesis causes a209g which is K70R
a425g	pcDNA3-Nod1FLAG-a425g	APB 238	Nod1-FLAG was cloned with a Kozak sequence into pcDNA3 between *KpnI* and *XhoI* restriction sites . This clone gives a 2.8kb dropout when cut with these enzymes. site directed mutagenesis causes a425g which is K142R

a728g	pcDNA3-Nod1FLAG-a728g	APB 239	Nod1-FLAG was cloned with a Kozak sequence into pcDNA3 between *KpnI* and *XhoI* restriction sites . This clone gives a 2.8kb dropout when cut with these enzymes. site directed mutagenesis causes a728g which is K243R
a971g	pcDNA3-NOD1FLAG-a971g	APB 220	NOD1-FLAG was cloned with a Kozak sequence into pcDNA3 between *KpnI* and *XhoI* restriction sites. This clone gives a 2.8kb dropout when cut with these enzymes. site directed mutagenesis causes a971g which is K324R
a983g	pcDNA3-Nod1FLAG-a983g	APB 240	Nod1-FLAG was cloned with a Kozak sequence into pcDNA3 between *KpnI* and *XhoI* restriction sites . This clone gives a 2.8kb dropout when cut with these enzymes. site directed mutagenesis causes a983g which is K328R

a1418g	pcDNA3-NOD1FLAG-a1418g	APB 221	NOD1-FLAG was cloned with a Kozak sequence into pcDNA3 between *KpnI* and *XhoI* restriction sites. This clone gives a 2.8kb dropout when cut with these enzymes. site directed mutagenesis causes a1418g which is K473R
a1745g	pcDNA3-NOD1FLAG-a1745g	APB 202	NOD1-FLAG was cloned with a Kozak sequence into pcDNA3 between *KpnI* and *XhoI* restriction sites. This clone gives a 2.8kb dropout when cut with these enzymes. site directed mutagenesis causes a1745g which is K582R
a1799g	pcDNA3-NOD1FLAG-a1799g	APB 208	NOD1-FLAG was cloned with a Kozak sequence into pcDNA3 between *KpnI* and *XhoI* restriction sites. This clone gives a 2.8kb dropout when cut with these enzymes. site directed mutagenesis causes a1799g which is K800R

a1853g	pcDNA3-NOD1FLAG-a1853g	APB 203	NOD1-FLAG was cloned with a Kozak sequence into pcDNA3 between *KpnI* and *XhoI* restriction sites. This clone gives a 2.8kb dropout when cut with these enzymes. site directed mutagenesis causes a1853g which is K618R
a2111g	pcDNA3-NOD1FLAG-a2111g	APB 222	NOD1-FLAG was cloned with a Kozak sequence into pcDNA3 between *KpnI* and *XhoI* restriction sites. This clone gives a 2.8kb dropout when cut with these enzymes. site directed mutagenesis causes a2111g which is K704R
a2237g	pcDNA3-NOD1FLAG-a2237g	APB 223	NOD1-FLAG was cloned with a Kozak sequence into pcDNA3 between *KpnI* and *XhoI* restriction sites. This clone gives a 2.8kb dropout when cut with these enzymes. site directed mutagenesis causes a2237g which is K746R

a2261g	pcDNA3-NOD1FLAG-a2261g	APB 204	NOD1-FLAG was cloned with a Kozak sequence into pcDNA3 between *KpnI* and *XhoI* restriction sites. This clone gives a 2.8kb dropout when cut with these enzymes. site directed mutagenesis causes a2261g which is K754R
a2333g	pcDNA3-NOD1FLAG-a2333g	APB 209	NOD1-FLAG was cloned with a Kozak sequence into pcDNA3 between *KpnI* and *XhoI* restriction sites. This clone gives a 2.8kb dropout when cut with these enzymes. site directed mutagenesis causes a2333g which is K778R
a2351g	pcDNA3-NOD1FLAG-a2351g	APB 205	NOD1-FLAG was cloned with a Kozak sequence into pcDNA3 between *KpnI* and *XhoI* restriction sites. This clone gives a 2.8kb dropout when cut with these enzymes. site directed mutagenesis causes a2351g which is K784R

a2405g	pcDNA3-NOD1FLAG-a2405g	APB 206	NOD1-FLAG was cloned with a Kozak sequence into pcDNA3 between *KpnI* and *XhoI* restriction sites. This clone gives a 2.8kb dropout when cut with these enzymes. site directed mutagenesis causes a2405g which is K802R
a2426g	pcDNA3-Nod1FLAG-a2426g	APB 241	Nod1-FLAG was cloned with a Kozak sequence into pcDNA3 between *KpnI* and *XhoI* restriction sites . This clone gives a 2.8kb dropout when cut with these enzymes. site directed mutagenesis causes a2426g which is K809R
a2696g	pcDNA3-NOD1FLAG-a2696g	APB 224	NOD1-FLAG was cloned with a Kozak sequence into pcDNA3 between *KpnI* and *XhoI* restriction sites. This clone gives a 2.8kb dropout when cut with these enzymes. site directed mutagenesis causes a2696g which is K899R

a2810g	pcDNA3-NOD1FLAG-a2810g	APB 225	NOD1-FLAG was cloned with a Kozak sequence into pcDNA3 between *KpnI* and *XhoI* restriction sites. This clone gives a 2.8kb dropout when cut with these enzymes. site directed mutagenesis causes a2810g which is K937R
Nod1-CARD	pcDNA3-NOD1FLAG-CARD	APB 263	NOD1-FLAG-CARD was cloned with a Kozak sequence into pcDNA3 *KpnI* and *XhoI* restriction sites. This clone gives a 0.5 kb dropout when cut with these enzymes.
Nod1-NBD	pcDNA3-NOD1FLAG-NBD	APB 237	NOD1-FLAG-NBD was cloned with a Kozak sequence into pcDNA3 *KpnI* and *XhoI* restriction sites. This clone gives a 1.1 kb dropout when cut with these enzymes.
Nod1-LRR_alone	pcDNA3-NOD1FLAG-LRR_alone	APB 229	NOD1-FLAG-LRR_alone was cloned with a Kozak sequence into pcDNA3 *KpnI* and *XhoI* restriction sites. This clone gives a 1.124 kb

			dropout when cut with these enzymes.
Nod1ΔCARD	pcDNA3-NOD1FLAG-ΔCARD	APB 226	NOD1-FLAG-ΔCARD was cloned with a Kozak sequence into pcDNA3 *KpnI* and *XhoI* restriction sites. This clone gives a 2.384 kb dropout when cut with these enzymes.
Nod1ΔNBD	pcDNA3-NOD1FLAG-ΔNBD	APB 227	NOD1-FLAG-ΔNBD was cloned with a Kozak sequence into pcDNA3 *KpnI* and *XhoI* restriction sites. This clone gives a 1.618 kb dropout when cut with these enzymes.
Nod1ΔLRR	pcDNA3-NOD1FLAG-ΔLRR	APB 228	NOD1-FLAG-ΔLRR was cloned with a Kozak sequence into pcDNA3 *KpnI* and *XhoI* restriction sites. This clone gives a 1.766 kb dropout when cut with these enzymes.
sspH2-LRR	pcDNA3-2xHAsspH2LRR	APB 234	This clone expresses a double hemagluttinin tagged version of the Salmonella SL1344 SspH2 LRR

			domain (residues 171-481) constitutively expressed in mammalian cells from the pcDNA3 backbone. sspH2LRR was amplified using sspH2LRRfor and sspH2LRRrev oligos and cloned into pcDNA3-2xHA using the *SrfI* and *BamHI* sites. This clone will be used to test binding partner interactions. This is clone A2 that has correct dropout with *HindIII* and *EcoRI* digestion and has been sequenced. Strain Genotype: F- mcrA Δ(mrr-hsdRMS-mcrBC) φ80lacZΔM15 ΔlacX74 recA1 endA1 araD139Δ(ara, leu)7697 galU galK λ-rpsL nupG
sspH2-NEL	pcDNA3-2xHAsspH2NEL	APB 235	This clone expresses a double hemagluttinin tagged version of the Salmonella SL1344 SspH2 NEL domain (residues 492-788) constitutively expressed in mammalian cells from the pcDNA3

			backbone. sspH2NEL was amplified using sspH2NELfor and sspH2NELrev oligos and cloned into pcDNA3-2xHA using the SrfI and BamHI sites. This clone will be used to test binding partner interactions. This is clone B2 that has correct dropout with *HindIII* and *EcoRI* digestion and has been sequenced. Strain Genotype: F- mcrA Δ(mrr-hsdRMS-mcrBC) φ80lacZΔM15 ΔlacX74 recA1 endA1 araD139Δ(ara, leu)7697 galU galK λ-rpsL nupG

2.3 Western Blotting

Proteins were separated on 4-20% acrylamide 1.0mm gels or 10% acrylamide 1.5mm gels and separated at 180V for 75 min. Once gels were run, they were transferred to nitrocellulose membranes using the Transblot turbo transfer machine (BioRad) with the 1.5 mm gel run setting 2x to ensure protein transfer. Once transferred, the nitrocellulose membranes were dried for 1 hour between 2 dry stacks of membrane transfer towel. Once 1 hour had elapsed, the nitrocellulose membrane was rehydrated completely with TBS for 2 minutes. This ensures that the proteins in the nitrocellulose are firmly cemented. Membranes were then blocked with TBS blocking buffer (927-60001; Li-Cor) for 1 hour at room temperature with gentle rotation, and incubated in 0.2% v/v Tween in TBS blocking buffer with primary (overnight at 4°C, with gentle rotation) and secondary antibodies (1 hour at room temperature, gentle rotation) using gentle in the following concentrations: mouse α-FLAG (clone M2) 1:2 500; rabbit α-FLAG (SAB4301135; Sigma) 1:2 500; rat α-HA (clone 3F10 (Roche Diagnostics); mouse α-Myc (9E10; Santa Cruz Biotechnology) 1:2 500; goat α-mouse (926-68020; IRDye680LT) 1:5 000; goat α-rabbit (925-32211; IRDye800CW) 1:5 000; goat α-rat (926-32219; IRDye800CW) 1:5 000. Proteins were imaged on a LiCor Odyssey and visualized using Licor Image Studio detection software.

2.4 NOD1/ NOD2 functional assays

HeLa cells were cultured as outlined above, and seeded at either 2.5×10^5 cells per well in a 6-well dish or at 6×10^4 cells per well of a 24-well dish. Cells were transfected with a total 1µg or 0.25 µg respectively of equivalently proportioned plasmid DNA using JetPrime transfection reagent (Polyplus) at 60-80% cell confluency. 2 days after transfection, cells had media replaced with 0.5% FBS in DMEM with Nod1/ Nod2 agonist (1µg/ml C12-iE-DAP (Invivogen)+ 10ng/ml human interferon gamma (AbD serotec) and 5µg/ml L-18 MDP (InvivoGen) + 10ng/ml human

interferon gamma, respectively). Cells were stimulated overnight and the following day, supernatants were collected and quantified using a human IL-8 ELISA kit according to the manufacturer's specifications (BD-Bioscience). For NF-κB pathway inhibition experiments, 20μM of Bay 11-7082 (Sigma-Aldrich) was pre-incubated with samples for 45 mins to allow for Bay 11 to bind to its target, before replacement of media and addition of agonist.

2.5 THP-1 functional assays
THP-1 cells were cultures as outlined above, and 1×10^6 THP-1 cells were nucleofected with 1 μg of total plasmid using Lonza Nucleofection kit FF-100 protocol (Lonza) and seeded in a 6-well dish supplemented with RPMI with 100 ng/mL phorbol-12-myristate 13-acetate (PMA, Sigma-Aldrich, Saint Luis, MO, USA) for 48 hours (195, 196). Cell differentiation was verified by evaluating cell adhesion and spreading under an optical microscope at 10x magnification. THP-1 cells, were washed and had their media replaced with fresh RPMI with 100ng/mL lipopolysaccharide (LPS) for 3 hours. This was followed by another cell wash and replacing the media again with RPMI and 10μM Nigericin for 1 hour. Supernatants were collected and quantified using a human IL-1β ELISA kit according to the manufacturer's specifications (BD-Bio-Science).

2.6 Immunoprecipitation

2.6.1 Manual immunoprecipitation assay

For manual immunoprecipitations HEK293T cells were seeded at 1×10^6 cells per 10 cm dish and transfected when cells reached 60-80% confluency with a total of 6μg of equivalently proportioned plasmid DNA using JetPrime transfection reagent (Polyplus). Lysates were harvested by washing HEK293T cells with PBS, and applying 800μl lysis buffer (20 mM Tris/HCl, pH 7.5, 150 mM NaCl, and 1% Nonidet P-40 (all from Sigma)) supplemented with

EDTA-free protease inhibitor mixture cocktail (Roche Applied Science). This was incubated on ice for 10 minutes. Debris was precipitated at 16 000xg and 4°C for 20 minutes, and the supernatant was collected. Immunoprecipitations were performed as per the outlined protocol from Invitrogen. In brief, 20µl Dynabeads™ Protein G beads (Invitrogen) were coupled to 2.5µg α-HA (high affinity) antibody (Roche Diagnostics) or 5µg α-FLAG (M2 clone) antibody for 10 mins with end-over-end/ medium shaking. Beads were then washed to ensure that the only antibodies present are coupled to the magnetic beads. Antibody-coupled beads were incubated overnight at 4°C with end-over-end rotation to facilitate protein-bead binding. Immunoprecipitated proteins were analyzed via Western blot with α-HA (Roche Applied Sciences), α-FLAG (SAB4301135; Sigma)/α-FLAG (clone M2) antibodies as identified above, to confirm expression of NELs and NLRs respectively.

2.6.2 Automated immunoprecipitation for mass spectrometry

This protocol was done in collaboration with Shu Luo from the Julien Lab. I prepared the cell lysate, and assisted in preparing the KingFisher machine. Transfected HEK293T cell lysate supernatant was prepared as outlined above. Automated immunoprecipitation was performed using the KingFisher Duo Prime Purification System (5400110; Thermo Scientific). The IP protocol was adapted and modified from Invitrogen manual (publication No. MAN0016198) and executed on BindIt software (v4.0.0.45). All reagents were added to a 96 deep-well plate prior to launching the run, allowing for parallel processing of different samples. In brief, 20 µL of Protein G Dynabeads (Invitrogen; 10003D) were binding to 7 µg of anti-DYKDDDDK antibody (SAB4301135; Sigma) in 200 µL of PBS-T (Phosphate Buffered Saline with 0.02% Tween 20) for 10 min, and subsequently washed with 200 µL PBS-T. The Dynabeads with the bound antibody complex then undergo binding to 800 µL of transfected cell lysates (~2.5 mg protein)

for 10 min at RT, and washed 2X with 500 µL PBS. The bound proteins were eluted from Dynabeads using 30 µL of 4x Laemmli buffer (Bio-Rad) without reducing agents and heated to 70˚C for 10 min. The eluants were collected from the plate, and diluted with 20 µL ddH₂O to run on an SDS-PAGE gel.

2.7 Mass spectrometry

2.7.1 In-gel sample preparation for mass spectrometry

This procedure was done by Shu Luo in the Julien lab. The eluted IP samples were run on a precast SDS-PAGE (Mini-PROTEAN TGX Stain-Free Protein Gels, 4-20%, 10 well, 50 µl; Bio-Rad) at 160 V for 10 min. The proteins in the gel were fixed by incubating with 50% EtOH, 2% phosphoric acid at room temperature for 30 min, then the gel was washed twice with ddH₂O for 10 min. The gel was subsequently stained by Blue-Silver stain (20% pure ethanol, 10% phosphoric acid, 10% w/v ammonium sulfate, 0.12% w/v Coomassie Blue G-250) at room temperature overnight.

After staining, the gel was washed twice with ddH₂O for 20 min. Each lane was cut into four fractions of gel pieces and transferred to a round-bottom 96-well plate to be repetitively destained by 150 µL destaining solution (50 mM ammonium bicarbonate, 50% acetonitrile) in each well at 37˚C. The gel pieces were then dried by incubating with acetonitrile at 37˚C, rehydrated and reduced with 175 µL of reducing solution (5 mM β-mercaptoethanol, 100 mM ammonium bicarbonate) at 37˚C for 30 min, and alkylated with 175 µL of alkylating solution (50 mM iodoacetamide, 100 mM ammonium bicarbonate) at 37˚C for 30 min. The gel pieces were washed twice with 175 µL of 100 mM ammonium bicarbonate at 37˚C for 10 min, and completely dried by incubating with acetonitrile at 37˚C. Proteins in each well were digested by

1 µg of sequencing-grade trypsin (Promega Inc.) in 75 µL of 50 mM ammonium bicarbonate and incubated overnight.

Tryptic peptides in the gel pieces were extracted by incubating with 2% acetonitrile, 1% formic acid, then with 50% acetonitrile, 0.5% formic acid, each at 37˚C for 1 h. The extracted peptides were transferred to another round-bottom 96-well plate, dried using a Genevac (EZ-2 plus). Each sample was injected in 4 gel-fractionated injections.

2.7.2 Mass spectrometry analyses

This procedure was done by Shu Luo in the Julien lab. Peptides were separated using a nanoflow-HPLC (Thermo Scientific EASY-nLC 1200 System) coupled to Orbitrap Fusion Lumos Tribrid Mass Spectrometer (Thermo Fisher Scientific). A trap column (5 µm, 100 Å, 100 µm × 2 cm, Acclaim PepMap 100 nanoViper C18; Thermo Fisher Scientific) and an analytical column (2 µm, 100 Å, 50 µm × 15 cm, PepMap RSLC C18; Thermo Fisher Scientific) were used for the reverse phase separation of the peptide mixture. Peptides were eluted over a linear gradient over the course of 90 min from 3.85% to 36.8% acetonitrile in 0.1% formic acid. Data were analyzed using ProteinProspector (v5.22.1) against the concatenated database of the human proteome (SwissProt.2017.11.01. random.concat), with maximum false discovery rate at 5% for proteins, and 1% for peptides. Search parameters included a maximum of 3 missed trypsin cleavages, a precursor mass tolerance of 15 ppm, a fragment mass tolerance of 0.8 Da, with the constant modification carbamidomethylation (C), and variable modifications of acetyl (protein N-term), deamidated (N/Q), oxidation (M), and GlyGly (uncleaved K). The maximum number of variable modifications was set to 4.

2.8 Statistical analysis

All error bars are representative of SD. NOD1 and NOD2 activation were analyzed in HeLa cells and statistical analyses were determined by non-parametric Student t test (Mann-Whitney U test). The semi-quantitative mass spectrometry peptide fragment analysis was analyzed by linear regression with 95% confidence intervals (seen as a solid line and dotted line, respectively). NOD1 lysine variants activation in HeLa cells were analyzed by 1-way ANOVA with Dunnett's multiple comparison test to a control sample (NOD1 + EV or against NOD1 + SspH2). All Statistical comparisons were performed using Prism 6.01.

2.9 Microscopy

Adherent THP-1 cells in cell culture were imaged at 10x magnification using the confocal and GFP filters before and after cell wash with PBS using the EVOS cell imaging system (Invitrogen, Thermo Fisher Scientific).

CHAPTER 3 – RESULTS
3.1 SspH2 interacts with multiple NLRs

As it stands there is a paucity of information on the way that SspH2 interacts with host receptors inside the cell. What is known so far is that SspH2 interacts with NOD1 to super-activate it in a manner that is dependent on the catalytic cysteine of SspH2 (56). The fact that SspH2 has only been documented to interact with 1 immune intracellular receptor sparked my curiosity, because there are many different receptors present inside of host cells that contribute to anti-bacterial immune responses. Therefore, I was curious as to what other receptors SspH2 could be interacting with inside of host epithelial cells.

To ensure that I would be able to effectively ask this question of other receptors, I first recapitulated the already documented binding characteristics of SspH2 to NOD1. I confirmed, in my own hands, that NOD1 is able to interact with both SspH2 and SspH2C580A, which are the catalytically active and inactive forms of SspH2, respectively. I identified this interaction by reciprocally co-immunoprecipitating (Co-IPing) NOD1 and SspH2 in cell lysate (Fig. 3.1A). I found that the band intensity of co-IPed SspH2C580A was reduced relative to SspH2 wild-type. Nonetheless the reciprocal co-IP of SspH2C580A and NOD1 are suggestive of their interaction (Fig. 3.1A).

To start investigating other intracellular receptors, I moved my focus onto NOD2, another prototypical member of the NLR family of receptors. I found that both SspH2 and SspH2C580A were capable of interacting with NOD2 through reciprocal co-IP, however the signal intensity for SspH2C580A co-IPs were reduced compared to SspH2. (Fig 3.1B). This might indicate that SspH2C580 may play a role facilitating increased strength of protein interaction.

To take my inquiry even further, and beyond just the NLRC family, which NOD1 and NOD2 are a part of, I wanted to know if SspH2 could interact with proteins of other NLR families. I chose to look at NLRP3, a well studied member of the NLRP family of proteins (197) By utilizing co-IP, I found that SspH2 and SspH2C580A can also interact with NLRP3. But, like with NOD1 and NOD2 the signal intensity of the SspH2C580A co-IP protein signal was not as intense as SspH2, indicating a possible role that the catalytic cysteine plays in facilitating strong protein interaction with the NLRs (Fig 3.1C).

Because *Salmonella* injects many different NELs to mediate infection, I next wanted to ensure that the interactions found between SspH2 and NLR proteins were specific to SspH2, or whether it was just a property of NELs. Previously, it has been shown that NOD1 does not interact with SspH1 (56), a closely related protein which has 69% sequence homology with SspH2 and is present in the cell at the same time during *Salmonella* infection (198). By utilizing reciprocal co-IP I observed that SspH1 does not interact with NOD2 (Fig 3.1D). This finding also extends to NLRP3, which also does not interact with SspH1 (Fig 3.1E). It should be noted that SspH1 is expressed less in the cell lysate of both of these experiments compared to SspH2, and thus there may be weak protein interactions with the NLRs that is below the limit of detection.

To control for whether any of the transfected proteins interact with our immunoprecipitation (IP) materials, I expressed all constructs, and immunoprecipitated without any specific antibodies. I perceived that the magnetic IP beads were incapable of binding to NOD1-FLAG, NOD2-FLAG, NLRP3-FLAG, HA-SspH2, HA-SspH2C580A or HA-empty vector (EV) (Fig 3.1F). Taken together, these data indicate that SspH2 is capable of specifically interacting with multiple NLRs which originate from the NLRC and NLRP families.
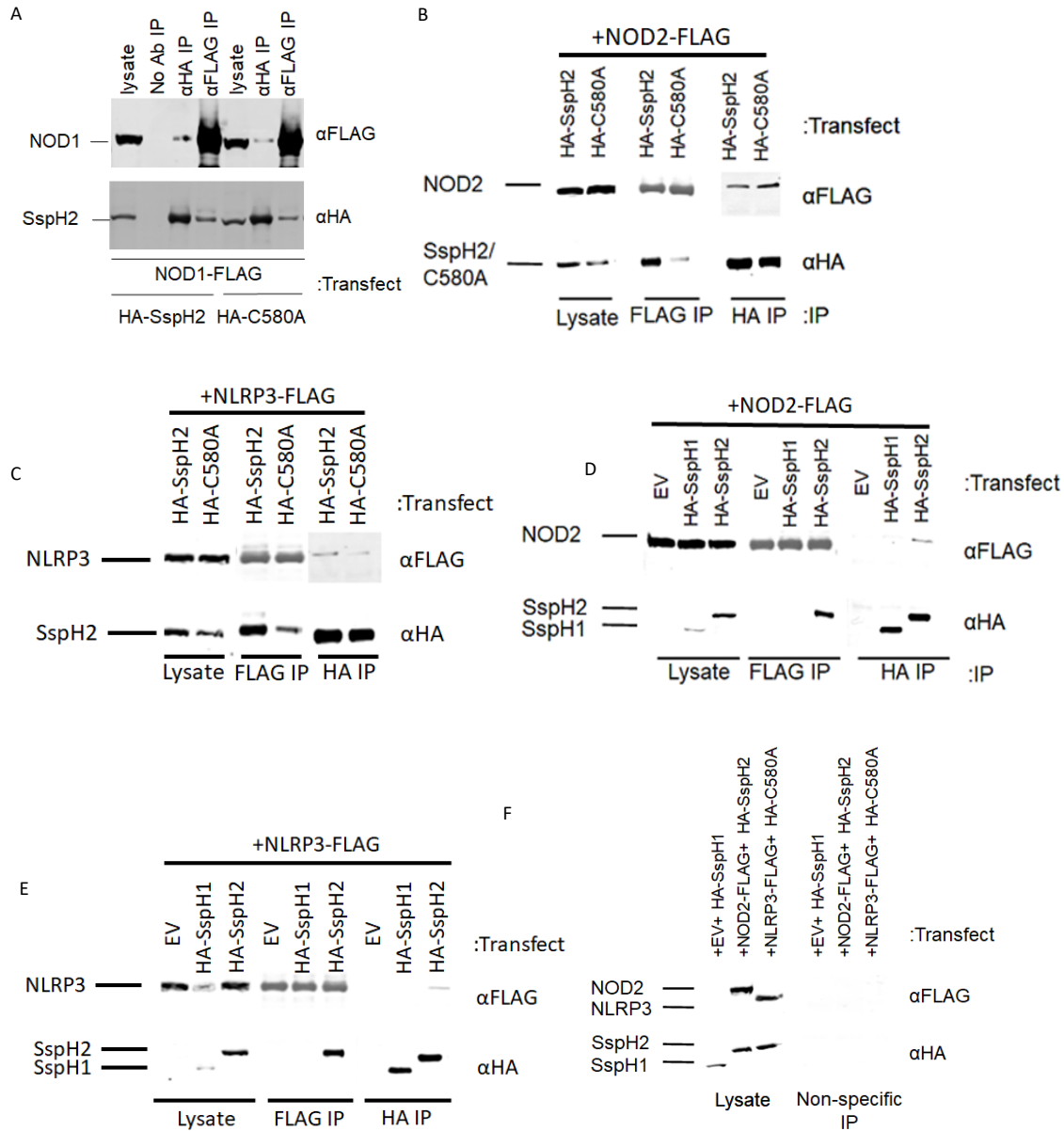
Figure 3.1. Interactions between *S. Typhimurium* SspH2 and NLRs.

Plasmids were transiently transfected in HEK293T cells and subjected to reciprocal co-immunoprecipitation (co-IP) analysis, imaged by western blot. **A.** Reciprocal co-IP analysis of NOD1 with SspH2 or SspH2 C580A **B.** Reciprocal co-IP analysis of NOD2 with SspH2 or SspH2C580A. **C.** Reciprocal co-IP analysis of NLRP3 with SspH2 or SspH2 C580A. **D.** Reciprocal co-IP analysis of NOD2 with SspH2 or SspH1. **E.** Reciprocal co-IP analysis of

NLRP3 with SspH2 or SspH1. **F.** Reciprocal co-IP analysis without binding of antibody to magnetic beads of NOD2, NLRP3, SspH1, SspH2, SspH2C580A, and empty vector (EV). IPs and immunoblotting were performed with indicated antibodies.

3.2 SspH2 LRR and NEL domains mediate interaction with NLRs.
Due to SspH2 having the ability to interact with multiple NLRs, I was curious to find out which

of SspH2's domains, its amino terminal-LRR domain or its carboxy-terminal NEL domain (52),

was responsible for mediating these interactions. To investigate how these domains individually

contribute to NLR binding, I transiently transfected HEK 293T cells with the individual SspH2

domains alongside the afore-mentioned NLRs (NOD1, NOD2, and NLRP3). I utilized SspH2

constructs made by Bhavsar *et. al.* (56), which consisted of the SspH2 LRR domain (residues

171-479) and the SspH2 NEL domain (residues 492-788). By utilizing co-IP, I was able to gather

insights as to how each SspH2 domain interacted with NOD1, NOD2, and NLRP3. I found that

both the LRR and NEL domain of SspH2 appeared to interact with NOD1 (Fig 3.2A). This result

was consistent across NOD2 (Fig 3.2B) and NLRP3 (Fig 3.2C). It is notable, that in these

experiments the SspH2 NEL band is more intense than the SspH2 LRR band in the lysate, which

may account for the intensity difference seen in the FLAG IP. However, more NLR is co-IPed by

SspH2 LRR compared to SspH2 NEL, despite the lower expression levels of SspH2 LRR. This

may indicate that there is different binding strength between the SspH2 regions and all of the

NLRs tested where SspH2 LRR interacts better with NLRs than SspH2 NEL. This data in

aggregate suggests that both SspH2 domains facilitate interactions with full-length host NLRs.
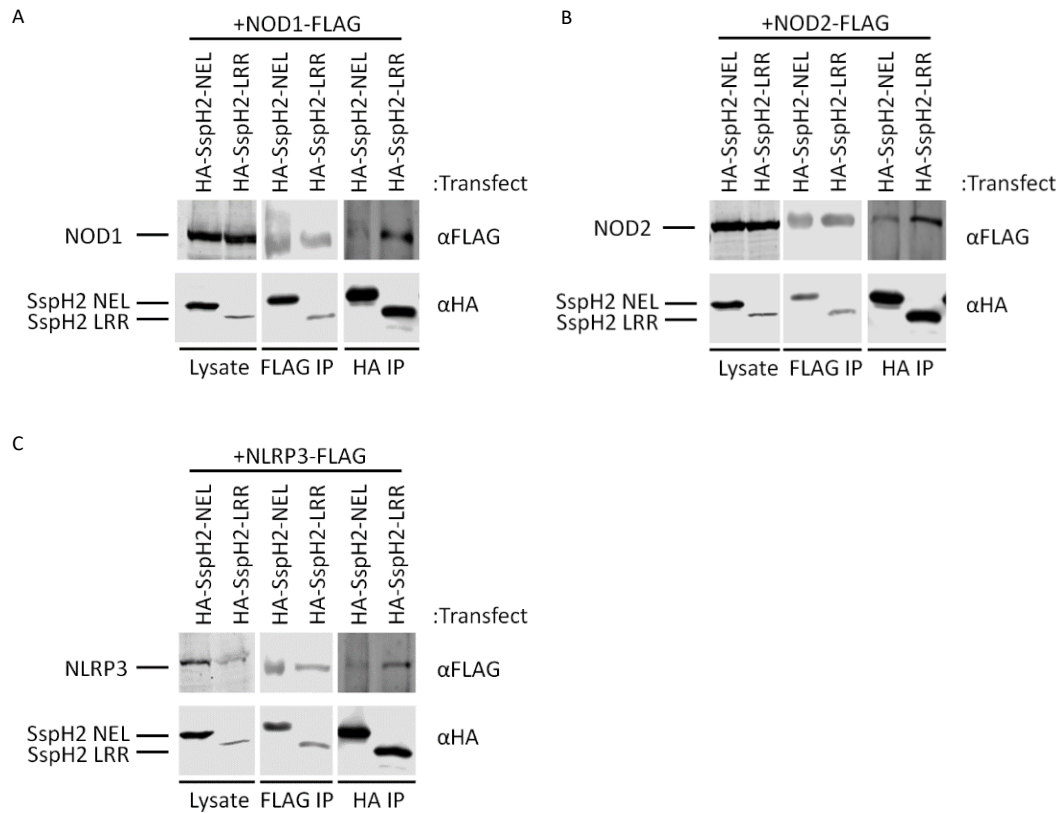
Figure 3.2. *S.* typhimurium SspH2 domain interaction with multiple NLRs.
Plasmids were transiently transfected in HEK293T cells and reciprocal co-IP analyses were performed with SspH2 domain fragments with **A.** NOD1, **B.** NOD2, and **C.** NLRP3. IPs and immunoblotting were performed with indicated antibodies.

3.3 The NOD1 NBD and LRR domains interact with SspH2.
After determining that both domains of SspH2 interacted with all of the NLRs tested, I wanted to

focus in on the NOD1 interaction, to further my understanding of how an archetypical NLR

interaction occurs. It has been previously reported that SspH2 interacts with SGT1 and NOD1

(56). However, the mechanistic details of how SspH2 interacts with NOD1 remain unexplored.

To further hone in on this binding interaction, I created domain deletions of NOD1 using single-

step and two-step PCR. I transiently transfected NOD1 domain fragments alone (CARD

[residues 1-160], NBD [residues 134-584], and LRR [residues 697-1053]), or single domain

deletion constructs (ΔCARD [residues 160-1053], ΔNBD [residues 1-160 & 580-1053], and

ΔLRR [residues 1-584]) to identify whether these proteins could be expressed in cell culture and

identify which domains are critical for NOD1 interaction with SspH2 (Fig. 3.3A). These

expressed proteins correlated to the expected observed size of each of the NOD1 domains.

Through reciprocal co-IP in HEK293T cells, I determined that the NBD and LRR domains of

NOD1 interact with SspH2, while the CARD region was not required (Fig. 3.3B). In summary,

these data show that NOD1 interacts with SspH2 through its NBD and LRR domains.
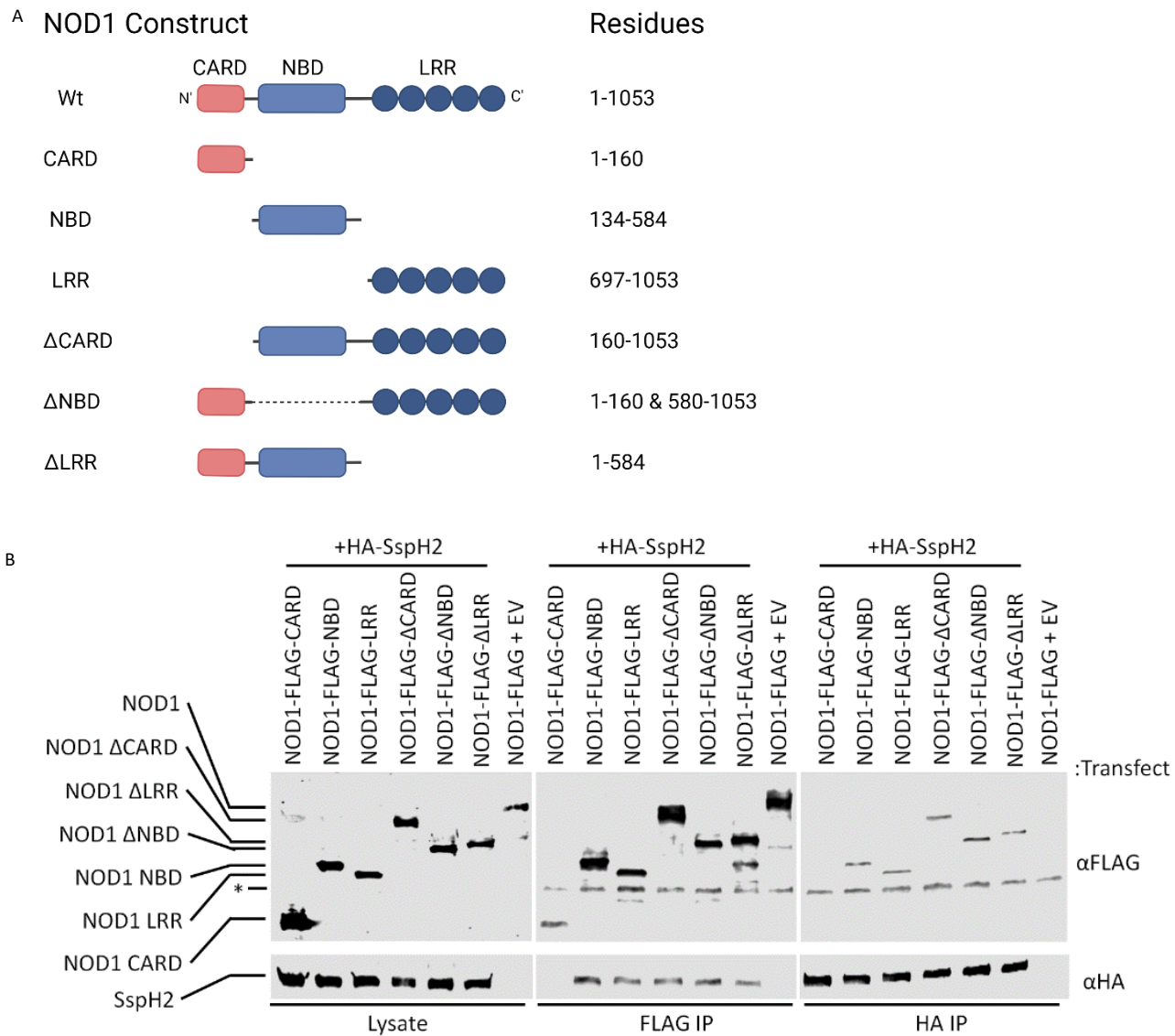
Figure 3.3. NOD1 domain fragment interactions with SspH2.

A. Schematic diagram of NOD1 domain fragments. Created with Biorender.com. **B.** Reciprocal co-immunoprecipitation (co-IP) of NOD1 domain fragments with SspH2 transiently expressed in HEK293T cells. IPs and immunoblotting were performed with indicated antibodies. * non-specific bands.

3.4 SspH2 super-activates NOD1.
Upon observing which domains of NOD1 and SspH2 were interacting with each other, I next

wanted to elucidate more clearly the specific pathway that this interaction signals through. To be

able to ask this question, I first needed to be able to recapitulate experiments that showed

reported super-activation of NOD1 with SspH2 (56). I was able to reproduce the previously

observed results of NOD1 super-activation with NOD1 in HeLa cells. There is a significant

(P<0.0001) difference between IL-8 secreted in the absence and presence of exogenous NOD1 of

~10 fold, (Fig. 3.4). I observed that the presence of SspH2 induced super-activation of NOD1 by

~4 fold over NOD1 activation alone, and confirmed that SspH2C580A did not induce the same

super-activation as the wild-type SspH2 (Fig. 3.4). This indicates that SspH2 super-activates

NOD1 beyond normal activation with NOD1 agonist, which is dependent on the catalytic

activity of SspH2.
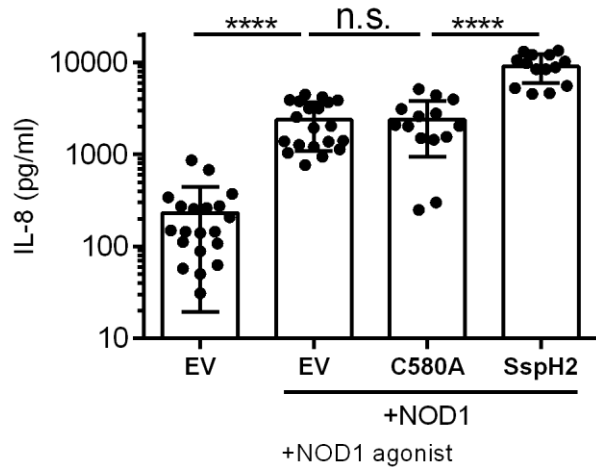
Figure 3.4. Functional interaction between SspH2 and NOD1.

NLR functional assay illustrating IL-8 secretion in HeLa cells. NOD1, SspH2, SspH2C580A

(C580A) or empty vector (EV), were transiently transfected as indicated, in the presence of

NOD1 agonist (1µg/mL c12-iE-DAP and 10ng/mL human IFNγ). Data is presented as the mean

with standard deviation for 4-9 biological replicates with 2-3 technical replicates each. Each dot

represents 1 technical replicate. Data were analyzed using a non-parametric Mann-Whitney test

where **** denote $P < 0.0001$ and n.s. is no significance between the indicated sample groups.

See materials and methods for more details.

3.5 SspH2 super-activates NOD2.
Since I found that SspH2 also interacts with NOD2, I was curious as to what sort of functional response this would result in. There is a significant (P<0.0001) difference between IL-8 secreted in the absence and presence of exogenous NOD2 of ~25 fold, (Fig. 3.5). When expressed in HeLa cells, I saw that the interaction of SspH2 with NOD2 induces ~10 fold more IL-8 secretion above NOD2 stimulation. Furthermore, the interaction between NOD2 and SspH2C580A caused ~3-fold increase in IL-8 secretion. I also found that NOD2 activity was not increased by SspH1, and there is no statistical significance between NOD2+EV and NOD2+SspH1 which corroborates with the finding that SspH1 and NOD2 do not interact. To ensure that these results were a result of the protein being expressed, I checked for protein expression alongside the IL-8 secretion, and found all of the expected proteins present (Fig 3.5). This indicates that the presence of SspH2 super-activates NOD2, which is partially dependent on the catalytic activity of SspH2.
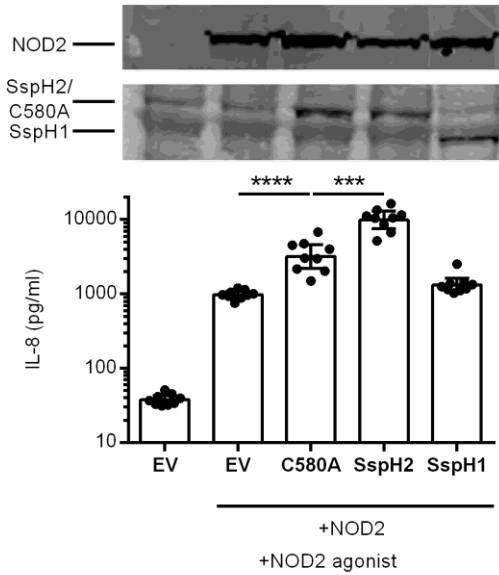
Figure 3.5. Functional interaction between SspH2 and NOD2.

NLR functional assay illustrating IL-8 secretion in HeLa cells. Cells are subsequently lysed for protein expression analysis. NOD2, SspH2, SspH2C580A (C580A) or empty vector (EV), were transiently transfected as indicated, in the presence of NOD2 agonist (5µg/mL MDP and 10ng/mL human IFNγ). Data is presented as the mean with standard deviation for 4 biological replicates with 2-3 technical replicates each. Each dot represents 1 technical replicate. Data were analyzed using a non-parametric Mann-Whitney test where ***, and **** denote $P < 0.001$, and < 0.0001 respectively, between the indicated sample groups. See materials and methods for more details.

3.6 SspH2 interaction with NLRCs mediates enhanced NLRC activation via NF-κB pathways.
NOD1 and NOD2 are thought to produce IL-8 through the activation of the NF-κB pathway

(199). To investigate whether SspH2 super-activation of NOD1 and NOD2 was through NF-κB,

IL-8 secretion assays were performed in the presence of the NF-κB pathway inhibitor, Bay-11.

Bay-11 inhibits NF-κB activation by preventing the phosphorylation of IκBα. This prevents p65

from traveling to the nucleus and binding to the NF-κB promoter, thus preventing initiating pro-

inflammatory cytokine release (200, 201).

My data shows that the NF-κB inhibitor Bay-11, reduced NOD1 activation. I measured this by

observing the levels of IL-8 secretion. This reduction was ~4.5 fold and ~9 fold in the absence

and presence of SspH2 respectively (Fig 3.6A). I also found that the levels of IL-8 being secreted

in the presence of NOD1+SspH2 with Bay11 compared to NOD1+EV with Bay11 were not

statistically significant (Fig. 3.6A). This indicates that NOD1 super-activation with SspH2 is

primarily being driven by NF-κB signaling. Due to SspH2 binding to both NOD1 and NOD2, I

also investigated the effect of Bay 11 on NOD2 super-activation. I found that NOD2 signaling

was also reduced in the presence of Bay-11. This reduction was ~2.5 fold and ~3 fold in the

absence and presence of SspH2, respectively (Fig 3.6B). I also found that the levels of IL-8

being secreted in the presence of NOD2+SspH2 with Bay11 compared to NOD2+EV with

Bay11 was significantly increased by ~4.5 fold (P<0.0001) (Fig. 3.6B). This indicates that

NOD2 super-activation with SspH2 may not entirely be due to NF-κB. This could be further

investigated by observing the contribution that MAPK signaling pathway is having on NOD2

signaling by inhibiting that signaling pathway. Taken together, these data indicate that SspH2

mediates increased NLR activation through NF-κB signaling in NOD1, and partially through

NF-κB in NOD2.
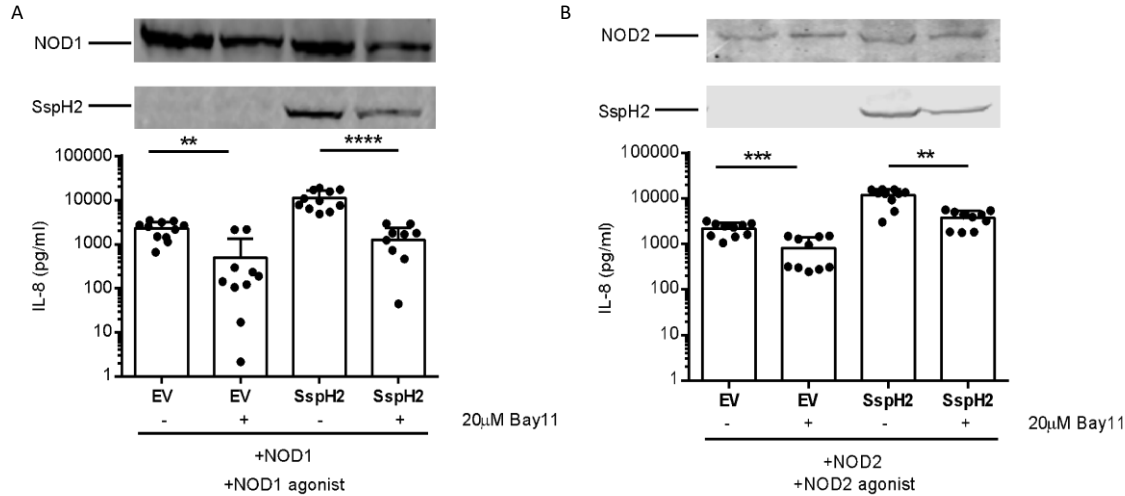
Figure 3.6. *S. typhimurium* SspH2 causes NLR activation through NF-κB pathway.

NLR functional assay illustrating IL-8 secretion in HeLa cells. Cells are subsequently lysed for protein expression analysis. **A.** NOD1, SspH2 or EV with NOD1 agonist (1µg/mL c12 iE-DAP and 10ng/mL human IFNγ) with or without the addition of 20µM Bay-11. **C.** NOD2, SspH2 or EV with NOD2 agonist (5µg/mL MDP and 10ng/mL human IFNγ) with or without the addition of NF-κB inhibitor, Bay11. NOD1 and NOD2 were tagged with FLAG. SspH2 was tagged with HA. Data is presented as the mean with standard deviation for 4 biological replicates with 2-3 technical replicates each. Each dot represents 1 technical replicate. Data were analyzed using a non-parametric Mann-Whitney test and **, ***, and **** denote $P < 0.01, < 0.001, < 0.0001$ respectively, between the indicated sample groups. See materials and methods for more details.

3.7 NLRP3 functional assays.
I have been previously able to show that NLRP3 also interacts with SspH2 (Fig. 3.1C, 3.1E, and

3.2C). To investigate the activation of NLRP3, I utilized THP-1 monocytes, which are a well-

recognized model for studying NLRP3 activation. NLRP3 activation initiates the assembly of the

inflammasome, which initiates inflammatory cell death in response to infection. This is mediated

by secretion of pro-inflammatory cytokines such as IL-1β (160-165). To observe IL-1β secretion

as a functional output of inflammasome activation, the monocytes must be differentiated into

macrophages. Unfortunately, I was unable to successfully transfect SspH2 into this *in* vitro cell

model to examine the effects of SspH2 interaction on NLRP3 activation, thus I cannot show the

data here. However, the work that I performed to establish this assay is found in appendix 1.

3.8. SspH2-mediated NLR activation is not dependent on NLR stimulation by agonists.
Since SspH2 mediates increased NOD1 activation in the absence of agonist (56), I sought to

determine whether this effect was replicated in NOD2. I repeated the super-activation

experiments without NOD2 agonist (MDP/h-IFNγ). Intriguingly, in the absence of NOD2

agonist, both SspH2 wt and SspH2C580A induced a significant increase in IL-8 secretion.

SspH2 caused a ~14 fold increase in IL-8, while SspH2C580A caused a ~6 fold increase in IL-8

over baseline NOD2 (Fig 3.7A). There were also no statistically significant differences in IL-8

secretion between EV and EV+NOD2 groups, indicating that presence of NOD2 alone does not

increase IL-8 secretion over baseline (Fig 3.7A). This result is consistent with SspH2 and

SspH2C580A interactions with NOD2 in the presence of agonist and indicates that SspH2

mediated super-activation is not specifically dependent on the activated form of NOD2.

I next performed control experiments to determine what effect NLR agonists interacting with

SspH2 may contribute to the super-activation seen in the presence of NLRs. I observed that

SspH2 expression alone increased IL-8 secretion by ~3 fold (Fig 3.7B). This was increased to

~10 fold in the presence of NOD1 agonist (Fig 3.7C) and NOD2 agonist (Fig 3.7D). However, I observed that this is still approximately ~20 fold lower than enhancements observed in the presence of exogenous NLR. These data suggest that SspH2 is interacting with either endogenous NOD1/NOD2 (in the case of Fig 3.7 B-D) or is specifically interacting with NLR agonists (Fig 3.7 C & D) to contribute to the increased IL-8 secretion seen when interacting with transiently transfected NLRs.
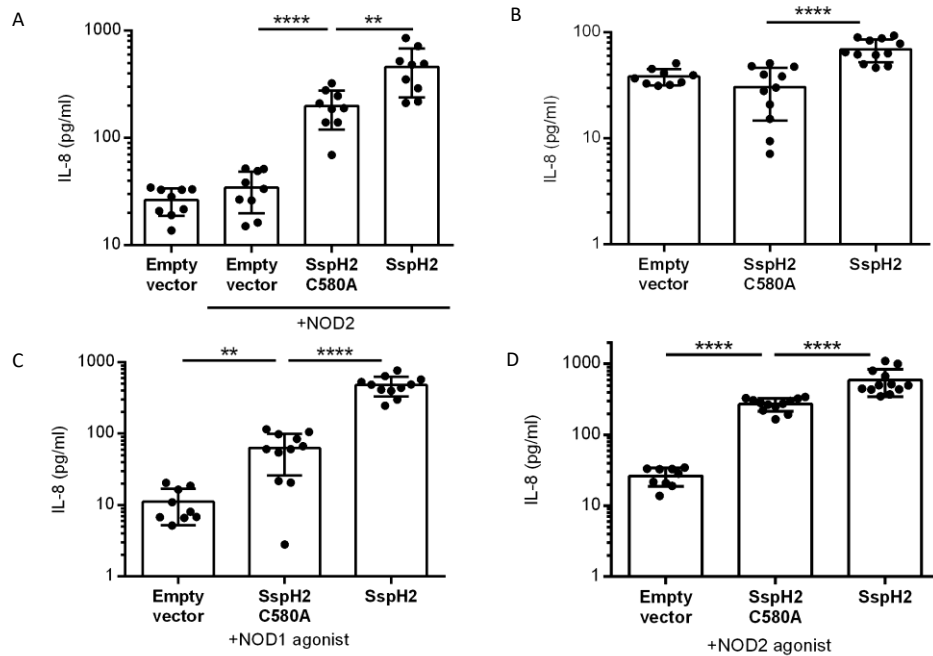
Figure 3.7. SspH2 activity, and SspH2 stimulation in the absence of NOD agonist.

IL-8 secretion assays of plasmids transiently transfected in HeLa cells. **A.** NOD2, SspH2, SspH2C580A (C580A), or empty vector (EV) as indicated in the absence of NOD2 agonist (5µg/mL MDP and 10ng/mL human IFNγ). **B-D.** SspH2, C580A, and EV as indicated, in the absence of agonist; **B)**, presence of NOD1 agonist (1µg/mL cDAP and 10ng/mL human IFNγ); **C)**, and presence of NOD2 agonist (5µg/mL MDP and 10ng/mL human IFNγ); **D)**. Data is presented as the mean with standard deviation for 3-4 biological replicates. Data were analyzed using a non-parametric Mann-Whitney test and ** and **** denote $P < 0.01$, $P < 0.0001$ respectively between the indicated sample groups. See materials and methods for more detail.

3.9 SspH2 interaction with NLRs does not cause poly-ubiquitination *in* vitro

It has been reported that SspH2 creates K48-linked polyubiquitin chains, suggesting that its

targets are meant for proteosomal degradation (202). K48-linked polyubiquitination indicates

proteasomal degradation, which would presumably diminish pro-inflammatory activities of

NLRs, due to reduced levels of NLR proteins in the cell. As I have observed so far, there is no

inhibition of NLR activation. Instead, there is super-activation, which is inconsistent with NLR

degradation. To better understand SspH2 ubiquitination of NOD1 *in vitro* I looked at the

ubiquitination pattern present on NLRs in the presence of SspH2. To do this, I transiently

transfected NLRs with EV/SspH2C580A/SspH2 and ubiquitin into HEK293T cells, and

immunoprecipitated the NLRs to look at their ubiquitination patterns by western blot. I identified

ubiquitination by observing the general staining pattern of ubiquitin on the immunoblots. My

findings indicate that in the presence of transiently transfected NOD1, SspH2, and ubiquitin

there was no distinct ubiquitin smearing, which if present, would indicate poly-ubiquitination.

There is however, a band of ubiquitin above where NOD1 is present, and no loss of NOD1 signal

in the presence of SspH2 compared to EV or SspH2C580A (Fig 3.8A). Furthermore, when

investigating SspH2's interaction of NOD2 in the presence of ubiquitin, there is no distinct

pattern of ubiquitin smearing, and a very faint band above NOD2 in the presence of SspH2,

coupled with a consistent signal intensity around NOD2 in the anti-myc stained western blot (Fig

3.8B). These results are mirrored with NLRP3 (3.8C).

These results are contrary to previously published SspH2 activity *in vitro* which claims that

SspH2 causes poly-ubiquitination when only the proteins are present in the reaction (202). These

findings are however, consistent with the previously reported findings that SspH2 causes mono-

ubiquitination of NOD1 *in vitro*, and does not cause degradation of NOD1 (56). It remains to be

identified whether poly-ubiquitination of these proteins is possible: to do that in cell culture

requires the use of proteasomal inhibitor, which was not used in these experiments. Thus, these data suggest that *in vitro*, SspH2 may cause mono-ubiquitination of multiple NLRs which is not utilized for protein degradation.
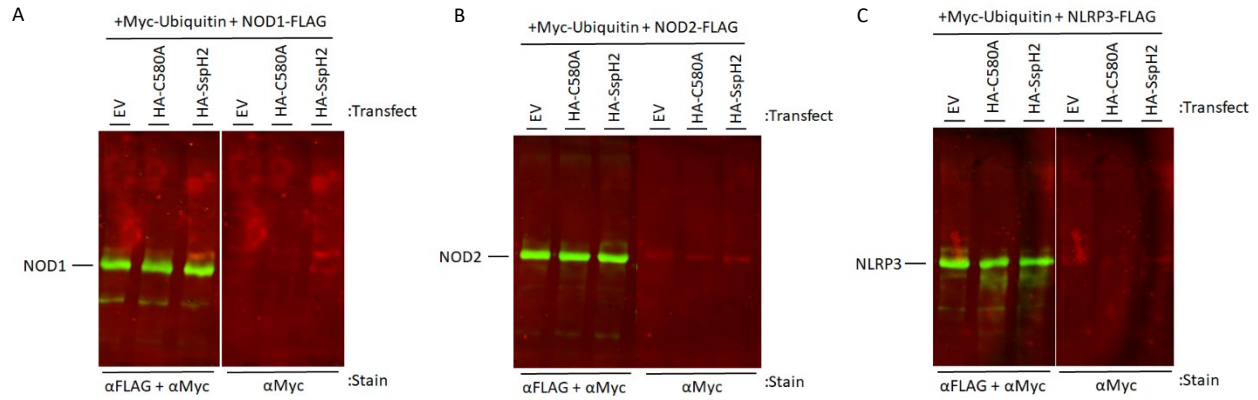
Figure 3.8. Identification of characteristic ubiquitination patterns.

Plasmids were transiently transfected into HEK293T cells, enriched via FLAG IP and subjected to Western blot analysis. All samples had EV, SspH2C580A or SspH2 expressed in them with either NOD1, NOD2, or NLRP3. The NLRs found in each blot are **A.** NOD1, **B.** NOD2, **C.** NLRP3. Immunoblotting was performed with indicated antibodies.

3.10 Identifying ubiquitination of NOD1 due to SspH2.

I next narrowed my focus to NOD1 interaction with SspH2 as a proof of concept. To further elucidate the mechanism by which SspH2 causes increased IL-8 secretion when interacting with NOD1, I identified putative ubiquitination sites on NOD1 via liquid chromatography mass spectrometry (LC-MS/MS). I transiently co-transfected FLAG-tagged NOD1, SspH2 (wt, C580A or empty vector) and ubiquitin in HEK293T cells, and harvested and lysed, the cells. I worked in conjunction with Shu Luo, a PhD student from the Julien lab to IP NOD1using anti-FLAG magnetic beads. Shu Luo then isolated NOD1-enriched sample bands using SDS-PAGE, and performed in-gel digestion with trypsin, followed by LC-MS/MS (Fig 3.9A). To identify ubiquitinated lysines, we searched the resultant peptides for the presence of remnant Gly-Gly motifs on lysine side chains (K-ε-GG), which is derived from the carboxy terminus of ubiquitin after trypsin digestion (203).

The overexpressed NOD1 protein was identified via more than a hundred distinct peptides with a NOD1 sequence coverage of ~80%, which are both very accurate identifiers for mass-spectrometry experiments (O. Julien, personal communication). We found that there were 12 ubiquitination sites in the presence of NOD1 and EV (Fig. 3.9B). There were 23 ubiquitination sites in the presence of SspH2C580A (Fig. 3.9C), and 22 sites on NOD1 in the presence of SspH2 (Fig. 3.9D). Because there were so many ubiquitin sites identified on NOD1 from the different combination of proteins, I first sought to identify ubiquitinated lysines that were uniquely present on in the presence of SspH2. I found one unique lysine on NOD1 at lysine 142 (Fig 3.9D). Through this data, we identified the first evidence of NOD1 ubiquitination in cells, albeit with over-expressed ubiquitin and NOD1, and found a SspH2-specific unique site of ubiquitination.
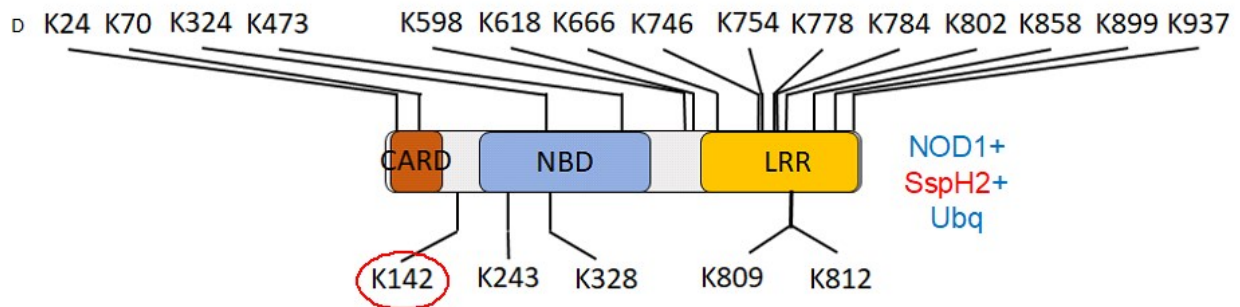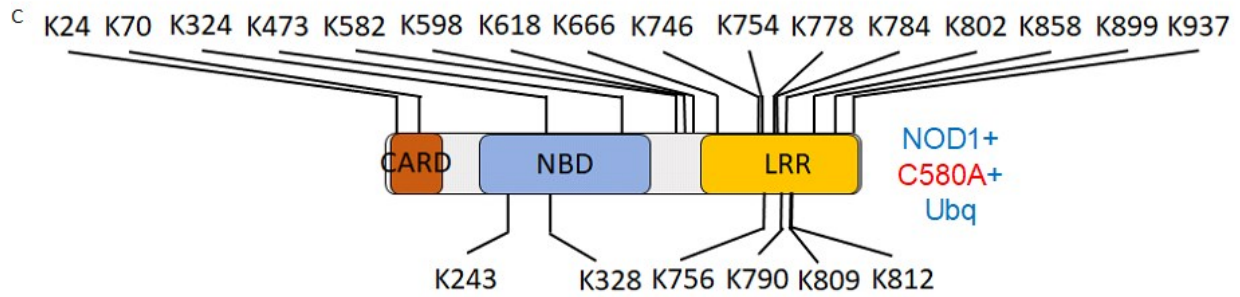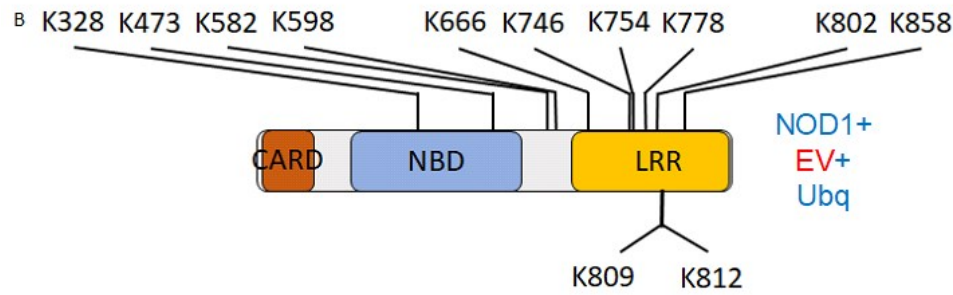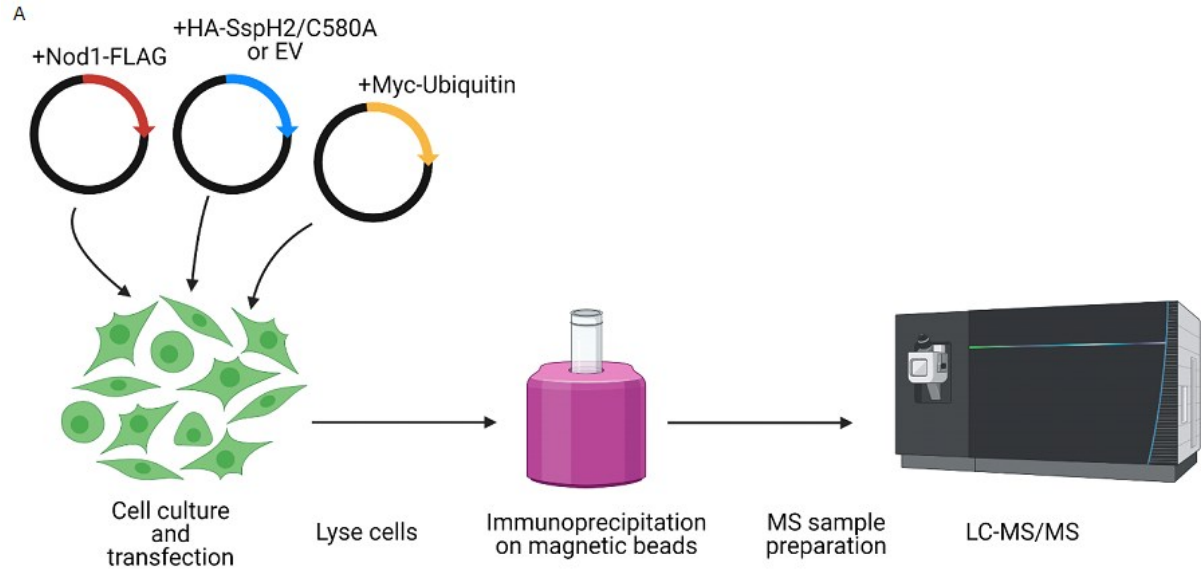
Figure 3.9. Mass spectrometry experimental design, and identification of ubiquitinated lysines between sample types.

A. Schematic diagram of mass spectrometry experiment (created with Biorender.com). All samples had NOD1 and ubiquitin protein transfected into HEK293T cells, and ubiquitination sites were identified by LC-MS/MS. **B.** ubiquitination sites identified with EV. **C.** ubiquitination sites identified with SspH2C580A. **D.** ubiquitination sites identified with SspH2.

3.11 Comparing ubiquitination sites on NOD1.

To ascertain whether any of the other ubiquitination sites on NOD1 were of possible importance for SspH2 activity, I performed a semi-quantitative analysis on the intensities of identical peptides present in all of the sample populations. I compared SspH2 to EV (Fig 3.10A), SspH2C580A to EV (Fig 3.10B) and SspH2 to SspH2C580A (Fig 3.10C). When comparing the maximum intensities found for each ubiquitinated lysine on NOD1, I performed a linear regression and applied a 95% confidence interval, and identified points as significant if they fell outside of the 95% confidence interval. None of the regressions showed a 45-degree association. My data analysis showed that lysines 473 and 746 were at a higher intensity in both SspH2 and SspH2C580A compared to EV (Fig 3.10D). Lysines 778 and 809 were at a lower intensity in both SspH2 and SspH2C580A compared to EV (Fig 3.10D). When I compared SspH2 to C580A, lysine 784 was at a higher intensity in SspH2, and lysine 328 was at a lower intensity in SspH2C580A (Fig 3.10D). Taken together, this gave direction for determining which lysines in NOD1 to mutate to ascertain SspH2 lysine dependency for super-activation.

A

B

C

D

```
        10        20        30        40        50
MEEQGHSEME IIPSESHPHI QLLDSNRELL VTHIRNTQCL VDNLLKNDYF
        60        70        80        90       100
SAEDAEIVCA CPTQPDKVR  ILDLVQSKGE EVSEFFLYLL QQLADAYVDL
       110       120       130       140       150
RPWLLEIGFS PSLLTQSKVV VNTDPVSRYT QQLRHHLGRD S FVLCYAQK
       160       170       180       190       200
EELLLEEIYM DTIMELVGFS NESLGSLNSL ACLLDHTTGI LNEQGETIFI
       210       220       230       240       250
LGDAGVGKSM LLQRLQSLWA TGRLDAGVKF FFHFRCRMFS CF ESDRLCL
       260       270       280       290       300
QDLLFKHYCY PERDPEEVFA FLLRFPHVAL FTFDGLDELH SDLDLSRVPD
       310       320       330       340       350
SSCPWEPAHP LVLLANLLSG KLL GAS LL TARTGIEVPR QFLRKKVLLR
       360       370       380       390       400
GFSPSHLRAY ARRMFPERAL QDRLLSQLEA NPNLCSLCSV PLFCWIIFRC
       410       420       430       440       450
FQHFRAAFEG SPQLPDCTMT LTDVFLLVTE VHLNRMQPSS LVQRNTRSPV
       460       470       480       490       500
ETLHAGRDTL CSLGQVAHRG ME SLFVFTQ EEVQASGLQE RDMQLGFLRA
       510       520       530       540       550
LPELGPGGDQ QSYEFFHLTL QAFFTAFFLV LDDRVGTQEL LRFFQEWMPP
       560       570       580       590       600
AGAATTSCYP PFLPFQCLQG SGPAREDLFK N DHFQFTNL FLCGLLS AK
       610       620       630       640       650
QKLLRHLVPA AALRRKR AL WAHLFSSLRG YLKSLPRVQV ESFNQVQAMP
       660       670       680       690       700
TFIWMLRCIY ETQSQ VGQL AARGICANYL KLTYCNACSA DCSALSFVLH
       710       720       730       740       750
HFPKRLALDL DNNNLNDYGV RELQPCFSRL TVLRLSVNQI TDGGV VLSE
       760       770       780       790       800
ELT Y IVTY LGLYNNQITD VGARYVT IL DEC GLTHL  LGKNKITSEG
       810       820       830       840       850
G YLALAV N S SISEVGMW GNQVGDEGAK AFAEALRNHP SLTTLSLASN
       860       870       880       890       900
GISTEGG SL ARALQQNTSL EILWLTQNEL NDEVAESLAE MLKVNQTL H
       910       920       930       940       950
LWLIQNQITA KGTAQLADAL QSNTGITEIC LNGNLI PEE AKVYEDEKRI
ICF
```

= CARD

= NBD

= LRR

Figure 3.10. Semi quantitative analysis of mass spectrometric intensity values between sample types.

Gly-gly peptides were plotted as a function of their maximum intensities identified by LC-MS/MS and intensities are scaled on the plot to 1×10^{7}. A linear regression, denoted by the solid black line, was generated based upon this analysis and outliers from the 95% CI, denoted by the dashed line, were identified as residues of interest. **A.** comparison of SspH2 to EV. **B.**

comparison of SspH2C580A to EV. **C.** comparison of SspH2 to SspH2C580A. **D.** Summary diagram of amino acid sequence of NOD1 with Caspase Activation Recruitment Domain (CARD), Nucleotide Binding Domain (NBD), and Leucine Rich Repeat (LRR) regions highlighted. Individual lysine residues highlighted in black denote lysine residues that were identified with di-glycyl modifications in any sample. Red denotes di-glycyl residues that were upregulated in SspH2 vs SspH2 C580A. Blue denotes residues that were downregulated in SspH2 compared to SspH2 C580A. Light green denotes di-glycyl residues that were upregulated in both SspH2/ SspH2 C580A over empty vector (EV). Pink denotes di-glycyl residues that were downregulated in both SspH2/ SspH2 C580A over EV. See materials and methods for more details.

3.12 Four lysine residues on NOD1 are critical for its activation by SspH2.

Through my analysis, I selected 19 lysine residues that contained di-glycyl remnants that were identified to be of interest through semi-quantitative mass spectrometry analysis, and to ensure coverage of lysine residues on NOD1 (Fig 3.11A). These lysines were chosen via a hierarchy that put unique lysines first (K142), lysines identified outside of the linear regression (K328, K473, K776, K778, K784, and K809) second, and finally random lysines throughout the protein third.

To assess whether these lysine residues were required for basal NOD1 activity, I individually mutated the lysine residues to arginine to prevent ubiquitination and tested these NOD1 variants in my NOD1 functional assay (Fig. 3.11B). My data indicated that the mutation of lysine residues to arginine had no suppressive effects on the ability of NOD1 to be activated by its agonist (1µg/mL c12-iEDAP and primed by 10ng/mL human IFNγ). Interestingly, the mutation of lysine to arginine of NOD1 at positions 784, 802, and 858 increased IL-8 secretion slightly (Fig. 3.11B). To ensure that the mutation of lysine to arginine does not alter the ability of the NOD1 proteins to be expressed from transiently transfected cells, I confirmed that the NOD1 single lysine variants were detectable via western blot (Fig 3.11C).

To determine whether the mutated lysine to arginine residues were important for SspH2's super-activation of NOD1 activity, I repeated the NOD1 functional assay in the presence of SspH2. Lysine variants in the NOD1 CARD (K24) and NBD (K324, 328, and K473) domains abrogated the enhanced IL-8 secretion phenotype elicited by SspH2 more than 50% (Fig. 3.11D). Lysine variant 784 also decreased IL-8 mediated super-activation by ~30%. This result is modest in comparison to the other lysine mutants, and was not investigated further. It is notable that the

CARD region of NOD1 does not interact with SspH2, yet K24 ubiquitination in the CARD region seems to be important for SspH2-mediated super-activation of NOD1. Even more intriguingly, even though K142 ubiquitination was identified to only be present as a result of SspH2, it does not appear to be critical for super-activation of NOD1 via SspH2. To ensure that mutation of lysine residues 24, 324, 328, or 473 to arginine did not affect the ability of SspH2 to bind to NOD1, I performed reciprocal co-IP from cell lysates co-expressing SspH2 and the variant NOD1 constructs. This analysis indicated that SspH2 continues to interact with NOD1 even when these single lysine residues are mutated into arginine. Taken together, these data further support a model where SspH2 specifically ubiquitinates lysines in the N-terminal CARD and NBD domains of NOD1 to augment its pro-inflammatory signaling (Fig. 3.11A).

A

K24 K70 K324 K328 K473 K598 K618 K666 K746 K754 K778 K784 K802 K858 K899 K937

CARD   NBD   LRR

K142   K243   K328 K756 K790 K809 K812

B

% of Nod1 activation

+NOD1 agonist

EV NOD1 K24R K70R K142R K243R K324R K328R K473R K600R K618R K704R K746R K754R K778R K784R K802R K809R K858R K899R K937R

C

+EV   +EV   +EV

K618R K754R K784R K802R K858R K600R K778R Nod1 EV   K24R K70R K324R K473R K704R K746R K899R K937R Nod1 EV   EV NOD1 K142R K243R K328R K809R

Nod1 —

D

% of Nod1 activation

EV C580A SspH2 K24R K70R K142R K243R K324R K328R K473R K600R K618R K704R K746R K754R K778R K784R K802R K809R K858R K899R K937R
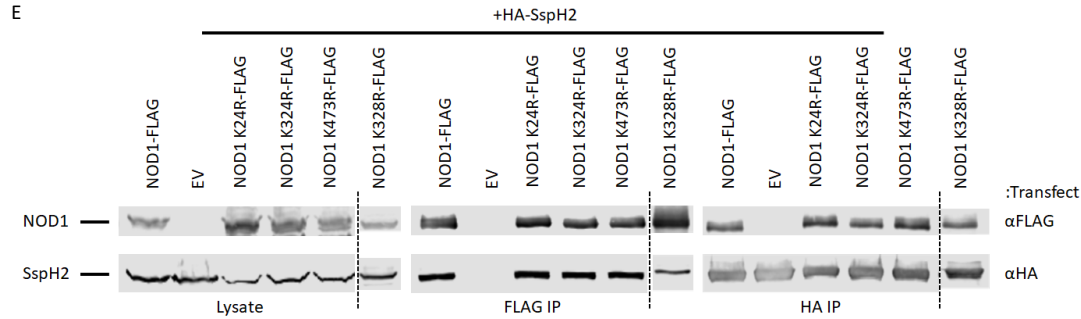
+NOD1   +SspH2
+NOD1 agonist

85

Figure 3.11. NOD1 point mutant activation capacity.

A. Schematic representation of all NOD1 lysines changed to arginine, with points of interest marked in red. **B.** IL-8 secretion assay in HeLa cells transiently expressing NOD1/NOD1 mutants in the presence of NOD1 agonist (1μg/mL cDAP and 10ng/mL human IFNγ). The dotted line represents the 100% activation level. **C.** Protein expression of NOD1 lysine variants or empty vector (EV) transiently expressed in HEK293T cells. NOD1 lysine variants were tagged with FLAG. Immunoblotting was performed with FLAG antibodies. **D.** IL-8 secretion assay in HeLa cells transiently expressing NOD1/NOD1 mutants in the presence of NOD1 agoinst (1μg/mL cDAP and 10ng/mL human IFNγ) and SspH2. The dotted line represents the 100% activation level. **E.** Reciprocal co-IP analysis of NOD1 lysine variants with SspH2 transiently expressed in HEK293T cells. NOD1 point mutants were tagged with FLAG. IPs and immunoblotting were performed with indicated antibodies. Data is presented as the mean with upper limit of standard deviation for 3-5 biological replicates. Data were analyzed using a One-way ANOVA, *, **, ***, and **** denote P < 0.01, P < 0.005, P < 0.001, and P < 0.0001 respectively between the indicated sample groups. See materials and methods for more details. Dashed line indicates samples run on another gel.

CHAPTER 4 – DISCUSSION

4.1 Summary of results.

Throughout my studies, I have used cell culture to uncover novel aspects of *Salmonella* bacterial effector biology. Using co-immunoprecipitations, I report that SspH2 is able to interact with 3 different tripartite NLRs: NOD1, NOD2, and NLRP3. Both SspH2-LRR and SspH2-NEL regions are able to interact with all 3 of these NLRs. Furthermore, the NBD, and LRR regions of NOD1 facilitate this interaction with SspH2. Using IL-8 ELISAs I was next able to demonstrate that SspH2 super-activates NOD1 and NOD2 in the presence of their respective agonists. The super-activation was mediated, in-part, by NF-κB activation. After identifying the binding capacities and functional consequences of SspH2 inside of host cells, I next looked at how SspH2 could be super-activating NLRs. I found that SspH2 does not elicit normal poly-ubiquitination characteristics when interacting with NLRs, and there is no apparent loss of NLR signal. However, SspH2 may be mono-ubiquitinating multiple NLRs to cause their super-activation. Using LC-MS/MS, I next looked at ubiquitination specifically on NOD1. I found, for the first time that NOD1 shows patterns of ubiquitination on its own. I further found that there was SspH2-specific ubiquitination occurring on NOD1, and that some ubiquitin sites showed stronger relative signal intensities in the presence of SspH2. However, the lysine residues highlighted from LC-MS/MS required further validation analyses to identify important lysine residues. I mutated all lysine residues of interest identified with LC-MS/MS, and found that 4 sites in the NBD and CARD regions of NOD1 were important for SspH2-induced super-activation (Fig. 4.1).

4.2 SspH2 interacts with multiple NLRs.

One of the most fascinating aspects of my findings is the multiple different ways that SspH2 can engage with the host immune system. It was known previously that SspH2 could interact with

the NOD1 receptor (56), but there was no knowledge on whether it was able to interact with other NLRs. It is known previously that SspH2 can interact with multiple other proteins inside of the host cell, such as: UbcH5 (57), and SGT1 (56). However, my findings show that SspH2 can interact with NOD1, NOD2, and NLRP3, insinuating that it facilitates a multi-factorial approach to mediating pathogenesis.

Since SspH1 is able to interact with PKN1 via its LRR domain (204), and the LRR domain of SspH2 mediated interaction with SGT1 (56), I thought that perhaps the LRR domain of SspH2 may be mediating its interaction with the NLRs. From IP experiments, I found that both the LRR and NEL domains of SspH2 were responsible for interaction with NOD1, NOD2, and NLRP3. This was unexpected, as documented protein interactions with NOD1 and NOD2 are via homotypic interaction (e.g. homotypic CARD interactions with RIP2) and the LRR is known to sense pathogens (205), and be used for interaction with HSP70/90 (118).

Given that SspH2 super-activates NOD1 (56), and that the CARD region of NOD1 is required for downstream signaling by interacting with RIP2 (108, 116), it could be assumed that SspH2 might be interacting with this domain. It also could be reasoned that because the LRR domain is used to sense bacterial subunits like iE-DAP (117), SspH2 may be interacting solely with the LRR domain. By utilizing co-IP to investigate the interaction of NOD1 domains with SspH2, I was able to find that CARD is actually the only NOD1 domain that SspH2 does NOT interact with and SspH2 interacts with NOD1 NBD and LRR. Furthermore, the fact that SspH2 interacts with 2 domains is interesting to note. It remains to be seen which domain of SspH2 interacts with which domain of NOD1. This could be done as a future experiment using the same constructs outlined above in my thesis to further elucidate the interaction mechanisms of SspH2. It would also be interesting to see whether these binding characteristics were the same for NOD2 and

NLRP3, or whether the introduction of an additional CARD region (in NOD2) or the pyrin domain (in NLRP3) altered the binding pattern.

The physiological importance of these interactions during a *S.* typhimurium infection remains to be determined. To identify whether these protein interactions are present during human cell infection, fluorescently-tagged SspH2 could be expressed in *S.* typhimurium and used to infect human gut epithelial cells that express different fluorescently-tagged NLRs. The cells could then be imaged to identify any overlap of the fluorescent signals to verify if these protein interactions occur in human cell infection.

4.3 SspH2 super-activates multiple NLRs.

Upon interacting with NOD1, SspH2 has been shown to super-activate NOD1, inducing higher than normal IL-8 secretion (56). Since SspH2 interacts with multiple different NLRs, I wanted to know whether this super-activation was similar when interacting with NOD2, and NLRP3. SspH2 is able to super-activate both NOD1 and NOD2. The super-activation of NOD2 is present with or without NOD2 agonist. NOD1 is super-activated to induce ~3x more IL-8 secretion, while NOD2 is super-activated to induce ~10x more IL-8 secretion. SspH2C580A was also able to induce some additional super-activation of NOD2, which was not the case in NOD1. This may hint that there is possibly something about the physical nature of SspH2 that can cause super-activation of NOD2. One notable difference between NOD1 and NOD2 is that NOD2 has two CARD motifs (134), compared to the single CARD motif in NOD1 (111). This difference could possibly contribute to the change in IL-8 secretion magnitudes, but there may also be different protein interaction patterns or ubiquitination of NOD2 which may contribute to this observed difference in activations.

4.4 SspH2 activity is mediated in part through NF-κB.

The NF-κB pathway is subject to much regulation by multiple proteins injected into host cells by *Salmonella,* such as GogB, SpvB, SseK1-3, SspH1 and SspH2 (206). The only protein that is not encoded by SPI-I, and does not inhibit NF-κB activity, is SspH2. It is interesting to note that even though SspH1 and SspH2 are very similar in sequence (~70% sequence homology), and target the same pathway, they have opposing NF-κB pathway functions (207). Other examples of *Salmonella* effector proteins with antagonistic functions, *e.g.,* SptP antagonism of the SopE/SopE2/SopB, are well-studied and suggest that dynamic regulation of critical host cell processes is important to *Salmonella* pathogenesis (206).

I was able to infer that NOD1 and NOD2 super-activation is mediated in part by NF-κB by inhibiting NF-κB signaling from both NLRs with Bay11. BAY11 irreversibly inhibits NF-κB activation by blocking the phosphorylation of IκBα, which suppresses the nuclear translocation of p65 and its binding to NF-κB response elements, thus effectively preventing pro-inflammatory cytokine production (200, 201). I found that NOD1 super-activation was completely abrogated in NOD1, but NOD2 is only inhibited ~3 fold by Bay11. This could be interpreted to mean that the other 6-7 fold increase over baseline could be due to an alternative pathway which results in IL-8 secretion. This could possibly be caused by MAPK activation, which is also activated by NOD2 (208). This could be tested by utilizing a MAPK phosphorylation western blot from cells transfected with NOD2 and SspH2, and stimulated with NOD2 agonist. This could also be tested by blocking the MAPK pathway with inhibitors of MAPK P38 like SB203580, SB202190, or BIRB-796 (209).

4.5 SspH2 ubiquitination of other host proteins.

When *S.* typhimurium infects host epithelial cells it alters not only the actin architecture to facilitate invasion of the cell, but it also greatly alters the host ubiquitinome. It has been reported that this infection mediates ubiquitination-mediated Rho GTPase (e.g. CDC42, and LUBAC) and NF-κB activities. It is known that SspH2 can interact with actin cytoskeletal components such as filamin (58). It has also been found that in HEK293T cells, SspH2 was found to be able to ubiquitinate actin cytoskeletal/co-chaperone proteins like ACTR8, ARPC5, FLNA, MYH9, and SGT1 (210). In this paper, the authors utilize mass spectrometry targeting di-glycyl proteomics to systematically and quantitatively monitor the changes in the host epithelial cell ubiquitinome in response to *S.* typhimurium infection. Their results insinuate that SspH2 does not ubiquitinate NLRs during bacterial infection in epithelial cells. An alternative reading of this could also be that they simply were unable to identify di-glycyl sites on NLRs during their mass spectrometry analysis. This is notable because the NLRs in this study were not over-expressed. Meanwhile, in *Yersinia pestis*, the bacterial E3 ligase, YopM, has been observed to decrease NLRP3 activation via K63 linked ubiquitination of NLRP3 (211). YopM is an unconventional E3 ubiquitin ligase, which contains an LRR domain, but no NEL domain (102).

It is notable that while there are reports that NLR signaling can be regulated by ubiquitination, there have been no reports of direct ubiquitination on NLRCs. NOD1 and NOD2 interact with host proteins to mediate downstream activation of NF-κB through homotypic CARD domain interaction with RIP2 (106, 114, 134, 135). This process involves many proteins interacting with RIP2 to increase or decrease signaling capacity to maintain appropriate levels of inflammatory activation. Polyubiquitination of RIP2 by host E3 ligases, *e.g.* XIAP, cIAP1/2, ITCH, and Pellino3 induces RIP2 activation upon NOD1/NOD2 stimulation (114, 134, 135). The

deubiquitinase proteins A20, OTULIN, and CYLD remove ubiquitin from RIP2 to repress its activation (130, 212, 213). Once RIP2 is ubiquitinated, TAK1 is recruited to phosphorylate IκBα of the IKK complex, leading to NF-κB translocation to the nucleus and production of pro-inflammatory cytokines (128). These conserved host signaling pathways downstream of receptors are where bacterial E3 ligases like IpaH4.5 and SspH1 usually modulate inflammation (214, 215). On the other hand, NLRP3 inflammasome activity can be regulated by host proteins through modification with ubiquitin. Ubiquitination via Pellino2 (216), and de-ubiquitination on the NLRP3 LRR domain via BRCC3 (212, 217) have been shown to activate NLRP3. Alternatively, de-ubiquitination via IRAK1 (216), and ubiquitination by TRIM31 have also been shown to decrease NLRP3 activity by inducing proteasomal degradation in the case of the latter (218).

It has been reported that SspH2 creates K48-linked polyubiquitin chains, suggesting that its targets are meant for proteosomal degradation (202). However, when identifying ubiquitin via immunoblot analysis from samples with ubiquitin and NLR, I did not observe the characteristic smear of poly-ubiquitination. This infers that SspH2 is mono-ubiquitinating NLRs to mediate its function, consistent with previously reported findings (56). In my experimental workflow with LC-MS/MS, I anticipated detecting enhanced, or differential ubiquitination of NOD1 in the presence of catalytically active SspH2 to mediate super-activation (52). Due to the absence of markedly identifiable increases in Gly-Gly lysine remnants (K-ε-GG) following trypsin digestion of NOD1, this suggests that ubiquitination by SspH2 is nuanced. I did however, find one ubiquitinated lysine that was present only in SspH2 at K142. I next looked at the semi-quantitative analysis of LC-MS/MS intensities, which revealed that the majority of the ubiquitinated lysines with statistically significant differential intensities between C580A and

SspH2 occurred in the LRR domain of NOD1. Surprisingly, I found that mutation of lysines in the LRR domain had little effect on SspH2's capacity to increase pro-inflammatory production. There are accounts that NOD1 can interact with ubiquitin at tyrosine 88 and glutamate 84 in the CARD region, and NOD2 interacts at the corresponding CARD region sites, isoleucine 104 and leucine 200. This binding of ubiquitin is distinct from post-translational ubiquitin modification, and prevents RIP2 binding to NLRs, to negatively regulate signaling (130, 131). There are also predictions of ubiquitin binding at K436 and K445 on NOD2 (130).

Out of the lysines mutated in the NDB and CARD regions, only 2/6 retained the ability to super-activate with SspH2. In the NBD region, all of the C-terminal lysines mutated (K324, K328 & K473) showed statistically significant decreases in SspH2-mediated super-activation. K324, 328, and K473 were all shown to be able to be expressed in cell culture and interact with SspH2. Based off of the identified NOD1 lysines that abrogate SspH2-super-activation, it could by hypothesized that all of these Lysines (K24, K324, K328, and K473) are all in proximity to each other. K784 is a specifically interesting lysine, as it exhibits increased basal activation and ~30% decrease in super-activation with SspH2. This reduction is modest when compared to the other lysine mutants (K24, K324, K328, and K473) that showed >50% reduction in SspH2- mediated super-activation. This lysine might be important for SspH2 interaction with SspH2 in the LRR domain. A more definitive answer could be obtained by using x-ray crystallography to visualize how NOD1 and SspH2 interact with one another.

My ubiquitination analyses focused on NOD1; thus, it is unclear if SspH2 would target both NOD2 CARD domains for ubiquitination. Further LC-MS/MS investigation are required to study this possibility. Due to the ability of SspH2 to interact with multiple NLRCs, it is tempting to

93

speculate that it interacts with other proteins within this family, or even across NLR families e.g., NLRP3.

4.6 Lysine placement on theoretical crystal structure of NOD1.

The theoretical protein structure of NOD1 has recently been released using artificial intelligence to predict, with great accuracy based on its ability to correctly identify already modeled proteins, how proteins would fold in 3D space (219). In this model, the lysines that were identified through mass-spectrometry are highlighted. The colours of the lysines correlate with where in NOD1 they are found: yellow is the CARD region, blue is the NBD region, and green is the LRR domain. 3 lysines, K324, K328, and K473 are present on the same plane, where K324 and K473 are both solvent exposed, and K328 is oriented into the protein. This incidence of lysines that are statistically significant for NOD1 super-activation being in the same plane is particularly interesting. This localization could suggest that this highlighted area in the NBD region is where the catalytic cysteine of SspH2 is exerting the majority of its activity, and could be where the NEL region of SspH2 is specifically binding to.

This hypothesis could be further tested by investigating which of the two individual domains of SspH2 is interacting with the NOD1 NBD region through co-IP. This interaction could be further investigated by using X-ray crystallography to fully elucidate where NOD1 NBD and SspH2 fully interact with one another. Being able to assess this information would give a greater understanding of how NELs could be interacting with NLRs, and allow for possible pharmacological treatments to be formulated.
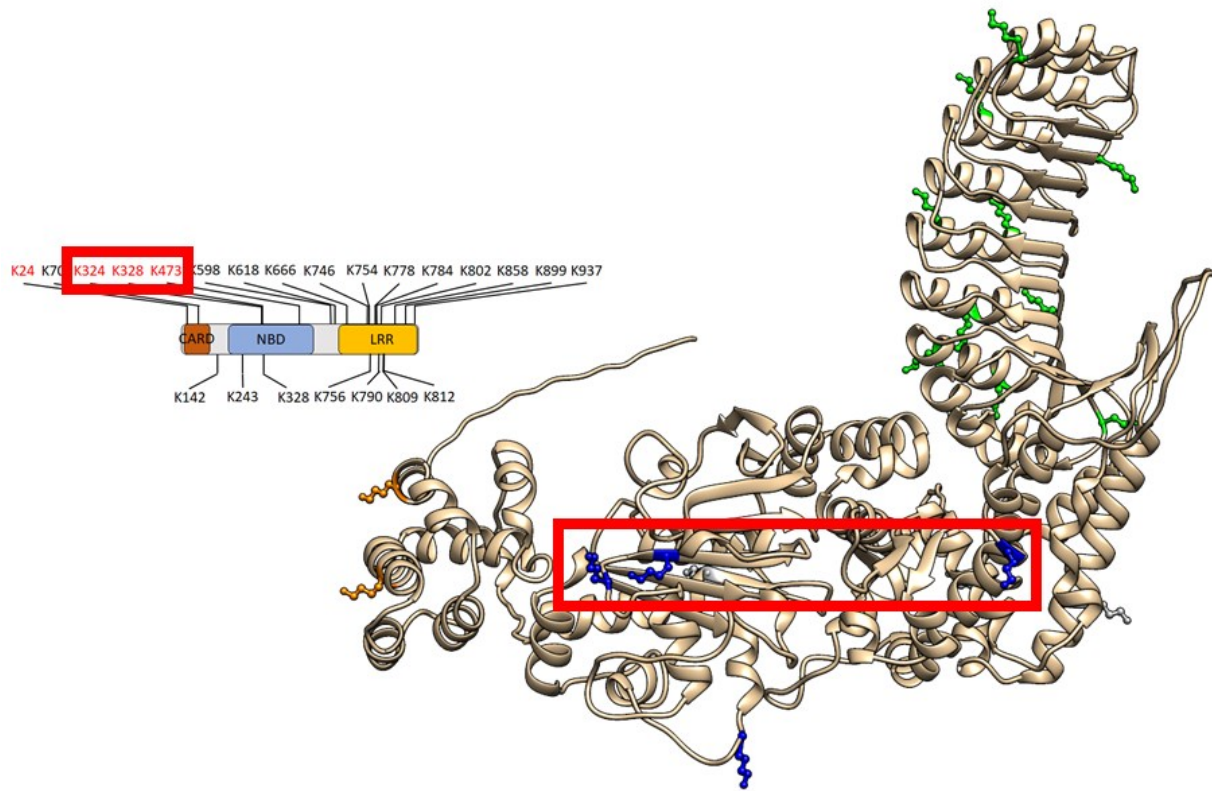
Figure 4.1. Lysine location on theoretical model of NOD1.

Conceptual domain model and theoretical structure of NOD1 using the AlphaFold modeling

system (219). The coloured amino acids are lysines found throughout NOD1. Lysine colour

correlates to which domain it is found in: yellow is the CARD region, blue is the NBD region,

and green is the LRR domain Outlined in red are the position of lysines, whose mutation reduces

NOD1 super-activation by SspH2.

4.7 THP-1 NLRP3 activation assay.

To further elucidate how SspH2 interacted with NLRs in the host cell, I sought to investigate the functional effects of SspH2 interaction with NLRP3. I initially looked to use a cell model that would allow me to recapitulate the NLRP3 inflammasome. THP1 cells are a model cell line to do this in an immune cell context. I was able to procure NLRP3 KO cells from the Muruve lab from University of Calgary, which had previously been used to identify NLRP3 function (194). I hoped to use them to be able to investigate how SspH2 affects cells that lack NLRP3, and compare these findings to cells expressing endogenous levels of NLRP3. This gives the benefit of seeing exactly how SspH2 could function inside of immune cells that would normally be targeted by *S.* typhimurium infection. However, I was unable to get a robust working system established for investigating the effect of SspH2 on NLRP3 using CRISPR edited THP1 cells. This avenue of investigation is an obvious next step in further exploring the effect of SspH2 on NLRs. NOD2 has been reported to interact with NLRP3 (135), so investigation into this pathway would be an interesting link between all of these NLRs.

I have already optimized the culturing and stimulation conditions for THP1 cells, but I believe that using non-edited THP1 cells may prove to be more fruitful. This is because non-edited cells could be heartier, as they have not been genetically modified, and thus be less susceptible to cell death following uptake of new genetic materials. I did not compare these CRISPR-modified cells to non-edited cells, so it remains to be seen. However, after transfecting the CRISPR-modified cells, I observed through microscopy that there are fewer adherent cells, compared to non-transfected cells. By being able to successfully transfect SspH2 into these cells, one could investigate how SspH2 could affect the inflammasome. If THP1 cells are unable to be used, there are also other methods of investigating inflammasome activation. For example, HEK293T cells

can be utilized to study inflammasome activation by transiently expressing all of the required components and then identifying IL-1β secretion (220).

4.8 Additional considerations.

NOD1 and NOD2 proteins are also known to interact with other proteins that affect their stability and functional capacities called chaperones (208). Some of these chaperones include HSP70/90 and SGT1 (208). I did not investigate the effect that SspH2 has on these proteins, or even whether SspH2 can interact with them at all. It is known however, that SspH2 does interact with SGT1 (56). This could also be a further avenue of study to fully explore the effect that SspH2 has on host NLRs.

Since my thesis was done in a cell culture model, it has the limitations of being restricted to biochemical functions. Further experiments could investigate the systemic effects of SspH2 interaction with NOD1/NOD2/NLRP3 during *S.* Typhimurium infection utilizing a mouse model. It would be interesting to speculate how blocking or interrupting the NLR mediated function during *S.* Typhimurium infections would affect the course of infection. This could be performed by creating NOD1/NOD2 specific inhibiting drugs to block this interaction, and seeing how well the mice were able to clear infection. The independent effects of SspH2 could be identified by utilizing a ΔSspH2 or SspH2C580A *S.* typhimurium mutant, and comparing it to wild-type infections with the NLR blocking drugs.

4.9 Final Conclusion.

Throughout my thesis, I make the novel discovery that SspH2, a *bona fide* member of the NEL family (102, 221), interacts with multiple members of the NLRC family to enhance pro-inflammatory signaling that result from targeted ubiquitination. Here, I report that the interaction

between the *S.* typhimurium E3 ubiquitin ligase SspH2 and NOD1 is facilitated by the NBD and LRR domains of NOD1. The interaction of SspH2 and NOD1 super-activates NOD1 signaling, and corroborates what we had found in our previous study (56). This super-activation is mediated through SspH2 specifically ubiquitinating NOD1 on lysine residues in the CARD and NBD regions of NOD1 (Fig. 4.1).

To my knowledge, this is the first report that mechanistically links NEL effector activity to functional enhancement of an NLR. Though my cell culture studies do not unequivocally demonstrate that SspH2 directly ubiquitinates NOD1, the report that YopM directly ubiquitinates NLRP3 (211) suggests that SspH2 might also work in a direct fashion. When NOD1 activates, it undergoes a structural change whereby its LRR domain un-inhibits access to its CARD and NBD regions (114), It remains to be seen what ubiquitination of NOD1 does to physically alter NOD1 and its ability to interact with other proteins in the cell but several models can be envisioned. One possibility is that by binding and ubiquitinating NOD1, SspH2 is mediating increased affinity between NOD1 and its agonist, thereby enhancing activation. Ubiquitination of NOD1 could also cause NOD1 to oligomerize more readily, allowing for enhanced interaction with downstream effectors. Another possibility is that ubiquitinating NOD1 in the vicinity of adapter binding sites, could alter interaction dynamics with RIP2, leading to increased IL-8 secretion (Fig. 4.2). Further study of protein visualization techniques like cryo-EM are required to discern between these models. My current work has illustrated the sophisticated nature of bacterial pathogenesis, and sheds new light on the mechanism by which a traditionally antimicrobial pathway is subverted for pathogenesis.
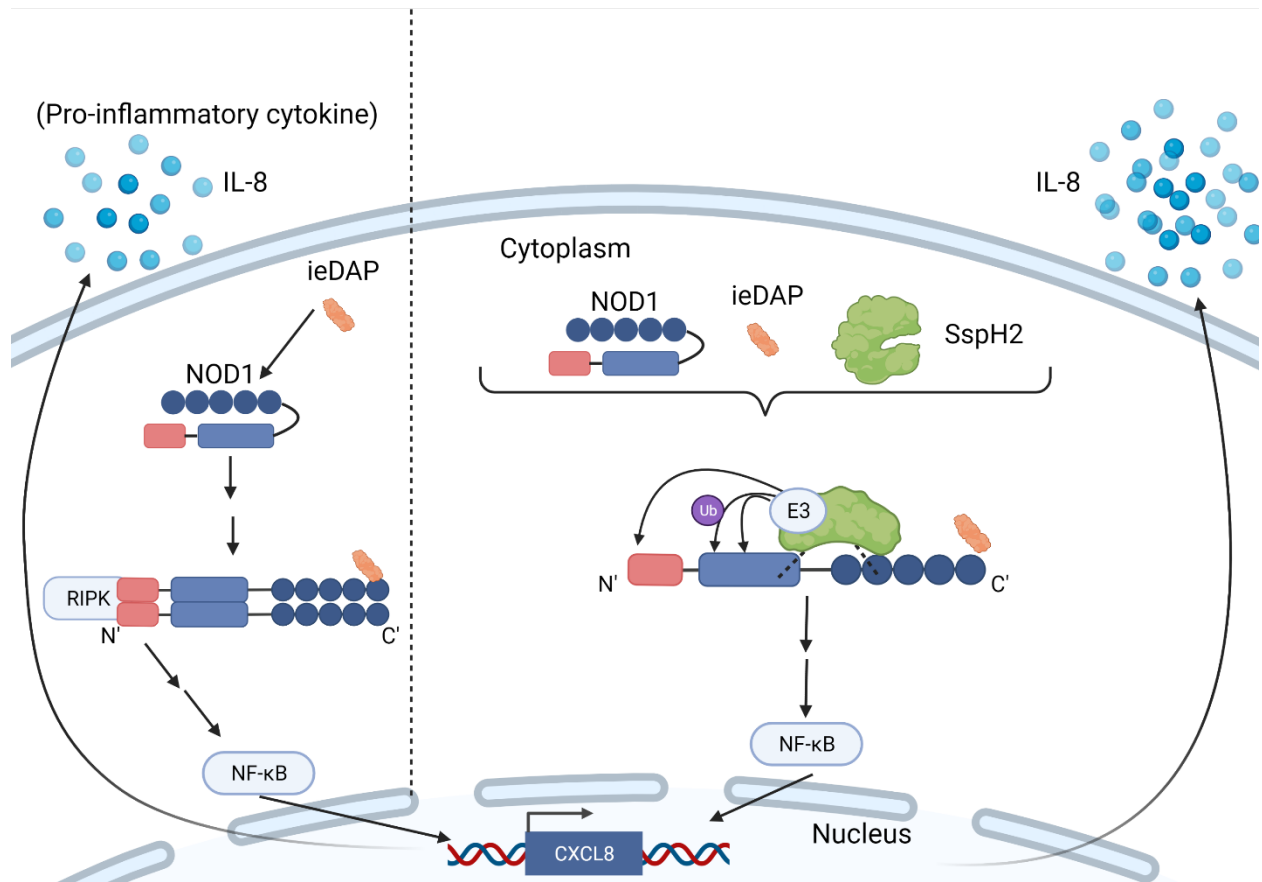
Figure 4.2. Model of SspH2 activation of NOD1 inside the cell.

(left) normal NOD1 activation from interaction with ieDAP, resulting in secretion of IL-8 cytokines. (right) NOD1 super-activation in the presence of SspH2. SspH2 interacts with the NBD and LRR domains of NOD1, and acts upon lysine residues in the CARD and NBD domains to super-activate NOD1 and cause increased IL-8 secretion.

REFERENCES

1. **Jajere, SM.** 2019. A review of Salmonella enterica with particular focus on the pathogenicity and virulence factors, host specificity and antimicrobial resistance including multidrug resistance. Vet. World. **12:**504-521. doi: 10.14202/vetworld.2019.504-521 [doi].

2. **Gal-Mor, O, Boyle, EC, Grassl, GA.** 2014. Same species, different diseases: how and why typhoidal and non-typhoidal Salmonella enterica serovars differ. Front. Microbiol. **5:**391. doi: 10.3389/fmicb.2014.00391 [doi].

3. **Crum-Cianflone, NF.** 2008. Salmonellosis and the gastrointestinal tract: more than just peanut butter. Curr. Gastroenterol. Rep. **10:**424-431. doi: 10.1007/s11894-008-0079-7 [doi].

4. **Chlebicz, A, Śliżewska, K.** 2018. Campylobacteriosis, Salmonellosis, Yersiniosis, and Listeriosis as Zoonotic Foodborne Diseases: A Review. Int. J. Environ. Res. Public. Health. **15:**863. doi: 10.3390/ijerph15050863. doi: 10.3390/ijerph15050863 [doi].

5. **World Health Organization.** 2018. Salmonella (non-typhoidal). .

6. **Kurtz, JR, Goggins, JA, McLachlan, JB.** 2017. Salmonella infection: Interplay between the bacteria and host immune system. Immunol. Lett. **190:**42-50. doi: S0165-2478(17)30201-8 [pii].

7. **Wemyss, MA, Pearson, JS.** 2019. Host Cell Death Responses to Non-typhoidal Salmonella Infection. Front. Immunol. **10:**1758. doi: 10.3389/fimmu.2019.01758 [doi].

8. **Broz, P, Ohlson, MB, Monack, DM.** 2012. Innate immune response to Salmonella typhimurium, a model enteric pathogen. Gut Microbes. **3:**62-70. doi: 10.4161/gmic.19141 [doi].

9. **Raffatellu, M, Chessa, D, Wilson, RP, Dusold, R, Rubino, S, Bäumler, AJ.** 2005. The Vi capsular antigen of Salmonella enterica serotype Typhi reduces Toll-like receptor-dependent interleukin-8 expression in the intestinal mucosa. Infect. Immun. **73:**3367-3374. doi: 73/6/3367 [pii].

10. **Herrero-Fresno, A, Olsen, JE.** 2018. Salmonella Typhimurium metabolism affects virulence in the host - A mini-review. Food Microbiol. **71:**98-110. doi: S0740-0020(16)31082-6 [pii].

11. **Wagner, C, Hensel, M.** 2011. Adhesive mechanisms of Salmonella enterica. Adv. Exp. Med. Biol. **715:**17-34. doi: 10.1007/978-94-007-0940-9_2 [doi].

12. **Jones, BD, Ghori, N, Falkow, S.** 1994. Salmonella typhimurium initiates murine infection by penetrating and destroying the specialized epithelial M cells of the Peyer's patches. J. Exp. Med. **180:**15-23. doi: 94275367 [pii].

13. **Jepson, MA, Collares-Buzato, CB, Clark, MA, Hirst, BH, Simmons, NL.** 1995. Rapid disruption of epithelial barrier function by Salmonella typhimurium is associated with structural

modification of intercellular junctions. Infect. Immun. **63:**356-359. doi: 10.1128/iai.63.1.356-359.1995 [doi].

14. **Vazquez-Torres, A, Jones-Carson, J, Bäumler, AJ, Falkow, S, Valdivia, R, Brown, W, Le, M, Berggren, R, Parks, WT, Fang, FC.** 1999. Extraintestinal dissemination of Salmonella by CD18-expressing phagocytes. Nature. **401:**804-808. doi: 10.1038/44593 [doi].

15. **Ohteki, T, Suzue, K, Maki, C, Ota, T, Koyasu, S.** 2001. Critical role of IL-15-IL-15R for antigen-presenting cell functions in the innate immune response. Nat. Immunol. **2:**1138-1143. doi: ni729 [pii].

16. **Niess, JH, Brand, S, Gu, X, Landsman, L, Jung, S, McCormick, BA, Vyas, JM, Boes, M, Ploegh, HL, Fox, JG, Littman, DR, Reinecker, HC.** 2005. CX3CR1-mediated dendritic cell access to the intestinal lumen and bacterial clearance. Science. **307:**254-258. doi: 307/5707/254 [pii].

17. **Tahoun, A, Mahajan, S, Paxton, E, Malterer, G, Donaldson, DS, Wang, D, Tan, A, Gillespie, TL, O'Shea, M, Roe, AJ, Shaw, DJ, Gally, DL, Lengeling, A, Mabbott, NA, Haas, J, Mahajan, A.** 2012. Salmonella transforms follicle-associated epithelial cells into M cells to promote intestinal invasion. Cell. Host Microbe. **12:**645-656. doi: S1931-3128(12)00354-X [pii].

18. **Raffatellu, M, Wilson, RP, Chessa, D, Andrews-Polymenis, H, Tran, QT, Lawhon, S, Khare, S, Adams, LG, Bäumler, AJ.** 2005. SipA, SopA, SopB, SopD, and SopE2 contribute to Salmonella enterica serotype typhimurium invasion of epithelial cells. Infect. Immun. **73:**146-154. doi: 73/1/146 [pii].

19. **Zhang, K, Riba, A, Nietschke, M, Torow, N, Repnik, U, Pütz, A, Fulde, M, Dupont, A, Hensel, M, Hornef, M.** 2018. Minimal SPI1-T3SS effector requirement for Salmonella enterocyte invasion and intracellular proliferation in vivo. PLoS Pathog. **14:**e1006925. doi: 10.1371/journal.ppat.1006925 [doi].

20. **Blocker, A, Jouihri, N, Larquet, E, Gounon, P, Ebel, F, Parsot, C, Sansonetti, P, Allaoui, A.** 2001. Structure and composition of the Shigella flexneri'needle complex', a part of its type III secreton. Molecular Microbiology. **39:**652-663. doi: 10.1046/j.1365-2958.2001.02200.x. https://onlinelibrary.wiley.com/doi/abs/10.1046/j.1365-2958.2001.02200.x.

21. **Kubori, T, Matsushima, Y, Nakamura, D, Uralil, J, Lara-Tejero, M, Sukhan, A, Galán, JE, Aizawa, S.** 1998. Supramolecular Structure of the Salmonella typhimurium Type III Protein Secretion System. Science. **280:**602-605. doi: 10.1126/science.280.5363.602. http://www.sciencemag.org/cgi/content/abstract/280/5363/602.

22. **Deng, W, Marshall, NC, Rowland, JL, Mccoy, JM, Worrall, LJ, Santos, AS, Strynadka, NCJ, Finlay, BB.** 2017. Assembly, structure, function and regulation of type III secretion systems. Nature Reviews. Microbiology. **15:**323-337. doi: 10.1038/nrmicro.2017.20. https://www.ncbi.nlm.nih.gov/pubmed/28392566.

23. **Abby, SS, Rocha, EPC.** 2012. The Non-Flagellar Type III Secretion System Evolved from the Bacterial Flagellum and Diversified into Host-Cell Adapted Systems. PLoS Genetics. **8:**e1002983. doi: 10.1371/journal.pgen.1002983.s017. https://hal-pasteur.archives-ouvertes.fr/pasteur-01374947.

24. **Burkinshaw, BJ, Strynadka, NCJ.** 2014. Assembly and structure of the T3SS. BBA - Molecular Cell Research. **1843:**1649-1663. doi: 10.1016/j.bbamcr.2014.01.035. https://www.sciencedirect.com/science/article/pii/S0167488914000470.

25. **Gaytán, MO, Martínez-Santos, VI, Soto, E, González-Pedrajo, B.** 2016. Type Three Secretion System in Attaching and Effacing Pathogens. Frontiers in Cellular and Infection Microbiology. **6:**129. doi: 10.3389/fcimb.2016.00129/full. https://www.ncbi.nlm.nih.gov/pubmed/27818950.

26. **Wagner, S, Grin, I, Malmsheimer, S, Singh, N, Torres-Vargas, CE, Westerhausen, S.** 2018. Bacterial type III secretion systems: a complex device for the delivery of bacterial effector proteins into eukaryotic host cells. FEMS Microbiology Letters. **365:**. doi: 10.1093/femsle/fny201. https://www.ncbi.nlm.nih.gov/pubmed/30107569.

27. **Sabbagh, SC, Forest, CG, Lepage, C, Leclerc, JM, Daigle, F.** 2010. So similar, yet so different: uncovering distinctive features in the genomes of Salmonella enterica serovars Typhimurium and Typhi. FEMS Microbiol. Lett. **305:**1-13. doi: 10.1111/j.1574-6968.2010.01904.x [doi].

28. **Wassenaar, TM, Gaastra, W.** 2001. Bacterial virulence: can we draw the line? FEMS Microbiol. Lett. **201:**1-7. doi: S0378-1097(01)00241-5 [pii].

29. **Galán, JE.** 1996. Molecular genetic bases of Salmonella entry into host cells. Mol. Microbiol. **20:**263-271. doi: 10.1111/j.1365-2958.1996.tb02615.x [doi].

30. **Marcus, SL, Brumell, JH, Pfeifer, CG, Finlay, BB.** 2000. Salmonella pathogenicity islands: big virulence in small packages. Microbes Infect. **2:**145-156. doi: S1286-4579(00)00273-2 [pii].

31. **Jajere, SM.** 2019. A review of Salmonella enterica with particular focus on the pathogenicity and virulence factors, host specificity and antimicrobial resistance including multidrug resistance. Veterinary World. **12:**504-521. doi: 10.14202/vetworld.2019.504-521. https://pubmed.ncbi.nlm.nih.gov/31190705 https://www.ncbi.nlm.nih.gov/pmc/articles/PMC6515828/.

32. **Galán, JE, Curtiss, R,3rd.** 1989. Cloning and molecular characterization of genes whose products allow Salmonella typhimurium to penetrate tissue culture cells. Proc. Natl. Acad. Sci. U. S. A. **86:**6383-6387. doi: 10.1073/pnas.86.16.6383 [doi].

33. **Hardt, WD, Chen, LM, Schuebel, KE, Bustelo, XR, Galán, JE.** 1998. S. typhimurium encodes an activator of Rho GTPases that induces membrane ruffling and nuclear responses in host cells. Cell. **93:**815-826. doi: S0092-8674(00)81442-7 [pii].

34. **Fu, Y, Galán, JE.** 1999. A salmonella protein antagonizes Rac-1 and Cdc42 to mediate host-cell recovery after bacterial invasion. Nature. **401:**293-297. doi: 10.1038/45829 [doi].

35. **Jesenberger, V, Procyk, KJ, Yuan, J, Reipert, S, Baccarini, M.** 2000. Salmonella-induced caspase-2 activation in macrophages: a novel mechanism in pathogen-mediated apoptosis. J. Exp. Med. **192:**1035-1046.

36. **Hersh, D, Monack, DM, Smith, MR, Ghori, N, Falkow, S, Zychlinsky, A.** 1999. The Salmonella invasin SipB induces macrophage apoptosis by binding to caspase-1. Proc. Natl. Acad. Sci. U. S. A. **96:**2396-2401. doi: 4845 [pii].

37. **Norris, FA, Wilson, MP, Wallis, TS, Galyov, EE, Majerus, PW.** 1998. SopB, a protein required for virulence of Salmonella dublin, is an inositol phosphate phosphatase. Proc. Natl. Acad. Sci. U. S. A. **95:**14057-14059. doi: 3515 [pii].

38. **Schmidt, H, Hensel, M.** 2004. Pathogenicity islands in bacterial pathogenesis. Clin. Microbiol. Rev. **17:**14-56. doi: 0038 [pii].

39. **Miao, EA, Scherer, CA, Tsolis, RM, Kingsley, RA, Adams, LG, Bäumler, AJ, Miller, SI.** 1999. Salmonella typhimurium leucine-rich repeat proteins are targeted to the SPI1 and SPI2 type III secretion systems. Molecular Microbiology. **34:**850-864. doi: 10.1046/j.1365-2958.1999.01651.x. https://onlinelibrary.wiley.com/doi/abs/10.1046/j.1365-2958.1999.01651.x.

40. **Shea, JE, Hensel, M, Gleeson, C, Holden, DW.** 1996. Identification of a virulence locus encoding a second type III secretion system in Salmonella typhimurium. Proc. Natl. Acad. Sci. U. S. A. **93:**2593-2597. doi: 10.1073/pnas.93.6.2593 [doi].

41. **Groisman, EA, Ochman, H.** 1997. How Salmonella became a pathogen. Trends Microbiol. **5:**343-349. doi: S0966-842X(97)01099-8 [pii].

42. **Carnell, SC, Bowen, A, Morgan, E, Maskell, DJ, Wallis, TS, Stevens, MP.** 2007. Role in virulence and protective efficacy in pigs of Salmonella enterica serovar Typhimurium secreted components identified by signature-tagged mutagenesis. Microbiology (Reading). **153:**1940-1952. doi: 10.1099/mic.0.2006/006726-0 [doi].

43. **Vazquez-Torres, A, Xu, Y, Jones-Carson, J, Holden, DW, Lucia, SM, Dinauer, MC, Mastroeni, P, Fang, FC.** 2000. Salmonella pathogenicity island 2-dependent evasion of the phagocyte NADPH oxidase. Science. **287:**1655-1658. doi: 8324 [pii].

44. **Chakravortty, D, Hansen-Wester, I, Hensel, M.** 2002. Salmonella pathogenicity island 2 mediates protection of intracellular Salmonella from reactive nitrogen intermediates. J. Exp. Med. **195:**1155-1166. doi: 011547 [pii].

45. **Uchiya, K, Barbieri, MA, Funato, K, Shah, AH, Stahl, PD, Groisman, EA.** 1999. A Salmonella virulence protein that inhibits cellular trafficking. Embo J. **18:**3924-3933. doi: 10.1093/emboj/18.14.3924 [doi].

46. **Hensel, M, Nikolaus, T, Egelseer, C.** 1999. Molecular and functional analysis indicates a mosaic structure of Salmonella pathogenicity island 2. Mol. Microbiol. **31:**489-498. doi: 10.1046/j.1365-2958.1999.01190.x [doi].

47. **Tsolis, RM, Townsend, SM, Miao, EA, Miller, SI, Ficht, TA, Adams, LG, Bäumler, AJ.** 1999. Identification of a putative Salmonella enterica serotype typhimurium host range factor with homology to IpaH and YopM by signature-tagged mutagenesis. Infect. Immun. **67:**6385-6393. https://pubmed.ncbi.nlm.nih.gov/10569754 https://www.ncbi.nlm.nih.gov/pmc/articles/PMC97046/.

48. **Pang, S, Octavia, S, Feng, L, Liu, B, Reeves, PR, Lan, R, Wang, L.** 2013. Genomic diversity and adaptation of Salmonella enterica serovar Typhimurium from analysis of six genomes of different phage types. BMC Genomics. **14:**718. doi: 10.1186/1471-2164-14-718. https://pubmed.ncbi.nlm.nih.gov/24138507 https://www.ncbi.nlm.nih.gov/pmc/articles/PMC3853940/.

49. **Proroga, YTR, Capuano, F, Capparelli, R, Bilei, S, Bernardo, M, Cocco, MP, Campagnuolo, R, Pasquale, V.** 2018. Characterization of non-typhoidal Salmonella enterica strains of human origin in central and southern Italy. Italian Journal of Food Safety. **7:**6888. doi: 10.4081/ijfs.2018.6888. https://pubmed.ncbi.nlm.nih.gov/29732321 https://www.ncbi.nlm.nih.gov/pmc/articles/PMC5913695/.

50. **Xu, X, Hensel, M.** 2010. Systematic analysis of the SsrAB virulon of Salmonella enterica. Infect. Immun. **78:**49-58. doi: 10.1128/IAI.00931-09. https://pubmed.ncbi.nlm.nih.gov/19858298 https://www.ncbi.nlm.nih.gov/pmc/articles/PMC2798222/.

51. **Nikolaus, T, Deiwick, J, Rappl, C, Freeman, JA, Schröder, W, Miller, SI, Hensel, M.** 2001. SseBCD proteins are secreted by the type III secretion system of Salmonella pathogenicity island 2 and function as a translocon. J. Bacteriol. **183:**6036-6045. doi: 10.1128/JB.183.20.6036-6045.2001. https://pubmed.ncbi.nlm.nih.gov/11567004 https://www.ncbi.nlm.nih.gov/pmc/articles/PMC99683/.

52. **Quezada, CM, Hicks, SW, Galán, JE, Stebbins, CE.** 2009. A Family of Salmonella Virulence Factors Functions as a Distinct Class of Autoregulated E3 Ubiquitin Ligases. Proceedings of the National Academy of Sciences of the United States of America. **106:**4864-4869. doi: 10.1073/pnas.0811058106. https://www.jstor.org/stable/40441909.

53. **Miao, EA, Miller, SI.** 2000. A conserved amino acid sequence directing intracellular type III secretion by Salmonella typhimurium. Proc. Natl. Acad. Sci. U. S. A. **97:**7539-7544. doi: 10.1073/pnas.97.13.7539. https://pubmed.ncbi.nlm.nih.gov/10861017 https://www.ncbi.nlm.nih.gov/pmc/articles/PMC16581/.

54. **Edwards, DJ, Streich,Frederick C.,,Jr, Ronchi, VP, Todaro, DR, Haas, AL.** 2014. Convergent evolution in the assembly of polyubiquitin degradation signals by the Shigella flexneri IpaH9.8 ligase. The Journal of Biological Chemistry. **289:**34114-34128. doi: 10.1074/jbc.M114.609164. https://pubmed.ncbi.nlm.nih.gov/25342744 https://www.ncbi.nlm.nih.gov/pmc/articles/PMC4256345/.

55. **Hicks, SW, Charron, G, Hang, HC, Galán, J,E.** 2011. Subcellular targeting of Salmonella virulence proteins by host-mediated S-palmitoylation. Cell Host & Microbe. **10:**9-20. doi: 10.1016/j.chom.2011.06.003. https://pubmed.ncbi.nlm.nih.gov/21767808 https://www.ncbi.nlm.nih.gov/pmc/articles/PMC4326042/.

56. **Bhavsar, AP, Brown, NF, Stoepel, J, Wiermer, M, Martin, DDO, Hsu, KJ, Imami, K, Ross, CJ, Hayden, MR, Foster, LJ, Li, X, Hieter, P, Finlay, BB.** 2013. The Salmonella Type III Effector SspH2 Specifically Exploits the NLR Co-chaperone Activity of SGT1 to Subvert Immunity. PLoS Pathogens. **9:**e1003518. doi: 10.1371/journal.ppat.1003518. https://www.ncbi.nlm.nih.gov/pubmed/23935490.

57. **Levin, I, Eakin, C, Blanc, M, Klevit, RE, Miller, SI, Brzovic, PS.** 2010. Identification of an unconventional E3 binding surface on the UbcH5 ~ Ub conjugate recognized by a pathogenic bacterial E3 ligase. Proc. Natl. Acad. Sci. U. S. A. **107:**2848-2853. doi: 10.1073/pnas.0914821107. https://pubmed.ncbi.nlm.nih.gov/20133640 https://www.ncbi.nlm.nih.gov/pmc/articles/PMC2840284/.

58. **Miao, EA, Brittnacher, M, Haraga, A, Jeng, RL, Welch, MD, Miller, SI.** 2003. Salmonella effectors translocated across the vacuolar membrane interact with the actin cytoskeleton. Molecular Microbiology. **48:**401-415. doi: 10.1046/j.1365-2958.2003.t01-1-03456.x. https://onlinelibrary.wiley.com/doi/abs/10.1046/j.1365-2958.2003.t01-1-03456.x.

59. **Halici, S, Zenk, SF, Jantsch, J, Hensel, M.** 2008. Functional analysis of the Salmonella pathogenicity island 2-mediated inhibition of antigen presentation in dendritic cells. Infect. Immun. **76:**4924-4933. doi: 10.1128/IAI.00531-08. https://pubmed.ncbi.nlm.nih.gov/18765734 https://www.ncbi.nlm.nih.gov/pmc/articles/PMC2573360/.

60. **McLaughlin, LM, Xu, H, Carden, SE, Fisher, S, Reyes, M, Heilshorn, SC, Monack, DM.** 2014. A microfluidic-based genetic screen to identify microbial virulence factors that inhibit dendritic cell migration. Integrative Biology : Quantitative Biosciences from Nano to Macro. **6:**438-449. doi: 10.1039/c3ib40177d. https://pubmed.ncbi.nlm.nih.gov/24599496 https://www.ncbi.nlm.nih.gov/pmc/articles/PMC4114769/.

61. **Hu, M, Zhao, W, Gao, W, Li, W, Meng, C, Yan, Q, Wang, Y, Zhou, X, Geng, S, Pan, Z, Cui, G, Jiao, X.** 2017. Recombinant Salmonella expressing SspH2-EscI fusion protein limits its colonization in mice. BMC Immunology. **18:**21. doi: 10.1186/s12865-017-0203-2. https://pubmed.ncbi.nlm.nih.gov/28468643 https://www.ncbi.nlm.nih.gov/pmc/articles/PMC5415771/.

62. **Hu, M, Zhao, W, Li, H, Gu, J, Yan, Q, Zhou, X, Pan, Z, Cui, G, Jiao, X.** 2018. Immunization with recombinant Salmonella expressing SspH2-EscI protects mice against wild type Salmonella infection. BMC Veterinary Research. **14:**79. doi: 10.1186/s12917-018-1404-5. https://pubmed.ncbi.nlm.nih.gov/29523140 https://www.ncbi.nlm.nih.gov/pmc/articles/PMC5845362/.

63. **Panthel, K, Meinel, KM, Domènech, V,E.Sevil, Retzbach, H, Igwe, EI, Hardt, W, Rüssmann, H.** 2005. Salmonella pathogenicity island 2-mediated overexpression of chimeric SspH2 proteins for simultaneous induction of antigen-specific CD4 and CD8 T cells. Infect. Immun. **73:**334-341. doi: 10.1128/IAI.73.1.334-341.2005. https://pubmed.ncbi.nlm.nih.gov/15618170 https://www.ncbi.nlm.nih.gov/pmc/articles/PMC538990/.

64. **Dikic, I.** 2017. Proteasomal and Autophagic Degradation Systems. Annu. Rev. Biochem. **86:**193-224. doi: 10.1146/annurev-biochem-061516-044908 [doi].

65. **Behrends, C, Harper, JW.** 2011. Constructing and decoding unconventional ubiquitin chains. Nat. Struct. Mol. Biol. **18:**520-528. doi: 10.1038/nsmb.2066 [doi].

66. **Mahajan, R, Delphin, C, Guan, T, Gerace, L, Melchior, F.** 1997. A small ubiquitin-related polypeptide involved in targeting RanGAP1 to nuclear pore complex protein RanBP2. Cell. **88:**97-107. doi: S0092-8674(00)81862-0 [pii].

67. **Matunis, MJ, Coutavas, E, Blobel, G.** 1996. A novel ubiquitin-like modification modulates the partitioning of the Ran-GTPase-activating protein RanGAP1 between the cytosol and the nuclear pore complex. J. Cell Biol. **135:**1457-1470. doi: 97133418 [pii].

68. **Loeb, KR, Haas, AL.** 1992. The interferon-inducible 15-kDa ubiquitin homolog conjugates to intracellular proteins. J. Biol. Chem. **267:**7806-7813. doi: S0021-9258(18)42585-9 [pii].

69. **Kamitani, T, Kito, K, Nguyen, HP, Yeh, ET.** 1997. Characterization of NEDD8, a developmentally down-regulated ubiquitin-like protein. J. Biol. Chem. **272:**28557-28562. doi: S0021-9258(18)38691-5 [pii].

70. **Lehmann, G, Udasin, RG, Livneh, I, Ciechanover, A.** 2017. Identification of UBact, a ubiquitin-like protein, along with other homologous components of a conjugation system and the proteasome in different gram-negative bacteria. Biochem. Biophys. Res. Commun. **483:**946-950. doi: S0006-291X(17)30046-3 [pii].

71. **Pearce, MJ, Mintseris, J, Ferreyra, J, Gygi, SP, Darwin, KH.** 2008. Ubiquitin-like protein involved in the proteasome pathway of Mycobacterium tuberculosis. Science. **322:**1104-1107. doi: 10.1126/science.1163885 [doi].

72. **Hershko, A, Ciechanover, A.** 1998. The ubiquitin system. Annu. Rev. Biochem. **67:**425-479. doi: 10.1146/annurev.biochem.67.1.425 [doi].

73. **Dye, BT, Schulman, BA.** 2007. Structural mechanisms underlying posttranslational modification by ubiquitin-like proteins. Annu. Rev. Biophys. Biomol. Struct. **36:**131-150. doi: 10.1146/annurev.biophys.36.040306.132820 [doi].

74. **Pickart, CM.** 2001. Mechanisms underlying ubiquitination. Annu. Rev. Biochem. **70:**503-533. doi: 70/1/503 [pii].

75. **Joazeiro, CA, Wing, SS, Huang, H, Leverson, JD, Hunter, T, Liu, YC.** 1999. The tyrosine kinase negative regulator c-Cbl as a RING-type, E2-dependent ubiquitin-protein ligase. Science. **286:**309-312. doi: 7886 [pii].

76. **Huang, L, Kinnucan, E, Wang, G, Beaudenon, S, Howley, PM, Huibregtse, JM, Pavletich, NP.** 1999. Structure of an E6AP-UbcH7 complex: insights into ubiquitination by the E2-E3 enzyme cascade. Science. **286:**1321-1326. doi: 7996 [pii].

77. **Eisenhaber, B, Chumak, N, Eisenhaber, F, Hauser, MT.** 2007. The ring between ring fingers (RBR) protein family. Genome Biol. **8:**209-209. doi: gb-2007-8-3-209 [pii].

78. **Schulman, BA.** 2011. Twists and turns in ubiquitin-like protein conjugation cascades. Protein Sci. **20:**1941-1954. doi: 10.1002/pro.750 [doi].

79. **Komander, D.** 2009. The emerging complexity of protein ubiquitination. Biochem. Soc. Trans. **37:**937-953. doi: 10.1042/BST0370937. https://doi.org/10.1042/BST0370937.

80. **van Wijk, SJ, Fulda, S, Dikic, I, Heilemann, M.** 2019. Visualizing ubiquitination in mammalian cells. EMBO Rep. **20:**e46520. doi: 10.15252/embr.201846520. Epub 2019 Jan 21. doi: 10.15252/embr.201846520 [doi].

81. **Vittal, V, Stewart, MD, Brzovic, PS, Klevit, RE.** 2015. Regulating the Regulators: Recent Revelations in the Control of E3 Ubiquitin Ligases. J. Biol. Chem. **290:**21244-21251. doi: 10.1074/jbc.R115.675165 [doi].

82. **Emmerich, CH, Ordureau, A, Strickson, S, Arthur, JS, Pedrioli, PG, Komander, D, Cohen, P.** 2013. Activation of the canonical IKK complex by K63/M1-linked hybrid ubiquitin chains. Proc. Natl. Acad. Sci. U. S. A. **110:**15247-15252. doi: 10.1073/pnas.1314715110 [doi].

83. **Yau, RG, Doerner, K, Castellanos, ER, Haakonsen, DL, Werner, A, Wang, N, Yang, XW, Martinez-Martin, N, Matsumoto, ML, Dixit, VM, Rape, M.** 2017. Assembly and Function of Heterotypic Ubiquitin Chains in Cell-Cycle and Protein Quality Control. Cell. **171:**918-933.e20. doi: S0092-8674(17)31134-0 [pii].

84. **Ikeda, F, Dikic, I.** 2008. Atypical ubiquitin chains: new molecular signals. 'Protein Modifications: Beyond the Usual Suspects' review series. EMBO Rep. **9:**536-542. doi: 10.1038/embor.2008.93 [doi].

85. **Kirisako, T, Kamei, K, Murata, S, Kato, M, Fukumoto, H, Kanie, M, Sano, S, Tokunaga, F, Tanaka, K, Iwai, K.** 2006. A ubiquitin ligase complex assembles linear polyubiquitin chains. Embo J. **25:**4877-4887. doi: 7601360 [pii].

86. **Trempe, JF.** 2011. Reading the ubiquitin postal code. Curr. Opin. Struct. Biol. **21:**792-801. doi: 10.1016/j.sbi.2011.09.009 [doi].

87. **Husnjak, K, Dikic, I.** 2012. Ubiquitin-binding proteins: decoders of ubiquitin-mediated cellular functions. Annu. Rev. Biochem. **81:**291-322. doi: 10.1146/annurev-biochem-051810-094654 [doi].

88. **Rahighi, S, Dikic, I.** 2012. Selectivity of the ubiquitin-binding modules. FEBS Lett. **586:**2705-2710. doi: 10.1016/j.febslet.2012.04.053 [doi].

89. **Randles, L, Walters, KJ.** 2012. Ubiquitin and its binding domains. Front. Biosci. (Landmark Ed). **17:**2140-2157. doi: 4042 [pii].

90. **Nijman, SM, Luna-Vargas, MP, Velds, A, Brummelkamp, TR, Dirac, AM, Sixma, TK, Bernards, R.** 2005. A genomic and functional inventory of deubiquitinating enzymes. Cell. **123:**773-786. doi: S0092-8674(05)01169-4 [pii].

91. **Mevissen, TET, Komander, D.** 2017. Mechanisms of Deubiquitinase Specificity and Regulation. Annu. Rev. Biochem. **86:**159-192. doi: 10.1146/annurev-biochem-061516-044916 [doi].

92. **Maculins, T, Fiskin, E, Bhogaraju, S, Dikic, I.** 2016. Bacteria-host relationship: ubiquitin ligases as weapons of invasion. Cell Res. **26:**499-510. doi: 10.1038/cr.2016.30 [doi].

93. **Mattoscio, D, Segré, CV, Chiocca, S.** 2013. Viral manipulation of cellular protein conjugation pathways: The SUMO lesson. World J. Virol. **2:**79-90. doi: 10.5501/wjv.v2.i2.79 [doi].

94. **Randow, F, Lehner, PJ.** 2009. Viral avoidance and exploitation of the ubiquitin system. Nat. Cell Biol. **11:**527-534. doi: 10.1038/ncb0509-527 [doi].

95. **Singer, AU, Rohde, JR, Lam, R, Skarina, T, Kagan, O, Dileo, R, Chirgadze, NY, Cuff, ME, Joachimiak, A, Tyers, M, Sansonetti, PJ, Parsot, C, Savchenko, A.** 2008. Structure of the Shigella T3SS effector IpaH defines a new class of E3 ubiquitin ligases. Nat. Struct. Mol. Biol. **15:**1293-1301. doi: 10.1038/nsmb.1511 [doi].

96. **Zhu, Y, Li, H, Hu, L, Wang, J, Zhou, Y, Pang, Z, Liu, L, Shao, F.** 2008. Structure of a Shigella effector reveals a new class of ubiquitin ligases. Nat. Struct. Mol. Biol. **15:**1302-1308. doi: 10.1038/nsmb.1517 [doi].

97. **Zouhir, S, Bernal-Bayard, J, Cordero-Alba, M, Cardenal-Muñoz, E, Guimaraes, B, Lazar, N, Ramos-Morales, F, Nessler, S.** 2014. The structure of the Slrp-Trx1 complex sheds

light on the autoinhibition mechanism of the type III secretion system effectors of the NEL family. Biochem. J. **464:**135-144. doi: 10.1042/BJ20140587 [doi].

98. **Keszei, AF, Tang, X, McCormick, C, Zeqiraj, E, Rohde, JR, Tyers, M, Sicheri, F.** 2014. Structure of an SspH1-PKN1 complex reveals the basis for host substrate recognition and mechanism of activation for a bacterial E3 ubiquitin ligase. Mol. Cell. Biol. **34:**362-373. doi: 10.1128/MCB.01360-13 [doi].

99. **Zheng, N, Shabek, N.** 2017. Ubiquitin Ligases: Structure, Function, and Regulation. Annu. Rev. Biochem. **86:**129-157. doi: 10.1146/annurev-biochem-060815-014922 [doi].

100. **Rohde, JR, Breitkreutz, A, Chenal, A, Sansonetti, PJ, Parsot, C.** 2007. Type III secretion effectors of the IpaH family are E3 ubiquitin ligases. Cell. Host Microbe. **1:**77-83. doi: S1931-3128(07)00006-6 [pii].

101. **Berglund, J, Gjondrekaj, R, Verney, E, Maupin-Furlow, JA, Edelmann, MJ.** 2020. Modification of the host ubiquitome by bacterial enzymes. Microbiol. Res. **235:**126429. doi: S0944-5013(19)31382-5 [pii].

102. **Norkowski, S, Schmidt, MA, Rüter, C.** 2018. The species-spanning family of LPX-motif harbouring effector proteins. Cell. Microbiol. **20:**e12945. doi: 10.1111/cmi.12945 [doi].

103. **Trindade, BC, Chen, GY.** 2020. NOD1 and NOD2 in inflammatory and infectious diseases. Immunol. Rev. **297:**139-161. doi: 10.1111/imr.12902 [doi].

104. **Moreira, LO, Zamboni, DS.** 2012. NOD1 and NOD2 Signaling in Infection and Inflammation. Frontiers in Immunology. **3:**328. doi: 10.3389/fimmu.2012.00328. https://pubmed.ncbi.nlm.nih.gov/23162548 https://www.ncbi.nlm.nih.gov/pmc/articles/PMC3492658/.

105. **Liwinski, T, Zheng, D, Elinav, E.** 2020. The microbiome and cytosolic innate immune receptors. Immunol. Rev. **297:**207-224. doi: 10.1111/imr.12901 [doi].

106. **Inohara, N, Koseki, T, del Peso, L, Hu, Y, Yee, C, Chen, S, Carrio, R, Merino, J, Liu, D, Ni, J, Nunez, G.** 1999. Nod1, an Apaf-1-like activator of caspase-9 and nuclear factor-kappaB. J. Biol. Chem. **274:**14560-14567.

107. **Travassos, LH, Carneiro, LA, Ramjeet, M, Hussey, S, Kim, YG, Magalhães, JG, Yuan, L, Soares, F, Chea, E, Le Bourhis, L, Boneca, IG, Allaoui, A, Jones, NL, Nuñez, G, Girardin, SE, Philpott, DJ.** 2010. Nod1 and Nod2 direct autophagy by recruiting ATG16L1 to the plasma membrane at the site of bacterial entry. Nat. Immunol. **11:**55-62. doi: 10.1038/ni.1823 [doi].

108. **Zurek, B, Proell, M, Wagner, RN, Schwarzenbacher, R, Kufer, TA.** 2012. Mutational analysis of human NOD1 and NOD2 NACHT domains reveals different modes of activation. Innate Immun. **18:**100-111. doi: 10.1177/1753425910394002 [doi].

109. **Moreira, LO, Zamboni, DS.** 2012. NOD1 and NOD2 Signaling in Infection and Inflammation. Front. Immunol. **3:**328. doi: 10.3389/fimmu.2012.00328 [doi].

110. **Bertin, J, Nir, W, Fischer, CM, Tayber, OV, Errada, PR, Grant, JR, Keilty, JJ, Gosselin, ML, Robison, KE, Wong, GHW, Glucksmann, MA, DiStefano, PS.** 1999. Human CARD4 Protein Is a Novel CED-4/Apaf-1 Cell Death Family Member That Activates NF-κB*. J. Biol. Chem. **274:**12955-12958. doi: https://doi.org/10.1074/jbc.274.19.12955. https://www.sciencedirect.com/science/article/pii/S0021925818368297.

111. **Manon, F, Favier, A, Núñez, G, Simorre, JP, Cusack, S.** 2007. Solution structure of NOD1 CARD and mutational analysis of its interaction with the CARD of downstream kinase RICK. J. Mol. Biol. **365:**160-174. doi: S0022-2836(06)01291-5 [pii].

112. **Srimathi, T, Robbins, SL, Dubas, RL, Hasegawa, M, Inohara, N, Park, YC.** 2008. Monomer/dimer transition of the caspase-recruitment domain of human Nod1. Biochemistry. **47:**1319-1325. doi: 10.1021/bi7016602 [doi].

113. **Coussens, NP, Mowers, JC, McDonald, C, Nuñez, G, Ramaswamy, S.** 2007. Crystal structure of the Nod1 caspase activation and recruitment domain. Biochem. Biophys. Res. Commun. **353:**1-5. doi: S0006-291X(06)02513-7 [pii].

114. **Inohara, N, Koseki, T, Lin, J, del Peso, L, Lucas, PC, Chen, FF, Ogura, Y, Núñez, G.** 2000. An induced proximity model for NF-kappa B activation in the Nod1/RICK and RIP signaling pathways. J. Biol. Chem. **275:**27823-27831. doi: S0021-9258(19)65057-X [pii].

115. **Tanabe, T, Chamaillard, M, Ogura, Y, Zhu, L, Qiu, S, Masumoto, J, Ghosh, P, Moran, A, Predergast, MM, Tromp, G, Williams, CJ, Inohara, N, Núñez, G.** 2004. Regulatory regions and critical residues of NOD2 involved in muramyl dipeptide recognition. Embo J. **23:**1587-1597. doi: 7600175 [pii].

116. **Girardin, SE, Jéhanno, M, Mengin-Lecreulx, D, Sansonetti, PJ, Alzari, PM, Philpott, DJ.** 2005. Identification of the critical residues involved in peptidoglycan detection by Nod1. J. Biol. Chem. **280:**38648-38656. doi: S0021-9258(19)37731-2 [pii].

117. **Laroui, H, Yan, Y, Narui, Y, Ingersoll, SA, Ayyadurai, S, Charania, MA, Zhou, F, Wang, B, Salaita, K, Sitaraman, SV, Merlin, D.** 2011. L-Ala-γ-D-Glu-meso-diaminopimelic acid (DAP) interacts directly with leucine-rich region domain of nucleotide-binding oligomerization domain 1, increasing phosphorylation activity of receptor-interacting serine/threonine-protein kinase 2 and its interaction with nucleotide-binding oligomerization domain 1. J. Biol. Chem. **286:**31003-31013. doi: S0021-9258(20)72381-1 [pii].

118. **Hahn, JS.** 2005. Regulation of Nod1 by Hsp90 chaperone complex. FEBS Lett. **579:**4513-4519. doi: S0014-5793(05)00874-4 [pii].

119. **Girardin, SE, Boneca, IG, Carneiro, LA, Antignac, A, Jéhanno, M, Viala, J, Tedin, K, Taha, MK, Labigne, A, Zähringer, U, Coyle, AJ, DiStefano, PS, Bertin, J, Sansonetti, PJ,**

Philpott, DJ. 2003. Nod1 detects a unique muropeptide from gram-negative bacterial peptidoglycan. Science. **300:**1584-1587. doi: 300/5625/1584 [pii].

120. **Inohara, N, Ogura, Y, Chen, FF, Muto, A, Nuñez, G.** 2001. Human Nod1 confers responsiveness to bacterial lipopolysaccharides. J. Biol. Chem. **276:**2551-2554. doi: S0021-9258(18)46599-4 [pii].

121. **Hasegawa, M, Yang, K, Hashimoto, M, Park, JH, Kim, YG, Fujimoto, Y, Nuñez, G, Fukase, K, Inohara, N.** 2006. Differential release and distribution of Nod1 and Nod2 immunostimulatory molecules among bacterial species and environments. J. Biol. Chem. **281:**29054-29063. doi: S0021-9258(19)33998-5 [pii].

122. **Girardin, SE, Travassos, LH, Hervé, M, Blanot, D, Boneca, IG, Philpott, DJ, Sansonetti, PJ, Mengin-Lecreulx, D.** 2003. Peptidoglycan Molecular Requirements Allowing Detection by Nod1 and Nod2. Journal of Biological Chemistry. **278:**41702-41708. doi: 10.1074/jbc.M307198200. http://www.jbc.org/content/278/43/41702.abstract.

123. **Askari, N, Correa, RG, Zhai, D, Reed, JC.** 2012. Expression, purification, and characterization of recombinant NOD1 (NLRC1): A NLR family member. J. Biotechnol. **157:**75-81. doi: 10.1016/j.jbiotec.2011.10.007 [doi].

124. **Keestra-Gounder, AM, Byndloss, MX, Seyffert, N, Young, BM, Chávez-Arroyo, A, Tsai, AY, Cevallos, SA, Winter, MG, Pham, OH, Tiffany, CR, de Jong, MF, Kerrinnes, T, Ravindran, R, Luciw, PA, McSorley, SJ, Bäumler, AJ, Tsolis, RM.** 2016. NOD1 and NOD2 signalling links ER stress with inflammation. Nature. **532:**394-397. doi: 10.1038/nature17631 [doi].

125. **Molinaro, R, Mukherjee, T, Flick, R, Philpott, DJ, Girardin, SE.** 2019. Trace levels of peptidoglycan in serum underlie the NOD-dependent cytokine response to endoplasmic reticulum stress. J. Biol. Chem. **294:**9007-9015. doi: 10.1074/jbc.RA119.007997 [doi].

126. **Kvarnhammar, AM, Petterson, T, Cardell, LO.** 2011. NOD-like receptors and RIG-I-like receptors in human eosinophils: activation by NOD1 and NOD2 agonists. Immunology. **134:**314-325. doi: 10.1111/j.1365-2567.2011.03492.x [doi].

127. **Yeretssian, G, Correa, RG, Doiron, K, Fitzgerald, P, Dillon, CP, Green, DR, Reed, JC, Saleh, M.** 2011. Non-apoptotic role of BID in inflammation and innate immunity. Nature. **474:**96-99. doi: 10.1038/nature09982 [doi].

128. **Hasegawa, M, Fujimoto, Y, Lucas, PC, Nakano, H, Fukase, K, Núñez, G, Inohara, N.** 2008. A critical role of RICK/RIP2 polyubiquitination in Nod-induced NF-kappaB activation. Embo J. **27:**373-383. doi: 7601962 [pii].

129. **Yamamoto-Furusho, JK, Barnich, N, Xavier, R, Hisamatsu, T, Podolsky, DK.** 2006. Centaurin beta1 down-regulates nucleotide-binding oligomerization domains 1- and 2-dependent NF-kappaB activation. J. Biol. Chem. **281:**36060-36070. doi: S0021-9258(20)68158-3 [pii].

130. **Martínez-Torres, RJ, Chamaillard, M.** 2019. The Ubiquitin Code of NODs Signaling Pathways in Health and Disease. Front. Immunol. **10:**2648. doi: 10.3389/fimmu.2019.02648 [doi].

131. **Ver Heul, AM, Fowler, CA, Ramaswamy, S, Piper, RC.** 2013. Ubiquitin regulates caspase recruitment domain-mediated signaling by nucleotide-binding oligomerization domain-containing proteins NOD1 and NOD2. J. Biol. Chem. **288:**6890-6902. doi: 10.1074/jbc.M112.413781 [doi].

132. **Ver Heul, AM, Gakhar, L, Piper, RC, Subramanian, R.** 2014. Crystal structure of a complex of NOD1 CARD and ubiquitin. PLoS One. **9:**e104017. doi: 10.1371/journal.pone.0104017 [doi].

133. **Fritz, JH, Le Bourhis, L, Sellge, G, Magalhaes, JG, Fsihi, H, Kufer, TA, Collins, C, Viala, J, Ferrero, RL, Girardin, SE, Philpott, DJ.** 2007. Nod1-mediated innate immune recognition of peptidoglycan contributes to the onset of adaptive immunity. Immunity. **26:**445-459. doi: S1074-7613(07)00212-9 [pii].

134. **Ogura, Y, Inohara, N, Benito, A, Chen, FF, Yamaoka, S, Nunez, G.** 2001. Nod2, a Nod1/Apaf-1 family member that is restricted to monocytes and activates NF-kappaB. J. Biol. Chem. **276:**4812-4818. doi: 10.1074/jbc.M008072200 [doi].

135. **Wagner, RN, Proell, M, Kufer, TA, Schwarzenbacher, R.** 2009. Evaluation of Nod-like receptor (NLR) effector domain interactions. PLoS One. **4:**e4931. doi: 10.1371/journal.pone.0004931 [doi].

136. **Mo, J, Boyle, JP, Howard, CB, Monie, TP, Davis, BK, Duncan, JA.** 2012. Pathogen sensing by nucleotide-binding oligomerization domain-containing protein 2 (NOD2) is mediated by direct binding to muramyl dipeptide and ATP. J. Biol. Chem. **287:**23057-23067. doi: 10.1074/jbc.M112.344283 [doi].

137. **Lauro, ML, D'Ambrosio, EA, Bahnson, BJ, Grimes, CL.** 2017. Molecular Recognition of Muramyl Dipeptide Occurs in the Leucine-rich Repeat Domain of Nod2. ACS Infect. Dis. **3:**264-270. doi: 10.1021/acsinfecdis.6b00154 [doi].

138. **Girardin, SE, Boneca, IG, Viala, J, Chamaillard, M, Labinge, A, Thomas, G, Philpott, DJ, Sansonetti, PJ.** 2003. Nod2 Is a General Sensor of Peptidoglycan through Muramyl Dipeptide (MDP) Detection. Journal of Biological Chemistry. **278:**8869-8872. doi: 10.1074/jbc.C200651200. http://www.jbc.org/content/278/11/8869.abstract.

139. **Grimes, CL, Ariyananda Lde, Z, Melnyk, JE, O'Shea, EK.** 2012. The innate immune protein Nod2 binds directly to MDP, a bacterial cell wall fragment. J. Am. Chem. Soc. **134:**13535-13537. doi: 10.1021/ja303883c [doi].

140. **Barnich, N, Aguirre, JE, Reinecker, HC, Xavier, R, Podolsky, DK.** 2005. Membrane recruitment of NOD2 in intestinal epithelial cells is essential for nuclear factor-{kappa}B activation in muramyl dipeptide recognition. J. Cell Biol. **170:**21-26. doi: jcb.200502153 [pii].

141. **Abbott, DW, Wilkins, A, Asara, JM, Cantley, LC.** 2004. The Crohn's disease protein, NOD2, requires RIP2 in order to induce ubiquitinylation of a novel site on NEMO. Curr. Biol. **14:**2217-2227. doi: S0960-9822(04)00988-1 [pii].

142. **Barnich, N, Hisamatsu, T, Aguirre, JE, Xavier, R, Reinecker, HC, Podolsky, DK.** 2005. GRIM-19 interacts with nucleotide oligomerization domain 2 and serves as downstream effector of anti-bacterial function in intestinal epithelial cells. J. Biol. Chem. **280:**19021-19026. doi: S0021-9258(20)67550-0 [pii].

143. **Mohanan, V, Grimes, CL.** 2014. The molecular chaperone HSP70 binds to and stabilizes NOD2, an important protein involved in Crohn disease. J. Biol. Chem. **289:**18987-18998. doi: 10.1074/jbc.M114.557686 [doi].

144. **Kobayashi, KS, Chamaillard, M, Ogura, Y, Henegariu, O, Inohara, N, Nunez, G, Flavell, RA.** 2005. Nod2-dependent regulation of innate and adaptive immunity in the intestinal tract. Science. **307:**731-734. doi: 307/5710/731 [pii].

145. **Jeong, YJ, Kang, MJ, Lee, SJ, Kim, CH, Kim, JC, Kim, TH, Kim, DJ, Kim, D, Núñez, G, Park, JH.** 2014. Nod2 and Rip2 contribute to innate immune responses in mouse neutrophils. Immunology. **143:**269-276. doi: 10.1111/imm.12307 [doi].

146. **Cooney, R, Baker, J, Brain, O, Danis, B, Pichulik, T, Allan, P, Ferguson, DJ, Campbell, BJ, Jewell, D, Simmons, A.** 2010. NOD2 stimulation induces autophagy in dendritic cells influencing bacterial handling and antigen presentation. Nat. Med. **16:**90-97. doi: 10.1038/nm.2069 [doi].

147. **Chen, CM, Gong, Y, Zhang, M, Chen, JJ.** 2004. Reciprocal cross-talk between Nod2 and TAK1 signaling pathways. J. Biol. Chem. **279:**25876-25882. doi: S0021-9258(20)66500-0 [pii].

148. **Humphries, F, Moynagh, PN.** 2015. Molecular and physiological roles of Pellino E3 ubiquitin ligases in immunity. Immunol. Rev. **266:**93-108. doi: 10.1111/imr.12306 [doi].

149. **Kobayashi, KS, Chamaillard, M, Ogura, Y, Henegariu, O, Inohara, N, Nuñez, G, Flavell, RA.** 2005. Nod2-dependent regulation of innate and adaptive immunity in the intestinal tract. Science. **307:**731-734. doi: 307/5710/731 [pii].

150. **Shaw, MH, Reimer, T, Sánchez-Valdepeñas, C, Warner, N, Kim, YG, Fresno, M, Nuñez, G.** 2009. T cell-intrinsic role of Nod2 in promoting type 1 immunity to Toxoplasma gondii. Nat. Immunol. **10:**1267-1274. doi: 10.1038/ni.1816 [doi].

151. **Divangahi, M, Mostowy, S, Coulombe, F, Kozak, R, Guillot, L, Veyrier, F, Kobayashi, KS, Flavell, RA, Gros, P, Behr, MA.** 2008. NOD2-deficient mice have impaired resistance to

Mycobacterium tuberculosis infection through defective innate and adaptive immunity. J. Immunol. **181:**7157-7165. doi: 181/10/7157 [pii].

152. **Watanabe, T, Kitani, A, Murray, PJ, Strober, W.** 2004. NOD2 is a negative regulator of Toll-like receptor 2-mediated T helper type 1 responses. Nat. Immunol. **5:**800-808. doi: ni1092 [pii].

153. **Gong, Q, Long, Z, Zhong, FL, Teo, DET, Jin, Y, Yin, Z, Boo, ZZ, Zhang, Y, Zhang, J, Yang, R, Bhushan, S, Reversade, B, Li, Z, Wu, B.** 2018. Structural basis of RIP2 activation and signaling. Nat. Commun. **9:**4993-9. doi: 10.1038/s41467-018-07447-9 [doi].

154. **Park, JH, Kim, YG, McDonald, C, Kanneganti, TD, Hasegawa, M, Body-Malapel, M, Inohara, N, Núñez, G.** 2007. RICK/RIP2 mediates innate immune responses induced through Nod1 and Nod2 but not TLRs. J. Immunol. **178:**2380-2386. doi: 178/4/2380 [pii].

155. **Chin, AI, Dempsey, PW, Bruhn, K, Miller, JF, Xu, Y, Cheng, G.** 2002. Involvement of receptor-interacting protein 2 in innate and adaptive immune responses. Nature. **416:**190-194. doi: 416190a [pii].

156. **Dorsch, M, Wang, A, Cheng, H, Lu, C, Bielecki, A, Charron, K, Clauser, K, Ren, H, Polakiewicz, RD, Parsons, T, Li, P, Ocain, T, Xu, Y.** 2006. Identification of a regulatory autophosphorylation site in the serine-threonine kinase RIP2. Cell. Signal. **18:**2223-2229. doi: S0898-6568(06)00108-2 [pii].

157. **Bertrand, MJ, Doiron, K, Labbé, K, Korneluk, RG, Barker, PA, Saleh, M.** 2009. Cellular inhibitors of apoptosis cIAP1 and cIAP2 are required for innate immunity signaling by the pattern recognition receptors NOD1 and NOD2. Immunity. **30:**789-801. doi: 10.1016/j.immuni.2009.04.011 [doi].

158. **Krieg, A, Correa, RG, Garrison, JB, Le Negrate, G, Welsh, K, Huang, Z, Knoefel, WT, Reed, JC.** 2009. XIAP mediates NOD signaling via interaction with RIP2. Proc. Natl. Acad. Sci. U. S. A. **106:**14524-14529. doi: 10.1073/pnas.0907131106 [doi].

159. **Yan, R, Liu, Z.** 2017. LRRK2 enhances Nod1/2-mediated inflammatory cytokine production by promoting Rip2 phosphorylation. Protein Cell. **8:**55-66. doi: 10.1007/s13238-016-0326-x [doi].

160. **Jo, EK, Kim, JK, Shin, DM, Sasakawa, C.** 2016. Molecular mechanisms regulating NLRP3 inflammasome activation. Cell. Mol. Immunol. **13:**148-159. doi: 10.1038/cmi.2015.95 [doi].

161. **Haneklaus, M, O'Neill, LA.** 2015. NLRP3 at the interface of metabolism and inflammation. Immunol. Rev. **265:**53-62. doi: 10.1111/imr.12285 [doi].

162. **Zhou, Y, Tong, Z, Jiang, S, Zheng, W, Zhao, J, Zhou, X.** 2020. The Roles of Endoplasmic Reticulum in NLRP3 Inflammasome Activation. Cells. **9:**1219. doi: 10.3390/cells9051219. doi: 10.3390/cells9051219 [doi].

163. **Swanson, KV, Deng, M, Ting, JP.** 2019. The NLRP3 inflammasome: molecular activation and regulation to therapeutics. Nat. Rev. Immunol. **19:**477-489. doi: 10.1038/s41577-019-0165-0 [doi].

164. **Shao, BZ, Xu, ZQ, Han, BZ, Su, DF, Liu, C.** 2015. NLRP3 inflammasome and its inhibitors: a review. Front. Pharmacol. **6:**262. doi: 10.3389/fphar.2015.00262 [doi].

165. **Tartey, S, Kanneganti, TD.** 2019. Differential role of the NLRP3 inflammasome in infection and tumorigenesis. Immunology. **156:**329-338. doi: 10.1111/imm.13046 [doi].

166. **Hoffman, HM, Mueller, JL, Broide, DH, Wanderer, AA, Kolodner, RD.** 2001. Mutation of a new gene encoding a putative pyrin-like protein causes familial cold autoinflammatory syndrome and Muckle-Wells syndrome. Nat. Genet. **29:**301-305. doi: ng756 [pii].

167. **Sharif, H, Wang, L, Wang, WL, Magupalli, VG, Andreeva, L, Qiao, Q, Hauenstein, AV, Wu, Z, Núñez, G, Mao, Y, Wu, H.** 2019. Structural mechanism for NEK7-licensed activation of NLRP3 inflammasome. Nature. **570:**338-343. doi: 10.1038/s41586-019-1295-z [doi].

168. **Inoue, M, Shinohara, ML.** 2013. NLRP3 Inflammasome and MS/EAE. Autoimmune Dis. **2013:**859145. doi: 10.1155/2013/859145 [doi].

169. **Hu, Z, Yan, C, Liu, P, Huang, Z, Ma, R, Zhang, C, Wang, R, Zhang, Y, Martinon, F, Miao, D, Deng, H, Wang, J, Chang, J, Chai, J.** 2013. Crystal structure of NLRC4 reveals its autoinhibition mechanism. Science. **341:**172-175. doi: 10.1126/science.1236381 [doi].

170. **Martinon, F, Burns, K, Tschopp, J.** 2002. The inflammasome: a molecular platform triggering activation of inflammatory caspases and processing of proIL-beta. Mol. Cell. **10:**417-426. doi: S1097-2765(02)00599-3 [pii].

171. **Gu, Y, Kuida, K, Tsutsui, H, Ku, G, Hsiao, K, Fleming, MA, Hayashi, N, Higashino, K, Okamura, H, Nakanishi, K, Kurimoto, M, Tanimoto, T, Flavell, RA, Sato, V, Harding, MW, Livingston, DJ, Su, MS.** 1997. Activation of interferon-gamma inducing factor mediated by interleukin-1beta converting enzyme. Science. **275:**206-209. doi: 10.1126/science.275.5297.206 [doi].

172. **Thornberry, NA, Bull, HG, Calaycay, JR, Chapman, KT, Howard, AD, Kostura, MJ, Miller, DK, Molineaux, SM, Weidner, JR, Aunins, J.** 1992. A novel heterodimeric cysteine protease is required for interleukin-1 beta processing in monocytes. Nature. **356:**768-774. doi: 10.1038/356768a0 [doi].

173. **Vanaja, SK, Rathinam, VA, Fitzgerald, KA.** 2015. Mechanisms of inflammasome activation: recent advances and novel insights. Trends Cell Biol. **25:**308-315. doi: S0962-8924(14)00220-7 [pii].

174. **Guarda, G, Zenger, M, Yazdi, AS, Schroder, K, Ferrero, I, Menu, P, Tardivel, A, Mattmann, C, Tschopp, J.** 2011. Differential expression of NLRP3 among hematopoietic cells. J. Immunol. **186:**2529-2534. doi: 10.4049/jimmunol.1002720 [doi].

175. **O'Connor, W,,Jr, Harton, JA, Zhu, X, Linhoff, MW, Ting, JP.** 2003. Cutting edge: CIAS1/cryopyrin/PYPAF1/NALP3/CATERPILLER 1.1 is an inducible inflammatory mediator with NF-kappa B suppressive properties. J. Immunol. **171:**6329-6333. doi: 10.4049/jimmunol.171.12.6329 [doi].

176. **Perregaux, D, Gabel, CA.** 1994. Interleukin-1 beta maturation and release in response to ATP and nigericin. Evidence that potassium depletion mediated by these agents is a necessary and common feature of their activity. J. Biol. Chem. **269:**15195-15203. doi: S0021-9258(17)36591-2 [pii].

177. **Heid, ME, Keyel, PA, Kamga, C, Shiva, S, Watkins, SC, Salter, RD.** 2013. Mitochondrial reactive oxygen species induces NLRP3-dependent lysosomal damage and inflammasome activation. J. Immunol. **191:**5230-5238. doi: 10.4049/jimmunol.1301490 [doi].

178. **Okada, M, Matsuzawa, A, Yoshimura, A, Ichijo, H.** 2014. The lysosome rupture-activated TAK1-JNK pathway regulates NLRP3 inflammasome activation. J. Biol. Chem. **289:**32926-32936. doi: 10.1074/jbc.M114.579961 [doi].

179. **Pan, Q, Mathison, J, Fearns, C, Kravchenko, VV, Da Silva Correia, J, Hoffman, HM, Kobayashi, KS, Bertin, J, Grant, EP, Coyle, AJ, Sutterwala, FS, Ogura, Y, Flavell, RA, Ulevitch, RJ.** 2007. MDP-induced interleukin-1beta processing requires Nod2 and CIAS1/NALP3. J. Leukoc. Biol. **82:**177-183. doi: jlb.1006627 [pii].

180. **Zhong, Y, Kinio, A, Saleh, M.** 2013. Functions of NOD-Like Receptors in Human Diseases. Front. Immunol. **4:**333. doi: 10.3389/fimmu.2013.00333 [doi].

181. **Toma, C, Higa, N, Koizumi, Y, Nakasone, N, Ogura, Y, McCoy, AJ, Franchi, L, Uematsu, S, Sagara, J, Taniguchi, S, Tsutsui, H, Akira, S, Tschopp, J, Núñez, G, Suzuki, T.** 2010. Pathogenic Vibrio activate NLRP3 inflammasome via cytotoxins and TLR/nucleotide-binding oligomerization domain-mediated NF-kappa B signaling. J. Immunol. **184:**5287-5297. doi: 10.4049/jimmunol.0903536 [doi].

182. **Hoegen, T, Tremel, N, Klein, M, Angele, B, Wagner, H, Kirschning, C, Pfister, HW, Fontana, A, Hammerschmidt, S, Koedel, U.** 2011. The NLRP3 inflammasome contributes to brain injury in pneumococcal meningitis and is activated through ATP-dependent lysosomal cathepsin B release. J. Immunol. **187:**5440-5451. doi: 10.4049/jimmunol.1100790 [doi].

183. **Brodsky, IE, Palm, NW, Sadanand, S, Ryndak, MB, Sutterwala, FS, Flavell, RA, Bliska, JB, Medzhitov, R.** 2010. A Yersinia effector protein promotes virulence by preventing inflammasome recognition of the type III secretion system. Cell. Host Microbe. **7:**376-387. doi: 10.1016/j.chom.2010.04.009 [doi].

184. **Zheng, Y, Lilo, S, Brodsky, IE, Zhang, Y, Medzhitov, R, Marcu, KB, Bliska, JB.** 2011. A Yersinia effector with enhanced inhibitory activity on the NF-κB pathway activates the NLRP3/ASC/caspase-1 inflammasome in macrophages. PLoS Pathog. **7:**e1002026. doi: 10.1371/journal.ppat.1002026 [doi].

185. **Thomas, PG, Dash, P, Aldridge, JR,Jr, Ellebedy, AH, Reynolds, C, Funk, AJ, Martin, WJ, Lamkanfi, M, Webby, RJ, Boyd, KL, Doherty, PC, Kanneganti, TD.** 2009. The intracellular sensor NLRP3 mediates key innate and healing responses to influenza A virus via the regulation of caspase-1. Immunity. **30:**566-575. doi: 10.1016/j.immuni.2009.02.006 [doi].

186. **Allen, IC, Scull, MA, Moore, CB, Holl, EK, McElvania-TeKippe, E, Taxman, DJ, Guthrie, EH, Pickles, RJ, Ting, JP.** 2009. The NLRP3 inflammasome mediates in vivo innate immunity to influenza A virus through recognition of viral RNA. Immunity. **30:**556-565. doi: 10.1016/j.immuni.2009.02.005 [doi].

187. **Hise, AG, Tomalka, J, Ganesan, S, Patel, K, Hall, BA, Brown, GD, Fitzgerald, KA.** 2009. An essential role for the NLRP3 inflammasome in host defense against the human fungal pathogen Candida albicans. Cell. Host Microbe. **5:**487-497. doi: 10.1016/j.chom.2009.05.002 [doi].

188. **Lima-Junior, DS, Costa, DL, Carregaro, V, Cunha, LD, Silva, AL, Mineo, TW, Gutierrez, FR, Bellio, M, Bortoluci, KR, Flavell, RA, Bozza, MT, Silva, JS, Zamboni, DS.** 2013. Inflammasome-derived IL-1β production induces nitric oxide-mediated resistance to Leishmania. Nat. Med. **19:**909-915. doi: 10.1038/nm.3221 [doi].

189. **Zaki, MH, Boyd, KL, Vogel, P, Kastan, MB, Lamkanfi, M, Kanneganti, TD.** 2010. The NLRP3 inflammasome protects against loss of epithelial integrity and mortality during experimental colitis. Immunity. **32:**379-391. doi: 10.1016/j.immuni.2010.03.003 [doi].

190. **Hirota, SA, Ng, J, Lueng, A, Khajah, M, Parhar, K, Li, Y, Lam, V, Potentier, MS, Ng, K, Bawa, M, McCafferty, DM, Rioux, KP, Ghosh, S, Xavier, RJ, Colgan, SP, Tschopp, J, Muruve, D, MacDonald, JA, Beck, PL.** 2011. NLRP3 inflammasome plays a key role in the regulation of intestinal homeostasis. Inflamm. Bowel Dis. **17:**1359-1372. doi: 10.1002/ibd.21478 [doi].

191. **Dinarello, CA.** 2005. Blocking IL-1 in systemic inflammation. J. Exp. Med. **201:**1355-1359. doi: jem.20050640 [pii].

192. **O'Neill, LA.** 2008. The interleukin-1 receptor/Toll-like receptor superfamily: 10 years of progress. Immunol. Rev. **226:**10-18. doi: 10.1111/j.1600-065X.2008.00701.x [doi].

193. **Dinarello, CA.** 2009. Immunological and inflammatory functions of the interleukin-1 family. Annu. Rev. Immunol. **27:**519-550. doi: 10.1146/annurev.immunol.021908.132612 [doi].

194. **Platnich, JM, Chung, H, Lau, A, Sandall, CF, Bondzi-Simpson, A, Chen, HM, Komada, T, Trotman-Grant, AC, Brandelli, JR, Chun, J, Beck, PL, Philpott, DJ, Girardin, SE, Ho, M, Johnson, RP, MacDonald, JA, Armstrong, GD, Muruve, DA.** 2018. Shiga Toxin/Lipopolysaccharide Activates Caspase-4 and Gasdermin D to Trigger Mitochondrial Reactive Oxygen Species Upstream of the NLRP3 Inflammasome. Cell. Rep. **25:**1525-1536.e7. doi: S2211-1247(18)31531-6 [pii].

195. **Gatto, M, Borim, PA, Wolf, IR, Fukuta da Cruz, T, Ferreira Mota, GA, Marques Braz, AM, Casella Amorim, B, Targino Valente, G, de Assis Golim, M, Venturini, J, Araújo Junior, JP, Pontillo, A, Sartori, A.** 2020. Transcriptional analysis of THP-1 cells infected with Leishmania infantum indicates no activation of the inflammasome platform. PLOS Neglected Tropical Diseases. **14:**e0007949. https://doi.org/10.1371/journal.pntd.0007949.

196. **Tedesco, S, De Majo, F, Kim, J, Trenti, A, Trevisi, L, Fadini, GP, Bolego, C, Zandstra, PW, Cignarella, A, Vitiello, L.** 2018. Convenience versus Biological Significance: Are PMA-Differentiated THP-1 Cells a Reliable Substitute for Blood-Derived Macrophages When Studying in Vitro Polarization? Frontiers in Pharmacology. **9:**71. https://www.frontiersin.org/article/10.3389/fphar.2018.00071.

197. **Kim, YK, Shin, JS, Nahm, MH.** 2016. NOD-Like Receptors in Infection, Immunity, and Diseases. Yonsei Med. J. **57:**5-14. doi: 10.3349/ymj.2016.57.1.5 [doi].

198. **Miao, EA, Scherer, CA, Tsolis, RM, Kingsley, RA, Adams, LG, Bäumler, AJ, Miller, SI.** 1999. Salmonella typhimurium leucine-rich repeat proteins are targeted to the SPI1 and SPI2 type III secretion systems. Molecular Microbiology. **34:**850-864. doi: 10.1046/j.1365-2958.1999.01651.x. https://onlinelibrary.wiley.com/doi/abs/10.1046/j.1365-2958.1999.01651.x.

199. **Le Bourhis, L, Werts, C.** 2007. Role of Nods in bacterial infection. Microb. Infect. **9:**629-636. doi: https://doi.org/10.1016/j.micinf.2007.01.014. https://www.sciencedirect.com/science/article/pii/S128645790700038X.

200. **Pierce, JW, Schoenleber, R, Jesmok, G, Best, J, Moore, SA, Collins, T, Gerritsen, ME.** 1997. Novel inhibitors of cytokine-induced IkappaBalpha phosphorylation and endothelial cell adhesion molecule expression show anti-inflammatory effects in vivo. J. Biol. Chem. **272:**21096-21103. doi: S0021-9258(19)65728-5 [pii].

201. **Sakurai, H, Suzuki, S, Kawasaki, N, Nakano, H, Okazaki, T, Chino, A, Doi, T, Saiki, I.** 2003. Tumor necrosis factor-alpha-induced IKK phosphorylation of NF-kappaB p65 on serine 536 is mediated through the TRAF2, TRAF5, and TAK1 signaling pathway. J. Biol. Chem. **278:**36916-36923. doi: S0021-9258(20)83509-1 [pii].

202. **Levin, I, Eakin, C, Blanc, MP, Klevit, RE, Miller, SI, Brzovic, PS.** 2010. Identification of an unconventional E3 binding surface on the UbcH5 ~ Ub conjugate recognized by a

pathogenic bacterial E3 ligase. Proc. Natl. Acad. Sci. U. S. A. **107:**2848-2853. doi: 10.1073/pnas.0914821107 [doi].

203. **Ordureau, A, Münch, C, Harper, JW.** 2015. Quantifying ubiquitin signaling. Mol. Cell. **58:**660-676. doi: S1097-2765(15)00134-3 [pii].

204. **Haraga, A, Miller, SI.** 2006. A Salmonella type III secretion effector interacts with the mammalian serine/threonine protein kinase PKN1. Cell. Microbiol. **8:**837-846. doi: CMI670 [pii].

205. **Proell, M, Riedl, SJ, Fritz, JH, Rojas, AM, Schwarzenbacher, R.** 2008. The Nod-like receptor (NLR) family: a tale of similarities and differences. PLoS One. **3:**e2119. doi: 10.1371/journal.pone.0002119 [doi].

206. **Jennings, E, Thurston, TLM, Holden, DW.** 2017. Salmonella SPI-2 Type III Secretion System Effectors: Molecular Mechanisms And Physiological Consequences. Cell Host & Microbe. **22:**217-231. doi: 10.1016/j.chom.2017.07.009.

207. **Figueira, R, Holden, DW.** 2012. Functions of the Salmonella pathogenicity island 2 (SPI-2) type III secretion system effectors. Microbiology (Reading). **158:**1147-1161. doi: 10.1099/mic.0.058115-0 [doi].

208. **Heim, VJ, Stafford, CA, Nachbur, U.** 2019. NOD Signaling and Cell Death. Front. Cell. Dev. Biol. **7:**208. doi: 10.3389/fcell.2019.00208 [doi].

209. **Burkhard, K, Shapiro, P.** 2010. Use of inhibitors in the study of MAP kinases. Methods Mol. Biol. **661:**107-122. doi: 10.1007/978-1-60761-795-2_6 [doi].

210. **Fiskin, E, Bionda, T, Dikic, I, Behrends, C.** 2016. Global Analysis of Host and Bacterial Ubiquitinome in Response to Salmonella Typhimurium Infection. Mol. Cell. **62:**967-981. doi: S1097-2765(16)30065-X [pii].

211. **Wei, C, Wang, Y, Du, Z, Guan, K, Cao, Y, Yang, H, Zhou, P, Wu, F, Chen, J, Wang, P, Zheng, Z, Zhang, P, Zhang, Y, Ma, S, Yang, R, Zhong, H, He, X.** 2016. The Yersinia Type III secretion effector YopM Is an E3 ubiquitin ligase that induced necrotic cell death by targeting NLRP3. Cell Death & Disease. **7:**e2519. doi: 10.1038/cddis.2016.413. https://doi.org/10.1038/cddis.2016.413.

212. **Cui, J, Chen, Y, Wang, HY, Wang, RF.** 2014. Mechanisms and pathways of innate immune activation and regulation in health and cancer. Hum. Vaccin Immunother. **10:**3270-3285. doi: 10.4161/21645515.2014.979640 [doi].

213. **Hrdinka, M, Fiil, BK, Zucca, M, Leske, D, Bagola, K, Yabal, M, Elliott, PR, Damgaard, RB, Komander, D, Jost, PJ, Gyrd-Hansen, M.** 2016. CYLD Limits Lys63- and Met1-Linked Ubiquitin at Receptor Complexes to Regulate Innate Immune Signaling. Cell. Rep. **14:**2846-2858. doi: S2211-1247(16)30183-8 [pii].

214. **Zheng, Z, Wei, C, Guan, K, Yuan, Y, Zhang, Y, Ma, S, Cao, Y, Wang, F, Zhong, H, He, X.** 2016. Bacterial E3 Ubiquitin Ligase IpaH4.5 of Shigella flexneri Targets TBK1 To Dampen the Host Antibacterial Response. J. Immunol. **196:**1199-1208. doi: 10.4049/jimmunol.1501045 [doi].

215. **Haraga, A, Miller, SI.** 2003. A Salmonella enterica serovar typhimurium translocated leucine-rich repeat effector protein inhibits NF-kappa B-dependent gene expression. Infect. Immun. **71:**4052-4058. doi: 1501 [pii].

216. **Rasaei, R, Sarodaya, N, Kim, KS, Ramakrishna, S, Hong, SH.** 2020. Importance of Deubiquitination in Macrophage-Mediated Viral Response and Inflammation. Int. J. Mol. Sci. **21:**8090. doi: 10.3390/ijms21218090. doi: 10.3390/ijms21218090 [doi].

217. **Man, SM, Kanneganti, TD.** 2015. Regulation of inflammasome activation. Immunol. Rev. **265:**6-21. doi: 10.1111/imr.12296 [doi].

218. **Song, H, Liu, B, Huai, W, Yu, Z, Wang, W, Zhao, J, Han, L, Jiang, G, Zhang, L, Gao, C, Zhao, W.** 2016. The E3 ubiquitin ligase TRIM31 attenuates NLRP3 inflammasome activation by promoting proteasomal degradation of NLRP3. Nature Communications. **7:**13727. doi: 10.1038/ncomms13727. https://doi.org/10.1038/ncomms13727.

219. **Jumper, J, Evans, R, Pritzel, A, Green, T, Figurnov, M, Ronneberger, O, Tunyasuvunakool, K, Bates, R, Žídek, A, Potapenko, A, Bridgland, A, Meyer, C, Kohl, SAA, Ballard, AJ, Cowie, A, Romera-Paredes, B, Nikolov, S, Jain, R, Adler, J, Back, T, Petersen, S, Reiman, D, Clancy, E, Zielinski, M, Steinegger, M, Pacholska, M, Berghammer, T, Bodenstein, S, Silver, D, Vinyals, O, Senior, AW, Kavukcuoglu, K, Kohli, P, Hassabis, D.** 2021. Highly accurate protein structure prediction with AlphaFold. Nature. **596:**583-589. doi: 10.1038/s41586-021-03819-2 [doi].

220. **Compan, V, López-Castejón, G.** 2016. Functional Reconstruction of NLRs in HEK293 Cells, p. 217-221. *In* F. Di Virgilio and P. Pelegrín (eds.), NLR Proteins: Methods and Protocols. Springer New York, New York, NY. https://doi.org/10.1007/978-1-4939-3566-6_15.

221. **Werts, C, Rubino, S, Ling, A, Girardin, SE, Philpott, DJ.** 2011. Nod-like receptors in intestinal homeostasis, inflammation, and cancer. J. Leukoc. Biol. **90:**471-482. doi: 10.1189/jlb.0411183 [doi].

APPENDIX 1

CRISPR/Cas9 modified THP-1 cells are able to differentiate into macrophages.

Since I was able to see interaction with NLRP3 with SspH2, I sought to use a cellular model whereby I could observe the effects that SspH2 had on NLRP3 signaling. To do this, I endeavored to use THP-1 cells, which are a well-studied *in vitro* model for NLRP3 inflammasome activation. These are a good model because they are human cells, and have all of the necessary components for inflammasome activation in the cell already. In addition, the inflammasome is typically activated in macrophages (179). THP-1 cells are monocytes suspended in culture, but upon stimulation with phorbol 12-myristate 13-acetate (PMA), which is analogous to diacyl glycerol, these cells differentiate into adherent macrophages. This results in their secretion of IL-1β, which is measurable by ELISA.

I obtained CRISPR/Cas9 NLRP3 and mock KO cells from the Muruve lab at the University of Calgary that they had previously used to asses NLRP3 function *in vitro* (194). To ensure that these cells were culturable and able to differentiate from THP-1 cells into macrophages, I tested multiple different PMA stimulation conditions. I observed that in accordance with literature on NLRP3 activation (195, 196), 100ng/ml of PMA was sufficient to cause the majority of cells to have the flattened and adherent phenotype characteristic of macrophages (Fig S1). This data indicates that I was successfully able to differentiate THP-1 monocytes into macrophages to be used for further NLRP3 dependent activity studies.
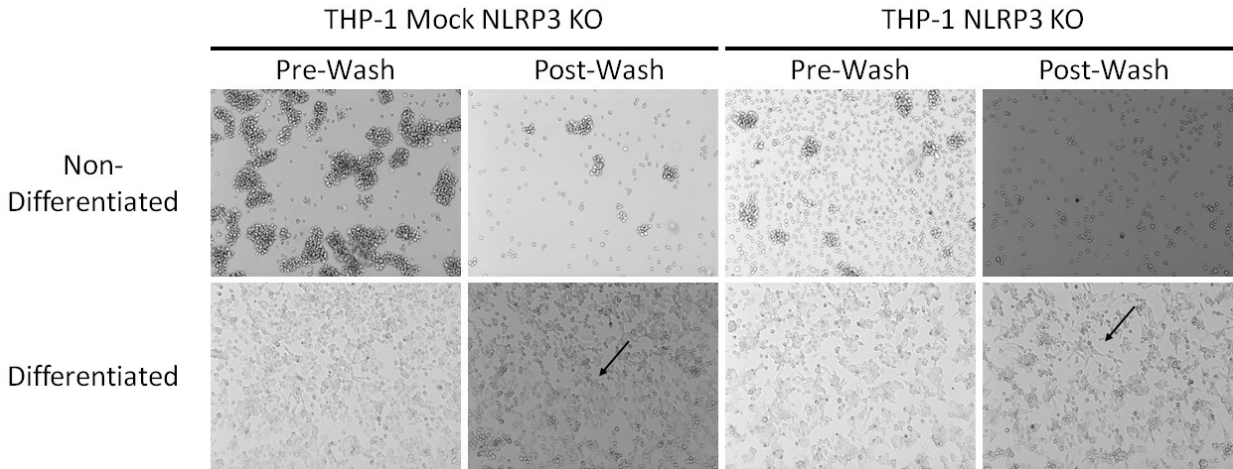
Supplementary Figure 1. THP1 cell culture differentiation.

THP-1 cells were stimulated with or without 100ng/mL PMA for 48 hours, and imaged pre- and post-wash. The arrows indicate adherent macrophages in culture.

THP-1 cell activation

I next assessed whether I am able to observe IL-1β secretion from the THP-1 cells following stimulation. LPS is known to prime THP-1 cells for activation by initiating the production of NLRP3 inflammasome components, and Nigericin induces K^+ efflux, which activates the NLRP3 inflammasome (195, 196). I investigated different concentrations LPS and nigericin for range-finding, in both the mock KO, which have NLRP3 present in them, and the NLRP3 KO THP-1 cells (Fig S2 A-B). I found that the optimal dosing of LPS, for NLRP3 priming, was 100ng/mL and the optimal nigericin concentration was between 5-10 µM for the THP-1 mock KO cells (Fig. S2A). The concentrations of LPS and nigericin had little discernable effect on the NLRP3 KO THP-1 cells. They were not able to secrete IL-1β at a comparable amount to mock KO THP-1s (~10x less), which functionally reaffirms that NLRP3 has been knocked out of these cells (Fig S2B). I next optimized the nigericin dosing for the mock KO THP-1 cells and found that 7.5 µM was an effective dose to observe stimulation of THP-1 cells (Fig S2C). Thus, this data indicates that I have optimised the experimental design for observing NLRP3 dependent activation through IL-1β secretion.
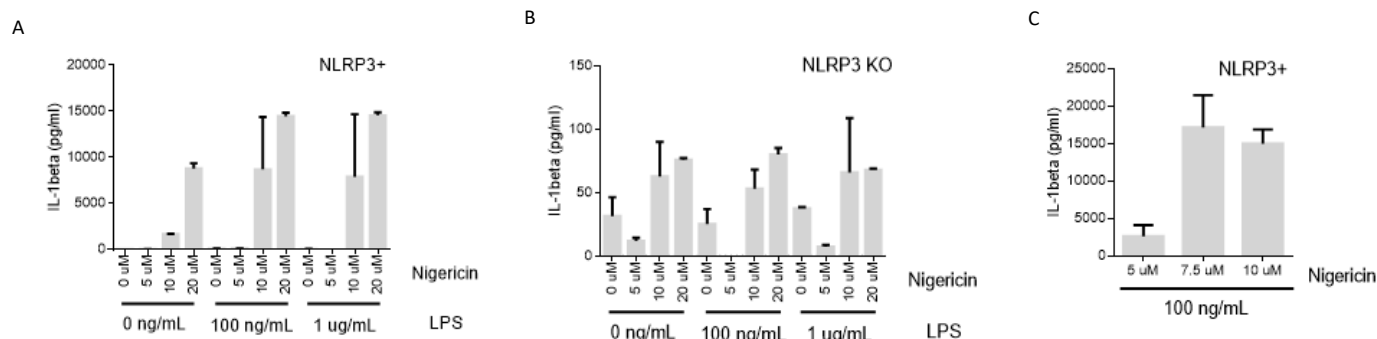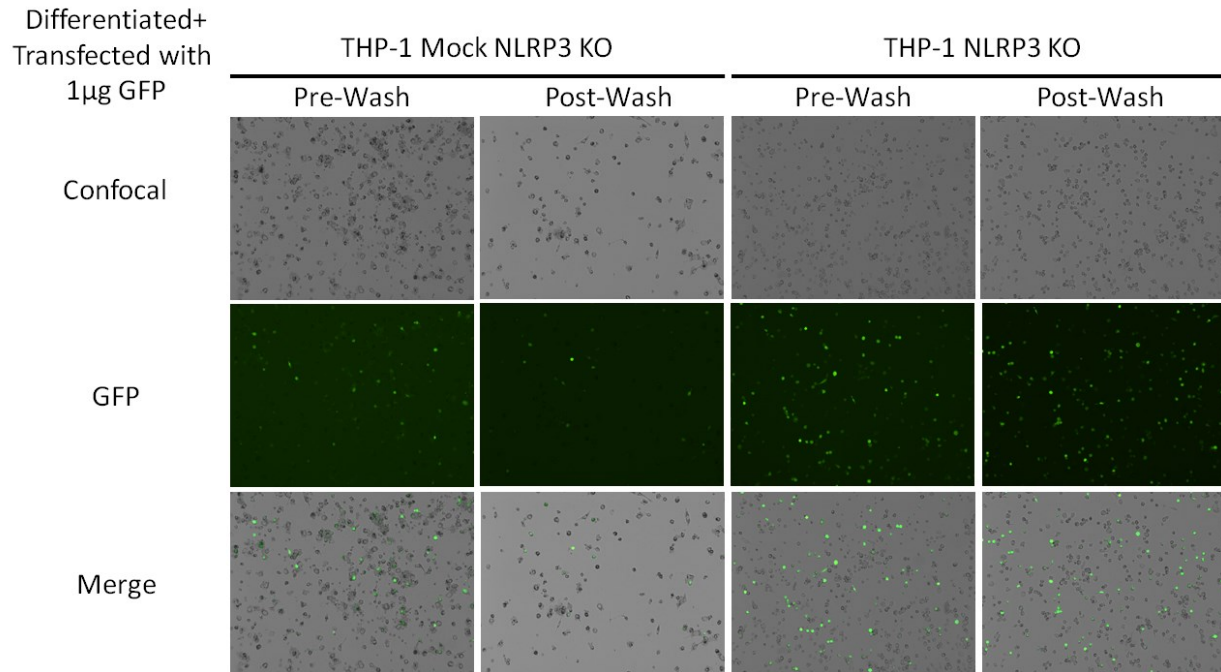
Supplementary Figure 2. THP-1 cell stimulation optimization.

IL-1β secretion assay performed on THP-1 cells stimulated with varying concentrations of Nigericin and LPS. **A.** THP-1 Mock KO (NLRP3+) cells were tested in the presence of 0ng-1μg/mL LPS and 0-20 μM Nigericin. **B.** THP-1 NLRP3 KO cells were tested in the presence of 0ng-1μg/mL LPS and 0-20 μM Nigericin. **C.** THP-1 Mock KO (NLRP3+) cells were further optimized with 100ng/mL and 5-10μM Nigericin. Data is presented as the mean with standard deviation for 1-2 biological replicates.

THP-1 cell transfection

I next sought to understand whether these cells can receive plasmids via electroporation by

transfecting these cells with GFP. I observed that these cells were able to uptake the GFP

plasmid and express GFP, but not at a high efficiency rate (Fig S3). I also found that

electroporating these cells in accordance with manufacturer specifications lead to poor viability

and a reduction of adherent cells observable after 48 hours (Fig S3). Thus, this data indicates that

THP-1 cells are transfectable.

Supplementary Figure 3. THP1 cell electroporation.

THP-1 cells were electroporated with 1µg of GFP plasmid and stimulated with PMA for 48 hours, and imaged pre- and post-wash.

Effect of transient expression of SspH2 in THP-1 cells

Seeing that THP-1 cells were able to uptake plasmids, and able to be effectively activated to produce IL-1β, I determined the effect of transfecting SspH2, SspH2C580A, or EV via electroporation. I observed that the addition of SspH2 or SspH2C580A had no statistically significant differences on IL-1β secretion between response groups in THP-1 mock KO and THP-1 NLRP3 KO cells cells (Fig S4A-D). I next sought to confirm, why that may be by observing whether the SspH2 constructs were detectable via Western blot. In THP-1 mock KO cells, I could clearly identify GAPDH in the THP-1 cell lysates, but could not detect any SspH2 bands in the presence or absence of NLRP3 stimuli (Fig. S4E). This result was replicated in THP-1 NLRP3 KO cells (Fig. S4F). Taken together, these data indicate that I could not see any discernable difference in IL-1β secretion from THP-1 cells transfected with SspH2, SspH2C580A or EV, however this was likely due to the inability for the protein to be effectively transfected into the cells. This could be remedied by using a different cell system, such as expression of the inflammasome in HEK293T cells to measure IL-1β secretion (220), or by using non CRISPR-edited THP-1 cells so that the cells are more vital, and less likely to be adversely affected by transfection.
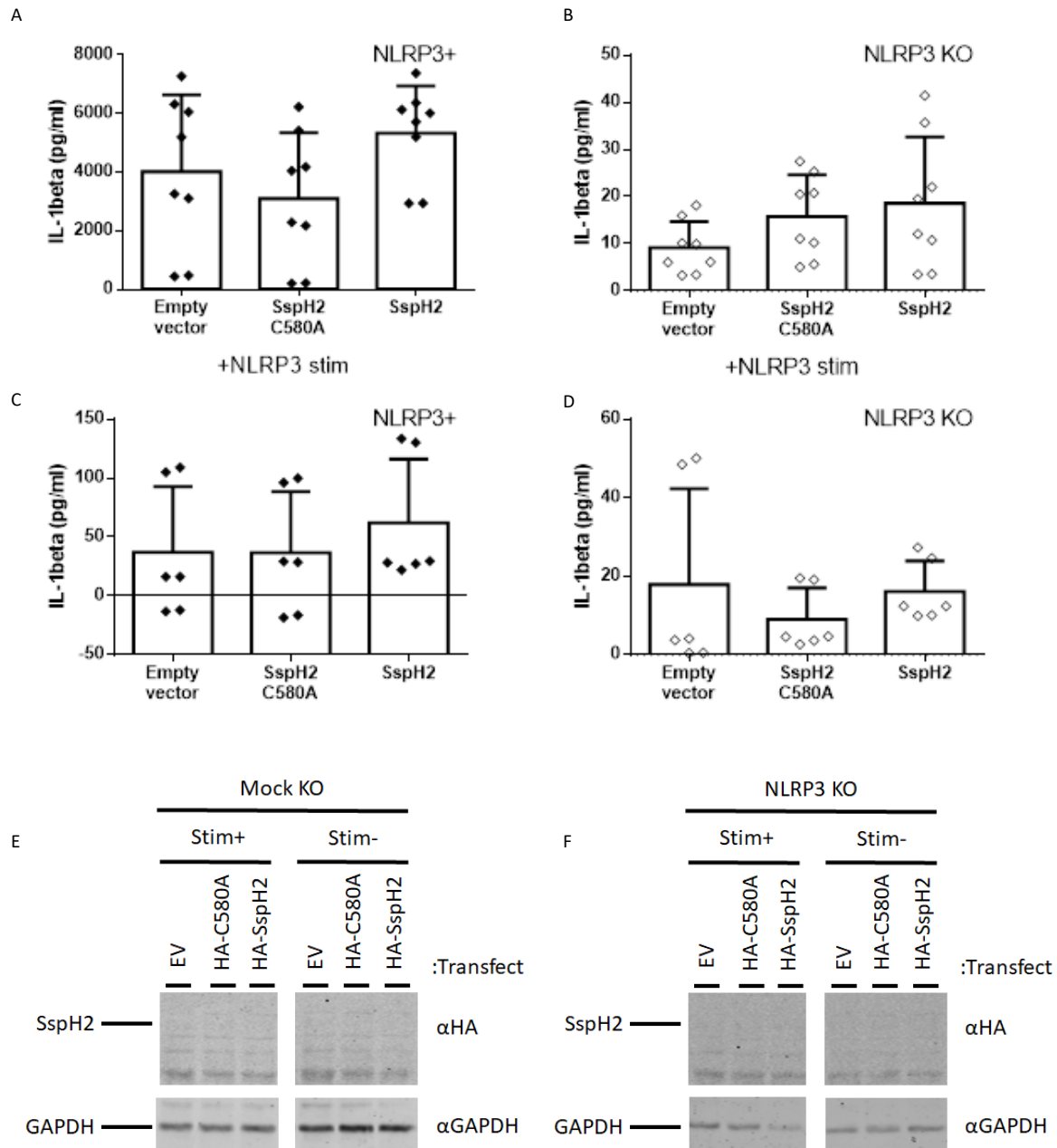
Supplementary Figure 4. THP1 IL-1β assays.

THP-1 cells were electroporated and stimulated with 100ng/mL PMA and 100ng LPS. **A.** IL-1β

secretion assay in THP-1 mock KO cells (NLRP3+) transiently expressing SspH2, SspH2C580A

(C580A), or empty vector (EV) as indicated in the presence of NLRP3 agonist (7.5µM

Nigericin). **B.** IL-1β secretion assay in THP-1 NLRP3 KO cells transiently expressing SspH2,

SspH2C580A (C580A), or empty vector (EV) as indicated in the presence of NLRP3 agonist (7.5μM Nigericin). **C.** IL-1β secretion assay in THP-1 mock KO (NLRP3+) cells transiently expressing SspH2, SspH2C580A (C580A), or empty vector (EV) as indicated. **D.** IL-1β secretion assay in THP-1 NLRP3 KO cells transiently expressing SspH2, SspH2C580A (C580A), or empty vector (EV) as indicated. **E.** Western blot analysis of Mock KO THP-1 cells in the presence/absence of NLRP3 agonist (7.5μM Nigericin). **F.** Western blot analysis of NLRP3 KO THP-1 cells in the presence/absence of NLRP3 agonist (7.5μM Nigericin). Data is presented as the mean with standard deviation for 3 biological replicates. Data were analyzed using a non-parametric Mann-Whitney test. See materials and methods for more detail. Protein expression in THP-1 cell lysate following transient electroporation of indicated constructs.